Western Australia School of Mines:

Minerals, Energy and Chemical Engineering

Solid Phase Extraction of Precious Metals from Aqueous Solution Using Magnetic Particles

April Rose Malagum Calderon

0000-0001-5384-5718

This thesis is presented for the Degree of

Doctor of Philosophy in Mining and Metallurgical Engineering

Of

Curtin University

October 2024

DECLARATION

To the best of my knowledge and belief this report contains no material previously published by any other person except where due acknowledgment has been made.

This thesis contains no material which has been accepted for the award of any other degree or diploma in any university.

April Rose Malagum Calderon

Abstract

Precious metals such as Pt, Pd, Rh, and Au are important in electronics, catalysis, medical/dental, chemical, and pharmaceutical industries due to their inherent characteristics, such as high catalytic activity, excellent mechanical strength, and high resistance to corrosion and oxidation. Spent catalysts, waste electrical and electronic equipment (WEEE) and waste effluents from electroplating and jewellery industries contain significant amounts of precious metals sometimes higher than that of natural ores and are considered as urban mines for these expensive metals. The extraction of precious metals from these secondary sources has become an important research area and technology. Hydrometallurgical techniques are the preferred methods of extraction specifically due to their applicability to low metal concentrations. Solid phase extraction (SPE) using magnetic particles is proposed to provide an economical, efficient, and environment friendly approach to solve this problem. In this method, adsorbents with magnetic properties are added to the sample solution and the target precious metals adsorbed onto the surface of the particle. The loaded magnetic particles are harvested using an external magnetic field and then stripped of precious metals.

The purpose of this study is to investigate the application of solid-phase extraction (SPE) method utilising commonly available and wastes-derived magnetic adsorbents for the recovery of gold, platinum, and palladium from aqueous solution. Two different magnetic particles were investigated in this study; maghemite-rich iron oxide composite prepared by thermal oxidation of synthetic magnetite samples, and a nickeliferous iron sulphide obtained from nickel mining waste tailings. XRD and BJH-BET methods were used to determine the mineralogy of the prepared adsorbents and surface characteristics respectively. Adsorption tests were conducted, and optimum conditions were determined. Adsorption isotherms were also plotted using different adsorption models. SEM and XPS were used to determine the interaction between the adsorbate and adsorbent. Finally, desorption of the recovered precious metals on adsorbents was attempted using different reagents.

Maghemite-rich composite

Magnetite is known to readily oxidise and transform to maghemite, a polymorph of magnetite and is also magnetic. Thus, a composite was prepared by thermal oxidation of synthetic magnetite at 350ºC for 18hours. XRD pattern of the prepared magnetic composite showed 445% maghemite, with 33% and 23% of hematite and magnetite

respectively. BET-BJH results showed a mesoporous material with specific surface area of 6.2686 m^2/g and an average pore width of 12.5nm. The capacity of the prepared adsorbent to recover gold from chloride solution was investigated in a simulated single component system. Results revealed that maximum recovery was achieved at pH 6.5 and 24h contact time with 99.78% Au recovery. The optimum recovery was obtained at a pH that corresponds to the point of zero charge (PZC) of the composite material where Au in the solution exists as $AuOH(H_2O)^o$ complex and can easily be adsorbed because the electrostatic repulsion is very minimal. The ionic strength between the adsorbate and adsorbent decreases as chloride concentration in the solution increases because chloride ions may adsorb onto the surface of the maghemite-rich iron oxide hindering the electrostatic approach of Au complexes to active sites. The overall result showed a chemisorption mechanism. Thiourea was found to be a promising eluant to desorb Au from the adsorbed maghemite-rich composite with 80.17% Au desorbed after 24 hours contact time.

Nickeliferous iron oxide

A naturally occurring magnetic nickeliferous iron sulphide mineral obtained by from nickel mining waste tailings was utilised to recover precious metals from chloride solution. The composite mineral was retrieved via handheld magnet prepared by crushing and grinding to achieve a particle size of D75 of 86.36 µm. and found to have 49.15% Fe, 26.9% S, 12% Ni, and other components in the XRD analysis. The BET-BJH showed a mesoporous material with specific surface area of 1.00 m^2/g and average pore width of 14.08nm. Adsorption experiments were conducted to recover gold, platinum, palladium, and rhodium in a chloride media using a single and multi-component systems. Results showed that Au uptake was fast, 100% Au was achieved after 15 mins contact time at pH<5.5. The adsorbent was reused showing an excellent Au loading capacity of about 6.9mg/g after 8^{th} use. A galvanic interaction is the potential mechanism of the Au uptake. Precipitation tests were investigated for Pt, Pd, and Rh where Pt was found to be stable at any pH range while Pd and Rh started to precipitate at pH 4 and 3.5 respectively. Results showed that at pH<4, 100% Pd was achieved after 1hr contact time while platinum reached 100% recovery after 24h contact time. On the other hand, Rh has a very minimal recovery thus, was not included in the further investigations. Thiourea as eluant gave promising result in desorbing precious metals from the nickeliferous adsorbent with very minimal Fe and Ni dissolution.

Acknowledgments

I would like to express my sincerest gratitude to my supervisors Assoc. Prof. Richard Alorro, Assoc. Prof. Bogale Tadesse, and my co-supervisors Prof. Kyoungkeun Yoo and Prof. Carlito Tabelin for their extraordinary patience and for sharing their brilliant ideas and exceptional contribution in this research.

Thank you also to Prof. Naoki Hiroyoshi, Assoc. Prof. Ilhwan Park, and the rest of professors and students from the Division of Sustainable Resources Engineering, Hokkaido University, Japan for an amazing 1-month internship which enabled me to gain additional knowledge in recycling and Japanese perspective on research and development.

I would also wish to acknowledge the R & D Center for Valuable Recycling (Global-Top R&D Program), Ministry of Environment, Republic of Korea (under project No. 2016002250004) for funding this research.

To my parents Billy and Jovencita, my siblings, and the rest of my family back in the Philippines for their undying support and for always being my strongest motivation.

And to my dear husband, Filbert, for believing in me since the beginning of this journey. For his unceasing love, understanding, and immeasurable support through this exciting ride and with God's grace we made it through together.

To our son, Travis James, for being my inspiration and my greatest achievement who gives me all the reason to strive harder and have the courage to dream a better future.

Also, to my friends: Kitchie, Daryl, the Marianos, the Griffins, my CFC Kalgoorlie family and Tita Emma for the never-ending coffee sessions and for being my cushion against the bumps along this road. For providing emotional, practical, and social support, making this journey smoother and more enjoyable.

And above all, to our Almighty God who gives me strength and made all these things possible.

Table of Contents

List of Figures

List of Tables

List of Equations

$AuCl_4^- + 3e^- \leftrightarrow Au^0 + 4Cl^- -$ ..... (Eq 1)

$Fe^{2+} + Fe^{3+} + 8OH^- \rightarrow Fe_3O_4 + 4H_2O$ ..... (Eq 2)

$4Fe^{3+} + 3BH_4^- + 9H_2O \rightarrow 4Fe^0 + 3H_2BO_3^- + 12H^+ + 6H_2$ ..... (Eq 3)

$3[Fe^{2+}Fe_2^{3+}]O_{4\ (magnetite)} \rightarrow 4[Fe_2^{3+}]O_{3\ (maghemite)} + Fe^{2+} + 2e^-$ ..... (Eq 4)

$\frac{C_e}{q_e} = \frac{1}{K_L q_m} + \frac{C_e}{q_m}$ ..... (Eq 5)

$R = \frac{1}{1+bC_0}$ ..... (Eq 6)

$\ln q_e = \ln K_F + \frac{1}{n} \ln C_e$ ..... (Eq 7)

Au uptake $\left[\frac{\mu mol}{g}\right] = (C_i - C_f) \times \frac{V}{W}$ ..... (Eq 8)

$Au^{3+} + 3e^- \rightarrow Au^0$ ..... (Eq 9)

$Fe_2O_3 + 2e^- + 6H^+ \rightarrow 2Fe^{2+} + 3H_2O$ ..... (Eq 10)

$2Au^{3+} + Fe_2O_3 + 6H^+ \rightarrow 2Au^0 + 2Fe^{2+} + 3H_2O$ ..... (Eq 11)

$2CS(NH_2)_2 + 2Fe^{3+} \rightarrow C_2S_2(NH)_2(NH_2)_2 + 2Fe^{2+} + 2H^+$ .....(Eq 12)

$2Au + C_2S_2(NH)_2((NH)_2)_2 + 2CS(NH_2)_2 + 2H^+ \rightarrow 2Au(CS(NH)_2)_2)_2^+$ ..... (Eq 13)

$q = kc$ ..... (Eq 14)

$PdCl_4^{2-} + 4OH^- \rightarrow Pd(OH)_{2(s)} + 4Cl^-$ ..... (Eq 15)

$Pd(OH)_2 \rightarrow Pd(O)_{(s)} + H_2O$ ..... (Eq 16)

$RhCl_6^{3-} + 6OH^- \rightarrow Rh(OH)_{3(s)} + 6Cl^-$ ..... (Eq 17)

$2Rh(OH)_3 \rightarrow Rh_2O_{3(s)} + 3H_2O$ ..... (Eq 18)

Chapter I

Introduction

I.1 Background of the Study

Platinum, palladium, rhodium and gold are the least abundant precious metals (PMs) in the earth's crust. These PMs have high industrial importance due to their immanent characteristics such as high catalytic activity, mechanical strength, and corrosion/oxidation-resistant properties Nikoloski and Ang (2013). Major applications of these PMs are in jewellery, electronics, catalysis, medical/dental, and pharmaceutical industries. The increasing global demand of these precious metals due to the above industrial uses, leads to higher extraction rates and can deplete accessible reserves more quickly.

As the population grows, there is an increase in the consumption of electronic devices such as smartphones, laptops, TVs, and household appliances, and the worldwide demand for Pt and Pd for automobile catalytic converters and petroleum hydro catalysts due to stricter environmental requirements on fuel emissions and efficiency, among others, leads to a larger quantity of electronics being discarded when they reach the end of their life cycle. Internet availability, mobile networks, new applications and services supplies at increasingly high speeds and techniques for handling big data, have provided new opportunities to the public for health, education, government, entertainment, and commerce. The rapid advancements in technology and the constant release of new products can also lead to shorter lifespans of electronic goods resulting to a massive generation of end-of-life electronic and electrical wastes (WEEE) which pose a major challenge in terms of waste management, environmental and health hazard, and availability of resources. For example, people may replace their devices more frequently, resulting in more electronic waste generation. Waste electrical and electronic equipment (WEEE) are heterogeneous materials that mainly contains glass, plastic, and metals. As shown in Table 1, the trace amounts of economically important critical materials including precious metals and other base metals are present in high concentrations in WEEE than their respective ores.

In many parts of the world, there is inadequate infrastructure for recycling electronic waste. This means that even though some people may want to recycle their old electronics, they may not have easy access to recycling facilities. In Queensland local council's survey in 2004/2005, the average household waste per capita was 341kg/year

and the number of recycled materials per capita was 49.8kg/year, a recycling rate of about 14.6% (Davis and Herat, 2008). Furthermore, the estimated amount of waste produced was 444,000 tonnes (2004/05) with only 23,000 tonnes being recycled (about 5%) (Queensland EPA, 2006). These numbers suggests that recycling is one of the best route to recover precious metals from e-wastes in order to sustain current demand of these precious metals.

Table 1. Typical composition of various secondary sources used for metal recovery (Sun et al., 2016)

	Base metal content, wt.%								Precious metal content, ppm		
Electronic Waste	**Cu**	**Sn**	**Fe**	**Al**	**Pb**	**Zn**	**Ni**	**Cr**	**Ag**	**Au**	**Pd**
ICT waste (<8mm)	50	2	4	2	2	3	2	1	640	120	-
Mobile phone scrap	13	0	5	2	0.3	0	0.1	0	1380	350	210
Portable audio scrap	21	0	23	1	0.1	0	1	0	150	10	4
Printed circuit board scrap	16	3	5	5	2	1	2	-	1000	250	100
Shredded WEEE <0.25mm	14	2	-	-	1	-	-	-	760	130	160
TV board scrap	10	2	28	10	1	-	0.3	-	280	20	10
Euro/kg (3 month average)[1]	5.3	16	0.4	1.5	1.7	1.8	13.2	6.4	632.1	37157	18654
Spent Catalyst	**Mo**	**Co**	**Ni**	**V**	**Fe**	**Zn**	**Al**	**Mg**	**Pt**	**Rh**	**Pd**
Spent catalyst (petroluem)	7	3	2.8	6.5	0.2	-	-	-			
Spent hydrotreatment catalyst	19	1	0.5	-	1.5	0.5	-	-			
Spent catalyst powder	13	0.1	2.5	0.1	-	-	27	-			
Spent automobile catalyst	-	-	-	-	-	-	25	8	800	50	120
Euro/kg (3 month average)[1]	16.6	25.3	13.2	308	0.4	1.8	1.5	2.1	40029	27207	18654

[1]The metal prices in the table are the 3-month(07/2014-09/2014) average price obtained from http://www.metalprices.com/

In 2010-2014, Australia's WEEE generation has grown from 410Mt to 587Mt or 43% (Golev et al., 2016). These wastes are considered as urban mines and are significant secondary sources of PGMs, gold and other base metals such as Fe and Cu being by far of major interest for recycling due to their inherent content and value. In 2014 alone, the estimated recovery value of WEEE and waste PCBs were $370M and $150M respectively. WEEE comprises 30% precious metals (PGM + Au) and several percentages of base metals. Although waste PCBs represented only 4% by weight, accounts 40% of the total recovery value due to high amounts of precious metals such as Au (59%) (Golev et al., 2016). The increase in waste electronics poses environmental and health risks due to the presence of hazardous materials such as lead, mercury and other retardants (Sun et al., 2016) and this statistic suggests that proper

management of e-waste, including recycling and safe disposal, is highly beneficial for the environment and economic reasons.

The extraction and recovery of precious metals from urban mines is still a vital area in metallurgical research and technological development inspite of several processes and techniques already established and commercialized (Sun et al., 2016, Akcil et al., 2015). The processing of waste materials containing precious metals is complicated due to a variety of reasons including low concentrations of precious metals and presence of multifarious components and high amounts of impurities. Several methods were proposed or established to recover precious metals from secondary sources, and these include physical, hydrometallurgical, bio-hydrometallurgical and pyrometallurgical processes based on conventional methods (Akcil et al., 2015, Wang et al., 2017a). Amongst these methods, hydrometallurgical processing has gained increasing attention and has been preferred over pyrometallurgical processing to recover precious metals due to low energy consumption, high recovery rate, easy operation, low equipment and investment cost, and low environmental impact (low or no gas emission and low or no dust generation, etc.) (Wang et al., 2017a, Akcil et al., 2015). Hydrometallurgical processing of urban mines comes after some pre-treatment steps such as sorting, and other physical or chemical separation processes. The dissolution of target precious metals from secondary sources is carried out through leaching using different lixiviants because of its ability to form complex ions which includes; cyanide, *aqua regia*, thiourea, thiosulfate, and halides (chloride, bromide, and iodide) (Zhang et al., 2012).

The next equally important step in hydrometallurgical processing of precious metals from secondary sources is the separation and purification of the dissolved metals from leaching solutions. This step presents a lot of difficulties and challenges related to selectivity, product purity and process efficiency among others. This is due to the dilute concentrations of precious metals in solution and the presence of huge quantities of impurity ions such as copper, iron, nickel and other base metals. A number of separation and purification methods are available and suggested by literature to recover precious metals from solution, including precipitation –cementation (Barakat et al., 2006, Park and Fray, 2009, Umeda et al., 2011), solvent extraction (Cui and Zhang, 2008, Paiva et al., 2017, Zhang et al., 2013), ion exchange (Marinho et al., 2011b, Nikoloski and Ang, 2014, Shen et al., 2011b) and solid phase extraction (adsorption) (Adhikari et al., 2013, Aktas et al., 2011, Alorro et al., 2010, Uheida et al., 2006b, Zazycki et al., 2017a). Among these methods, solid phase extraction (SPE) is regarded to be more attractive

and offers several advantages over the other methods including simpler and faster operation, higher capacity, less environmental impact, easy handling, and lower cost.

Solid phase extraction (SPE) has wide applications in several industries including hydrometallurgical processing, water treatment, biotechnology, and analytical systems. It is particularly useful for the extraction and purification of analytes that are present in low concentrations, as well as for the removal of unwanted matrix interferences (Giakisikli and Anthemidis, 2013b). This method is carried out by allowing the desired analyte from the solution to adhere or bond, either by ion exchange mechanism or chelating mechanism, at the surface of a solid material known as adsorbents. These adsorbents are usually in the form of spherical pellets, rods, or monoliths which can be categorised as organic (Adhikari et al., 2013, Aktas et al., 2011, Aktas and Morcali, 2011, Cui and Zhang, 2008), inorganic (Alorro et al., 2010, Homchuen et al., 2016, Uheida et al., 2006b) or organic-inorganic adsorbents (Ferreira et al., 2010, Mamani et al., 2013). The adsorbent material is the key and critical factor for efficient extraction, hence, must be properly selected and prepared.

The utilization of magnetic particles as adsorbents in solid phase extraction is considered one of the emerging technologies in the separation and purification of precious metal ions from hydrometallurgical processes. The method is known as magnetic solid phase extraction or MSPE and is a procedure based on the use of magnetic sorbents for the separation and pre-concentration of different organic and inorganic analytes from large sample volumes. Figure 1 illustrates the MSPE procedure. The magnetic sorbent is added to the sample solution and the target analyte is adsorbed onto the surface of the magnetic sorbent particles. The use of magnetic materials in solid phase extraction has received considerable attention in recent years due to the many advantages arising from the inherent characteristics of magnetic particles. By applying an external magnetic field, problems associated with filtration or phase separation in a conventional solid-liquid system can be easily performed with MSPE methodology (Giakisikli and Anthemidis, 2013b, Herrero-Latorre et al., 2015a). Generally, the adsorption process concerning the use of magnetic adsorbents include adsorption separation, magnetic recovery, adsorbent regeneration and reusability, and management of the used adsorbent and spent solution (Gómez-Pastora et al., 2014).

In this study, two types of magnetic particles were investigated to recover precious metals such as Au, Pt, Pd, and Rh, from chloride solution. These includes iron oxide composite (maghemite-rich) particles prepared from low temperature oxidation of

synthetic magnetite, and a natural magnetic iron sulphide obtained from a nickel mine waste from Western Australia. The maghemite-rich iron composite was prepared by low temperature oxidation of synthetic magnetite whilst the magnetic iron sulphide (consist primarily of pyrrhotite), is prepared by crushing, grinding and magnetic separation. The effects of different process parameters such as solution pH, contact time chloride concentration, and initial Au concentration, on the recovery of precious metals (Pt, Pd, Rh, and Au) were investigated. Adsorption isotherm studies and detailed characterisation using Scanning Electron Microscopy-Energy Dispersive X-ray (SEM-EDX), and X-ray Photoelectron Spectroscopy (XPS) were conducted to identify the mechanism of reaction of precious metal ions and the surfaces of magnetic adsorbents.

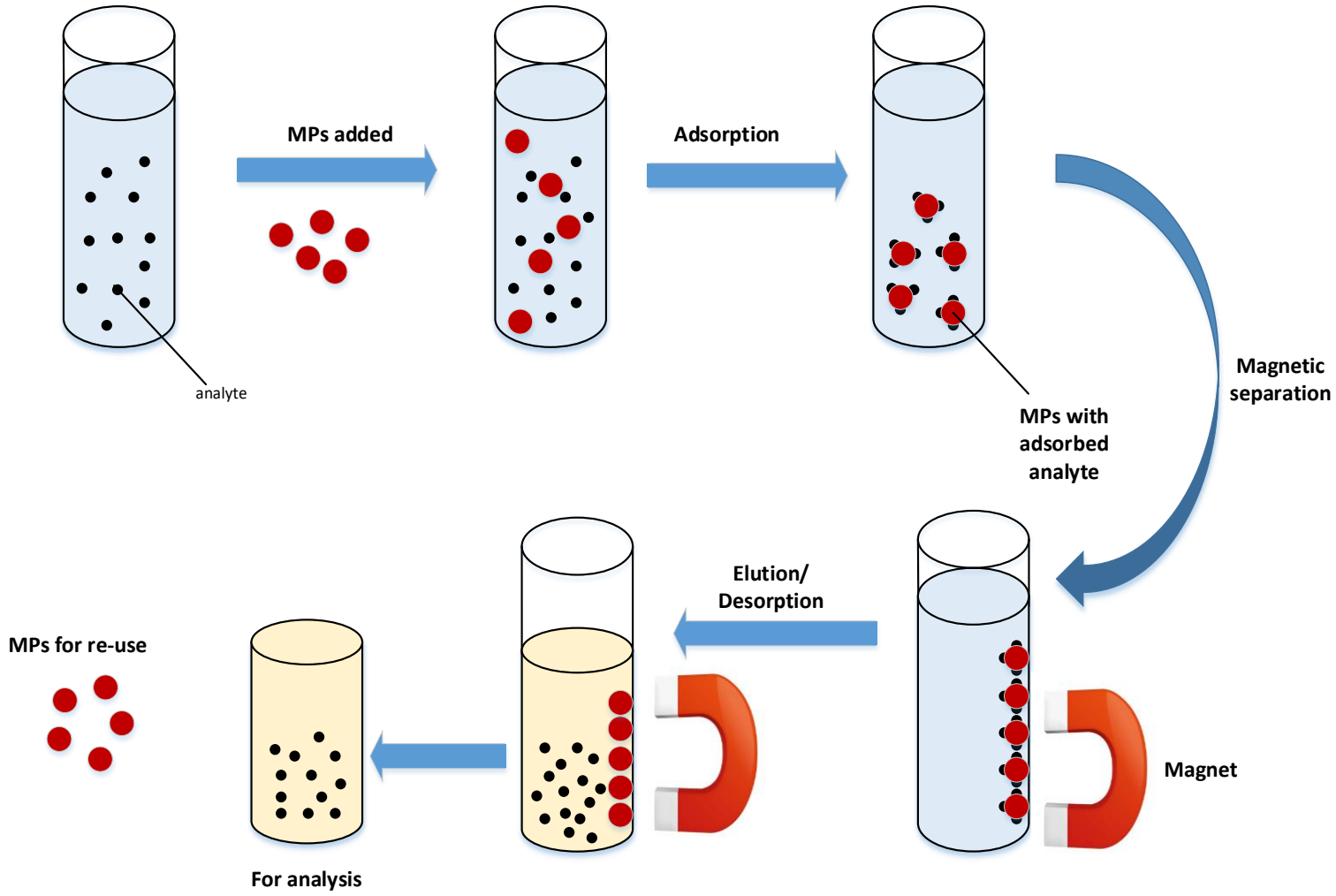

Figure 1. Schematic diagram for the MSPE process (Giakisikli and Anthemidis, 2013b)

I.2 Significance of the Study

The increase of population over the years has multifaceted impact on precious metals consumption. It drives higher demand in electronics, industrial applications, jewellery, and vehicles. The increase in industrial activity related to population growth fuels the need for more precious metals, while also presenting environmental and sustainability challenges related to resource depletion and recycling. For example, a typical electronic waste has an average concentration of; 701ppm Ag, 147ppm Au, and 100ppm Pd, while spent catalysts has 800ppm Pt, and 50ppm Rh (Sun. et. al., 2016). These amounts of precious metals in urban wastes have attracted researchers in developing methods for sustainable metal recovery while minimizing environmental impact. Magnetic solid phase extraction (MSPE) is one of the separation techniques that received considerable attention in the recent years. This method primarily uses magnetic particles as adsorbent for toxic elements and valuable metals from different aqueous streams. MSPE is considered because of its ease of phase separation primarily carried out by facile magnetic decantation as compared to traditional SPE aside from high adsorption capacity and selectivity. This research investigated the capability of the naturally-occurring and synthetic magnetic particles as adsorbent to recover precious metals such as gold, platinum, palladium, and rhodium from aqueous solution using magnetic solid phase extraction (MSPE) as a separation technique.

Magnetite is the most abundant magnetic particle in the earth's atmosphere and has extensively employed to separate and concentrate species from solution for analytical purposes in mineral processing, extractive metallurgy, wastewater treatment, among others. Magnetite can oxidise and form maghemite, a magnetic polymorph of magnetite where its electroneutrality, shape, and crystal structure is preserved. From the geochemical point of view, gold in the refractory ores is known to be occluded in the impenetrable bands of maghemite suggesting an excellent adsorbent capability. In this study, a maghemite composite material will be investigated in the recovery of precious metals from solutions.

Iron sulphides such as pyrrhotites are mined because they are associated with pentlandite, marcasite, etc., that usually contains significant amount of nickel and cobalt. Pyrrhotite specifically are often considered as overburden or waste rocks and are used as backfill in the open pit or underground mine. Depending on its mineralogy, pyrrhotite could possess an excellent magnetic characteristic and has reported to adsorb

heavy metals (mercury, lead, zinc and cadmium) and was found to play important roles in the deposition of gold complexes in the geochemical processes. This characteristic has demonstrated the potential of pyrrhotite as an effective adsorbent for metal ions from solutions.

This project will contribute another important low-concentration metal separation and purification technique in different fields primarily environmental remediation and recycling. In addition, this study primarily utilizes a cost-efficient adsorbent derived from readily available materials or waste; promote circular economy, waste valorisation.

I.3 Objective of the Study

The main objective of this study is to investigate adsorption capability of prepared magnetic adsorbents from synthetic and naturally occurring mineral on the recovery of precious metals such as Au, Pt, Pd, and Rh, from chloride solution. Specifically, it is aimed to:

1. characterize the prepared magnetic adsorbents for physical and chemical properties using range of analytical techniques;
2. evaluate the adsorption of precious metal ions (Au, Pt, Pd and Rh) in single component systems on the prepared magnetic adsorbents;
3. investigate the effects of different process variables such as pH, contact time, precious metals concentration, adsorbent dosage, and chloride concentration on the adsorption of precious metals;
4. conduct chemical speciation, adsorption isotherm and kinetic studies and relate to process mechanism; and
5. identify suitable desorption or stripping methods for precious metals adsorbed on magnetic particles.

Chapter II

Review of Related Studies

II.1 Precious Metals

Platinum group metals [platinum (Pt), palladium (Pd), iridium (Ir), osmium (Os), rhodium (Rh), ruthenium (Ru)] plus gold (Au) and silver (Ag) are called 'precious' metals (PMs). In the recent years, precious metals are regarded as industrial commodities. From the natural resources, the concentration of these precious metals is low and widely distributed (Kyriakakis, 2005). Precious metals has extensively consumed in modern and high technology application due to their excellent characteristics such as high melting points, naturally inert, and are highly resistant to corrosion (Nikoloski and Ang, 2014). The continuing demand of these precious metals to satisfy the needs of current practices and applications coupled with the depleting primary sources, have rendered recycling and reprocessing of waste materials containing precious metals highly attractive for economic and environmental reasons.

II.1.2 Platinum Group Metals (PGM)

Platinum Group Metals or PGMs such as Pd, Pt, and Rh are noble elements used extensively in the modern high technological activities such as in electronics, jewellery, pharmaceutical, dental, automotive, etc. due to their distinctive characteristics, such as high resistance to chemical attack, high melting points, electrical stability, and outstanding catalytic properties (Benson et al., 2000, Kim, 2000). For example, platinum, palladium, and Rhodium are widely exploited as automotive catalysts due to its conversion of carbon monoxide (CO) and hydrocarbons (HC) into carbon dioxide (CO_2) and moisture (H_2O), while Pt is well suited for fine jewellery due to its resistance to wear and tarnish, etc. Platinum group metals are typically found together in nature and are relatively rare. They are often extracted from ore deposits in underground mines or open-pit mines. Due to very low concentrations in the nature, PGMs are often mined as by-products of nickel and copper mining, primarily in the regions like South Africa, Russia, and North America, Zimbabwe, and Canada (Perez et al., 2019, Karim and Ting, 2021). In the last decades, the increasing demand of these PGMs, in conjunction with the rapidly increasing human population, offers a challenge as the low-abundant mineral deposits have started to decline. Hence, researchers are attracted to urgently recover these raw materials in a reliable, sustainable, and economical manner. Due to

more stricter emission policies and legislations, i.e., in the United States and European Union (EU), platinum group metals together with other metals such as rare-earths, scandium, antimony, beryllium, bismuth, cobalt and other metals are now considered critical raw materials (CRM) and are vital for economic development as well as improving life quality (Perez et al., 2019, Rao and Reddi, 2000, Crundwell Frank et al., 2011).

The main process technologies for the recovery of PGMs has 2 possible routes: (1) pyrometallurgical and/or (2) hydrometallurgical. Decades ago, pyrometallurgical method is preferred due to easy handling. However, several disadvantages are met within which involves a specific equipment that requires vast power to melt the metal at relatively high temperatures which makes it uneconomical (Steinlechner and Antrekowitsch, 2015). Moreover, this route is not ideal due to the possible hazardous gas emissions. For example, smelters cannot recover metallic iron or aluminium ending in slags, the presence of ceramic and glass materials increases the amount of slag production and losses precious metals recovery, and due to high temperatures, feed materials may produce dioxins and other toxins that are harmful to humans and environment. On the other hand, hydrometallurgical methods are more controllable, more efficient, and less or minimal production of harmful constituents. This method requires a suitable lixiviant and oxidant/reductant which makes the process more selective to target analytes.

II.1.3 Gold

Gold is one of the least abundant precious metals (PMs) in the Earth's crust, which has an average concentration of only about 0.005 g/t or 0.001 to 0.006 parts per million (Fosu, 2016). It is a precious metal that can be found in various forms and geological settings. Gold deposits are the concentrations of gold that accumulate in specific areas of the Earth's crust due to different geological processes. Several examples of gold deposition, which has its own characteristics, includes vein, placer, carlin-type, alluvial, among others. At present, gold has become an important metal in electronics, medical/dental, catalysis, aerospace engineering, pharmaceutical, and other industries (Iwasaki et al., 2009). This is due to its immanent characteristics, such as, excellent electrical conductivity and malleability, ductility, and high corrosion/oxidation-resistant properties (Homchuen et al., 2016, Nikoloski and Ang, 2014). Printed Circuit Boards (PCBs) in electronics production uses gold as plating on the surfaces, connector

pins and switches, for electrical conductivity and corrosion resistance. The rapid increase in the production of more advanced electronic goods, such as televisions, mobile phones and laptops, have resulted to massive increase in demand for gold and other precious metals. However, this has also resulted in massive generation of end-of-life electronic and electrical wastes (e-wastes), which pose major challenges globally due to problems associated with waste management and environmental and health hazards. Recycling of gold and other precious metals from e-wastes has become an attractive option due to its economic advantages.

The extraction and recovery of gold from e-wastes is an important area in metallurgical research despite of a number of processes and techniques already established and commercialised. Several methods were proposed or established including physical, pyrometallurgical, hydrometallurgical, and bio-hydrometallurgical process based on conventional methods (Tuncuk et al., 2012, Zhao et al., 2014, Syed, 2012). Amongst these methods, hydrometallurgical processing has gained increasing attention and has been preferred over pyrometallurgical processes due to low energy consumption, high recovery rate, easy operation, low equipment and investment cost, and low environmental impact (low or no gas emission and low or no dust generation, etc.) (Wang et al., 2017b, Tuncuk et al., 2012). However, an equally important step, which is the separation and recovery of the dissolved gold in the solution, presents several difficulties and challenges related to selectivity, product purity and process efficiency among others, especially when gold is present in low concentrations.

Various methods were proposed to recover gold from aqueous solutions. These include cementation (Navarro et al., 2004), solvent extraction (Li et al., 2012), coagulation (Lu et. al., 2011), ion-exchange (Aktas et al., 2011, Navarro et al., 2004), and adsorption (Homchuen et al., 2016, Lam et al., 2008) (Aktas et al., 2011, Alorro et al., 2010, Zazycki et al., 2017b). Amongst these methods, adsorption is highly preferred due to ease in handling, low cost, potential adsorbent regeneration, and high capacity (Aktas et al., 2011, Assadian et al., 2013). The major focus in adsorption is adsorbent selection and effectiveness especially when very low gold concentrations (<100 ppm) are considered. The needs to ensure high selectivity, low environmental impact, availability, re-usability, and the ease of preparation and phase separation are extremely relevant in this regard.

II.2. Hydrometallurgical Techniques

The processing of waste materials containing precious metals is complicated due to a variety of reasons including low concentrations of precious metals and presence of multifarious components and high amounts of impurities. Several methods were proposed or established to recover precious metals from secondary sources and these include physical, hydrometallurgical, bio-hydrometallurgical and pyrometallurgical processes based on conventional methods (Akcil et al., 2015, Wang et al., 2017a). Hydrometallurgical techniques such as leaching followed by refining, are commonly used in the recovery of precious metals from solutions. In comparison to pyrometallurgical processing, hydrometallurgical methods are more predictable, and more easily controlled. These techniques involve the use of aqueous solutions, often acidic or alkaline, to selectively dissolve and recover precious metals from ores, concentrates, or other materials (Akcil et al., 2015, Sun et al., 2016). Hydrometallurgical processing of urban mines comes after some pre-treatment steps such as sorting, magnetic separation, and other physical or chemical separation processes. The dissolution of target precious metals from secondary sources is a process typically involves leaching using different lixiviants such as cyanide, aqua regia, thiourea, thiosulfate, chloride, bromide, and iodide (Zhang et al., 2012). These reagents have been successful to a varying degree to solubilise the precious metals. Some of the key hydrometallurgical methods used for recovering precious metals are discussed in the succeeding sections:

II.2.1. Methods of separation and purification of precious metals from leach solutions

II.2.1.1 Precipitation-cementation

Precipitation-cementation is considered as a classical method of separating metals from aqueous solutions. It is carried out by adding a reducing agent onto the leached solution and allowing the desired metal ions to precipitate. The precipitate can be recovered by filtration, centrifugation, decantation, etc. Several studies reported the use of different reducing agents to precipitate out and recover precious metals (Au, Pd and Pt) from leach solutions of spent petroleum catalysts, waste PCBs, and industrial wastewaters. These reagents include aluminium powder (Kim et al., 2010), formic acid (Barakat et al., 2006), iron, zinc, and nickel wires or powders (Park and Fray 2009, Umeda et al. 2011).

Precipitation-cementation has been reported to have several drawbacks. For instance, in the case of precious metal recovery from chloride media, the formation of chloro-complexes in solution reduces the precipitation efficiency of the desired precious metal ions. In this manner, more reducing agent is required to achieve maximum recovery. And in addition, some metal impurities that are originally present in the sample, such as copper, iron, nickel, etc. also co-precipitates (Umeda et al. 2011). Removal of the co-precipitated metal impurities require additional procedures, such as neutralization, de-ammoniation or fusion, which render the process more tedious, labour intensive and uneconomical (Kim et al. 2010, Macaskie et al. 2007, Nikoloski and Ang 2014).

II.2.1.2 Solvent extraction

Solvent extraction (SX) is a separation and purification technique (liquid-liquid) commonly applied in copper, nickel, rare earths, and other metal processing including precious metals. It is a favourable method that requires understanding of kinetics and equilibrium principles especially of metals in low concentrations and complex formations. Several extractant systems have been investigated for the solvent extraction of precious metals and some of them are available commercially. These reagents can be classified into three: (a) compound formation (alkyl sulphides, phosphine sulphides, and hydroxyoximes) with applications in Pd extraction, (b) ion-pair formation (amines, ammonium salts, tributyl phosphate) with applications in Pd, Pt, Ir and Rh extractions, and (c) solvation (ketones, ethers) with applications in Au extraction (Cui and Zhang, 2008, Demopoulos, 1986). Palladium from waste PCBs and spent alumina catalyst was successfully recovered using different extractants such as di-isoamyl sulphide (S201) (Zhang and Zhang, 2014b), thioamine and thiodiglycolamide derivatives (Paiva et al., 2017) wherein under optimum conditions (10%S201, A/O ratio 5, and 2min), around 96% Pd was recovered. SX method is highly efficient and widely used for recovering PMs due to its ability to selectively target metals from complex solutions. However, several details will have to be carefully considered, such as selection of appropriate extractants and equipment handling, to avoid solute and reagent losses (Nikoloski and Ang, 2013, Wang et al., 2017a). This method is also known to have several drawbacks such as slow kinetics, low loading, difficult stripping, and the need for solution chemistry adjustments (pH, redox, etc.) (Demopoulos, 1986).

II.2.1.3 Ion-exchange

Ion-exchange was first identified in the 1800s when resins such as clays, aerolytes, and ultramarines were introduced. However, these conventional resins have poor selectivity towards precious metals and decompose irreversibly under acidic conditions. In the recent years, a chelating resin has been developed to rectify the issue (Nikoloski and Ang, 2013). Chelating resins are known to be insoluble materials that contain ligands capable of forming coordination complexes with metal ions and were used for the selective removal or recovery of metal ions from solutions via chemical bonding allowing efficient separation process. At present, numerous types of resins are commercially available for different applications such as water treatment, hydrometallurgical separation, food industries, and others. Several studies in the recovery of Pt and Pd from leach solutions of spent automotive catalysts were presented using various anion exchange resins such as Amberlite IRA-400AR, Amberlite IRA 420, Dowex 1, Ambejet 4200 Cl (Marinho et al., 2011a). 2011), and Diaion WA21J (Shen et al., 2011a). Results showed that the presence of base metal ions such as aluminium, nickel, and others hinders the uptake of Pd and Pt metal ions onto the resin beads. Pre-removal of base metal ions could help selectivity towards PMs ions but then makes the entire process tedious and could lead to additional costs and maintenance. In cases where the solution environment is acidic, it could lead to the decrease of the resin's ion exchange capacity and may affect re-usability. Therefore, the composition and nature of the samples, leaching agents, as well as the resin properties are carefully determined as these generally influence metal ion recovery (Marinho et al., 2011a).

II.2.1.4 Solid phase extraction

Solid phase extraction is a separation method that has found wide applications in several industries including hydrometallurgical processing, water treatment, biotechnology, and analytical systems. This method is carried out by allowing the desired analyte from the solution to adhere or bond, either by ion exchange mechanism or chelating mechanism, at the surface of a solid material known as adsorbents. These adsorbents are usually in the form of spherical pellets, rods, or monoliths which can be categorised as organic, inorganic or organic-inorganic adsorbents. In general, adsorbents should possess the following: large surface area, high adsorption capacity and selectivity, ease of preparation and regeneration, and cost effectiveness

(Zhang et al., 2016). Adsorption capacity can be enhanced selectivity towards target analytes by modifying the adsorbent surface. Surface modification or functionalization is a good way to improve adsorption capacity. This is done by introducing a functional group either a metal (or called bi metallic) or an organic functional group (Nikoloski and Ang, 2013). A review of various studies on different types of adsorbents and their application in the recovery of precious metals from aqueous solutions available in the literature are summarised in the following sub-sections:

A. Activated carbon, graphite/graphene

Adsorbent materials such as activated carbon and biosorbents, have been reported to successfully recover precious metals from the secondary sources. Activated carbon is widely applied in the recovery of gold and silver cyanide complexes in cyanide leaching of gold ores but still has limited applications in secondary gold processing. Amongst the noted advantages of using these adsorbents include high porosity, high exposed surface area, and low cost. Activated carbon as adsorbents is cost-effective as their raw materials are mainly derived from waste which makes it advantageous in the current issues on environmental issues and sustainable use of resources (Chand et al., 2009). The recovery of gold, copper, and nickel from spent mobile batteries by thiourea leaching followed by adsorption using activated carbon (AC) and biosorbents chitin (CTN) and chitosan (CTS) as adsorbents were investigated by Zazycki et al. (2017). Over 80% metal recoveries were obtained at optimum conditions and the adsorption was characterised by fast kinetics reaching equilibrium within 120 min. The maximum adsorption capacities of Au onto AC, CTN and CTS were 5.62 mg/g, 1.89 mg/g, and 3.11 mg/g respectively. AC showed higher affinity towards Cu with maximum adsorption capacity of 88.93 mg/g compared to CTN and CTS with only 56.52 mg/g and 47.00 mg/g respectively. Lastly, the maximum adsorption capacity of Ni towards AC, CTN, and CTS were found to be 57.62 mg/g, 23.60 mg/g, and 42.51 mg/g respectively.

The experiments of Chand et al. (2009) showed that barley straw carbon has a higher specific surface area compared to rice husk carbon (319 m^2/g vs 792m^2/g) as raw material in the preparation of activated carbon adsorbent, thus, a higher adsorption capacity for Au (III), Pd(II) and Pt(IV). Wu also used the recovered supercapacitor activated carbon (RSAC) in the adsorption f Ag(I) from aqueous solution with maximum adsorption capacity of 104.0 mg/g. The excellent adsorbent performance of

RSAC was due to various oxygen-containing ligands which can participate in the electrostatic attraction and reduction process (Wu et al., 2020). Graphene oxide was also used in the recovery of Au(III), Pd(II) and Pt(IV) from aqueous solution. Graphene oxide consists of carbon stacked together in a honeycomb structure which contains oxygen-linked functional groups makes it excellent in metal binding by electrostatic and coordination (Yang et al., 2010, Machida et al., 2006). Maximum adsorption capacities of Au(III), Pd(II) and Pt(IV) using GO adsorbent were 108.342mg/g, 80.775mg/g, and 71.378mg/g respectively.

B. Biosorbents

Biomass and biosorbents are materials derived or prepared from naturally abundant plants, waste biomass of algae, fungi and bacteria (Cui and Zhang 2008). Several studies have reported the utility of biomass and biosorbents in the recovery of precious metals from aqueous solutions and amongst the materials used was a low-cost adsorbent prepared by cross linking persimmon extract with sulphuric acid (CPT) in the recovery of Au (III). The maximum adsorption capacity of Au(III) towards CPT was higher than crude PT (1.52 mg/g vs 1.14 mg/g) . (Gurung et al., 2011, Gurung et al., 2012) They also developed a tetraethylenepentamine modified persimmon tannin prepared by sodium bicarbonate and TEPA stirred continuously for 24h and was able to produce a uniform gel particle (TEPA-PT). TEPA-PT was then investigated in the recovery of Au(III), Pd(II), and Pt(IV) where adsorption was attributed with electrostatic interaction. Gold(III) was found to further reduce to elemental Au^0. The maximum adsorbent capacity of Au(III), Pd(II), and Pt (IV) were 1168 mg/g, 187 mg/g, and 288.72 respectively. Adsorption of platinum from chloride solutions was investigated using carbonised pistachio nutshells (CPNS), an agricultural waste biomass. To activate the PNS, it underwent thermal carbonisation at 1000°C under argon atmosphere (Morcali et al., 2013). Platinum reached the maximum adsorption capacity of 38.31 mg/g which is two-fold (%) higher than the non-carbonised PNS.

Gold recoveries were compared using 16 different types of fallen leaves as biosorbent from the studies of Aktas et al. (2011) where 7 species demonstrated above 95% Au recovery. Egg-shell membrane and other proteins, bacteria, fungi, alfalfa, kraft mill lignin, among others were investigated (Cui and Zhang, 2008). The adsorption of precious metals on biosorbents and biomass is a very complex process characterised by physical or chemical adsorption onto cell walls, cell-associated materials, or cell

metabolism (Cui and Zhang 2008). They also noted that the mechanism also include complexation, chelation, microprecipitation and microbial reduction. Another perceived limitation for the use of biosorbents and biomass for precious metals recovery is the stability of the materials at highly acidic solutions. The components and structure of biosorbents may degrade or decompose in acidic pH decreasing their ability to uptake precious metals from solution.

C. Metal sulphides

Several authors used molybdenum disulphide (MoS_2), a novel material that recently attracted interest in the energy storage/conversion, microelectronic, and photocatalyst fields. The weak bonds between the S-Mo-S nanosheet layers readily forms two-dimensional (2D) morphology resulting to larger surface area providing greater ion adsorption and transport (Tong et al., 2018). Authors Feng et al. (2018) presented high selectivity of molybdenum disulphide adsorbent towards Au with the presence of other metal ions such as Cr(III), Co(II), Mn(II), Ni(II), Cu(II0, Zn(II), Cd(II), Ca(II), Mg(II) and Fe(II) ions. The adsorption mechanism was found to be attributed to strong affinity between Au and S atoms. The maximum adsorption capacity of Au was 1113 mg/g at pH=0.85. However, black MoS_2 may cause water contamination. Therefore, Zhao et al. (2020) successfully synthesized chitosan imbedded-MoS_2 (CS-MoS_2 -1, 2, 3) with different ratios resulting in a more sulphur-rich MoS_2 surface subsequently increased Au adsorption. The maximum adsorption capacity of CS-MoS_2 -1, 2, 3 for Au(III) were found to be 2012.46 mg/g, 2611.32 mg/g and 3108.79 mg/g respectively at pH=5.

Copper sulphide nanoparticles (CuNPs), a semiconductor transition metals extensively investigated for cancer photothermal therapy, are considered a promising candidate for metal ion recovery due to their natural sulphur-rich properties, non-toxicity, soil abundance and low-cost. Yao et al. (2019) used a solvothermal method in fabricating CuS nanoparticles and efficiently recovered Au(III), Pd(II), and Pt(IV) from solution. The order of adsorption was Au(III)>Pd(II)>Pt(IV) with maximum adsorption capacities of 574.7 mg/g, 222.2 mg/g, and 142.9 mg/g respectively.

D. Metal-organic framework adsorbents

Metal-organic functionalized (MOF) adsorbents are 1-,2-, or 3-dimensional inorganic-organic complexes that are highly porous comprising metal ions and organic

linkers. This structure has many advantages which includes controllable morphology, high achievable surface areas, high porosity with tunable pore structures, easy functionalization and more exposed chelating sites, which enables them to be extensively used in drug delivery, catalysis, metal ion sensing, among others (Xu et al., 2021, Lin et al., 2019). Most of MOFs are unstable in water, which limits their application for adsorption in aqueous solutions. The Zr_6 MOFs have by far shown popularity due to their superior stability. UiO-66 ($Zr_6(OH)_4O_4(BDC)_6$, BDC=benzene-1,4-dicarboxylate) was the first Zr_6 MOF reported and widely used (Shearer et al., 2016). UiO-66 was found to have good thermal and chemical stability up to ~540°C. UiO-66 was utilized by Lin's group in the recovery of precious metals via adsorption and showed maximum adsorption capacities of 120mg/g, 166 mg/g, and 280mg/g for Pd(II), Pt(IV) and Au(III) respectively. The authors also compared the adsorption performances of MOF-808, UiO-66, and MOF-802 towards Pd(II). Of all the MOFs, MOF-808 exhibited the highest Pd(II) adsorption capacity (163.9 mg/g) and performed extremely rapid adsorption kinetics, while MOF-802 exhibited high adsorption affinity for Pd(II) (Lin et al., 2017, Lin et al., 2019). Furthermore, the same authors introduced an amino acid group into UiO-66 (UiO-66-NH_2) and showed significantly better adsorption capacities for Pd(II), Pt(IV) and Au(III) with maximum adsorption capacity of 167mg/g, 193 mg/g and 495mg/g respectively at pH=1 (Lin et al., 2019). Thiol-containing groups was found to have high affinity for Au(III) (Fotoohi and Mercier, 2015). Therefore, a thiourea modified UiO-66 (UiO-66-TU) was adopted to recover Au(III) from solution. UiO-66-TU was found adsorbed Au(III) at maximum adsorption capacity of 326mg/g. Moreover, UiO-66-TU was found to be highly selective to Au from complex solution systems (Wu et al., 2017).

ZIF-8 is another MOF typically a zeolitic imidazole framework material with excellent thermal and chemical stability boiling water conditions, aqueous basic environment (NaOH), and in high pressure settings (Li et al., 2014). ZIF-8 was used in as adsorbent in the recovery of Au(III) from aqueous solution and achieved a good maximum adsorption capacity of 1192 mg/g at pH 2.5 (Hu et al., 2018). Subsequently, the authors Zhou et al. (2020) utilized ZIF-8 modified by ethanediamine (ZIF-8-NH_2) to recover Au(III) and A(I) and obtained a maximum adsorption capacities of 357 mg/g, and 222.25 mg/g respectively. The adsorption of Au(III) was found to be unaffected with co-existing ions such as Ni(II), Cd(II), and Zn(II) while the adsorption of Au(I) was affected by Ni(II). Wang et al. (2018) presented excellent adsorption efficiency of

thiourea modified ZIF-8 (ZIF-8-TU) towards Au(III) from solutions with maximum adsorption capacity of 4262.8 mg/g even with the decrease of surface area and pore volume.

E. Resin

Resins have been widely used for metal ion removal because they offer a highly effective and versatile method of purifying and separating ions from solutions and their ease of regeneration . Most types of resin have organic matrices with chemically bound functional groups that can create a chelating phenomenon towards the desired metal ions. Resin can withstand a wide range of pH levels makes them chemically stable making them suitable for various industrial and environmental applications (Amphlett et al., 2018). Lewatit TP 214 is a type of chelating polystyrene-containing thiourea groups resin that exhibits higher affinity for platinum where maximum adsorption capacity of 33.22mg/g (Morcali et al., 2013). The authors Xiong et. al (2014) synthesized polystyrene-2-aminothiazole (PS-AT), another type of chelating resin prepared by attaching 2-aminothiazole into chloromethylated polystyrene polymers. PS-AT results showed high selectivity towards Au because of the presence of nitrogen and sulphur on the surface of the adsorbent. The maximum adsorption capacity of Au(III) onto the PS-AT adsorbent was found to be 733.8 mg/g. Urea-modified phenolic resin (RFU) was synthesized by the Xiang et al. (2020) via hydrothermal method was also utilised in the recovery of Au (III) from acidic complex chloride solutions that also contains Cu(II), Fe(III), Ni(II), Co(II), and K(I). It was found out that RFU was highly selective to Au(III) mainly because Au may exist as negatively charged ions in acidic medium and highly attracted to the positive surface of RFU adsorbent. The maximum adsorption capacity of Au(III) can reach 1600 mg/g at pH=1.

F. Silica

Silica, in its various forms, is a versatile and effective adsorbent to recovery precious metals from solutions owing to its characteristics such as large surface area, porosity, chemical stability, ease of modification, low-cost, among others (Zhao et al., 2019a). Silica's large surface area and well-defined pore structure allows provides ample sites for adsorption as well as capture and retention of metal ions.

A macrocyclic polyether-modified nanosilica adsorbent was synthesized by the authors Bai et al. (2013) used in the recovery of Pd ions from solutions. The

incorporation of the macrocyclic polyether into the silica matrix formed ligands where the complexation between the Pd ions and adsorbent occurred. Adsorption capacity of Pd(II) was 83.3 mg/g. Two silica-based adsorbents were prepared via microemulsion polymerization by Saman et al. (2020), and these were silica nanocapsules (SiNC-FREE) and Cetyltrimethylammonium bromide (SiNC-CTAB). CTAB provides positively charge active sites allowing effective adsorption of anionic Pd complexes in the solution. The adsorption capacity of Pd(II) using SiNC-TAB was 124.5 mg/g higher compared to SiNC-FREE which was only 51.28 mg/g. Table 2 is the summary of adsorbents used for precious metals recovery.

Table 2. List of different adsorbents used for the recovery of precious metals from solutions.

Adsorbent		Metal Ions	Maximum metal uptake ($mg\ g^{-}$)	Ref
Activated carbon, graphite/graphene, biomass	AC	Au	5.62	Zazycki et al. (2017)
		Cu	88.93	
		Ni	57.62	
	CTN	Au	1.89	Zazycki et al. (2017)
		Cu	56.52	
		Ni	23.6	
	CTS	Au	3.11	Zazycki et al. (2017)
		Cu	47	
		Ni	42.51	
	RSAC	Ag (I)	104	Wu et al. (2020)
	GO	Au (III)	108.342	Yang et al. (2010)
		Pd(II)	80.775	
		Pt(IV)	71.378	
Biosorbents	CPT	Au(III)	1.52	Gurung et al. (2011)
	PT	Au(III)	1.14	Gurung et al. (2011)
	TEPA-PT	Au(III)	1168	Gurung et al. (2011)
		Pd(II)	187	
		Pt(IV)	288.72	
	CPNS	Pt	38.31	Morcali et al. (2013)
Metal Sulphides	MoS_2	Au	1113	Feng et al. (2018)
	CS-MoS2-1	Au(III)	2012.46	Zhao et al. (2020)
	CS-MoS2-2	Au(III)	2611.32	Zhao et al. (2020)
	CS-MoS2-3	Au(III)	3108.79	Zhao et al. (2020)
	CuNPs	Au(III)	574.7	Yao et al. (2019)
		Pd(II)	222.2	Yao et al. (2019)
		Pt(IV)	142.9	Yao et al. (2019)
Metal organic framework (MOF)	UiO-66 ($Zr_6(OH)_4O_4(BDC)_6$	Pd(II)	120	Lin et al. (2017)
		Pt(IV)	166	Lin et al. (2017)
		Au(III)	280	Lin et al. (2017)
	MOF-808	Pd(II)	163.9	Lin et al. (2019)
	UiO-66-NH_2	Pd(II)	167	Lin et al. (2019)
		Pt(IV)	193	Lin et al. (2019)
		Au(III)	495	Lin et al. (2019)
	UiO-66-TU	Au(III)	326	Wu et al. (2020)
	ZIF-8	Au(III)	1192	Li et al. (2014)
	ZIF-8-NH_2	Au(III)	357	Zhou et al. (2020)
		Au(I)	222.5	Zhou et al. (2020)
	ZIF-8-TU	Au(III)	4262.8	Wang et al. (2018)
Resin	Lewatit Tp-214	Pt	33.22	Morcali et al. (2013)
	PS-AT	Au(III)	733.8	Xiong et. al. 2014
	RFU	Au(III)	1600	Xiang et al. (2020)
Silica	Polyether-modified silica	Pd(II)	83.3	Bai et al. (2013)
	SiNC-CTAB	Pd(II)	124.5	Saman et al. (2020)
	SiNC-FREE	Pd(II)	52.28	Saman et al. (2020)

II.2.1.5 Magnetic solid phase extraction

The utilization of magnetic particles as adsorbents in solid phase extraction is considered one of the emerging technologies that in the separation and purification of precious metal ions from hydrometallurgical processes. The typical schematic diagram of MSPE process is shown in (Figure 1). The magnetic particles are generally added into the solution and are then stirred continuously to aide contact between the adsorbate and adsorbent for specific period. The magnetic particles are separated by an external magnetic field and immediately eluted in the solution where it losses its magnetic properties and washed with appropriate solvent. Desorption process will follow the addition of concentrated eluent in the suspension. Magnetic solid phase extraction is a highly significant technique in the field of analytical purposes in mineral processing, extractive metallurgy, waste water treatment, among others, particularly for the extraction and pre concentration of metal ions to separate and concentrate species from solution (Aghaei et al., 2017b, Herrero-Latorre et al., 2015b). The key element in the selectivity and sensitivity in magnetic solid phase extraction (MSPE) is the selection of suitable magnetic particle as adsorbents. The magnetic sorbent is added to the sample solution and the target analyte is adsorbed onto the surface of the magnetic sorbent particles (Giakisikli and Anthemidis, 2013; Herrero-Latorre et al., 2015). The use of magnetic materials in solid phase extraction has received considerable attention in recent years due to the many advantages arising from the inherent characteristics of magnetic particles such as high selectivity to target analytes, faster reaction kinetics, and its superparamagnetic property which can be activated by an external magnetic field or other different sources leaving no residual magnetism when magnetic field is removed (Uheida et al., 2006b).

MSPE can selectively target and extract specific metal ions from complex matrices. Magnetic particles are materials that exhibit magnetic properties made from various magnetic materials such as iron, nickel, and cobalt and their alloys or oxides. Because magnetic particles are prone to oxidation, surface modification is sometimes required to achieve high selectivity and maximum adsorption capacity. This is often achieved by functionalizing the magnetic particles with specific ligands or functional groups that have a high affinity for the target metal ions as shown in Figure 2 allowing the MSPE methods tailored to a wide range of metal ions and sample types. The versatility of this method makes MSPE applicable in diverse fields such as environmental monitoring, food safety, clinical analysis, and industrial process control. For example, nano

magnetic particles are easily utilized in the treatment of contaminant soils and wastewater streams due their particle size (1-100nm) either by direct injection into water-slurry streams or by attachment onto solid matrix to enhance treatment. Metallic iron nanoparticle is known to be best environmental remediation. A palladized iron (Pd/Fe) particles was prepared by soaking nano-Fe particles in ethanol solution containing 1wt% palladium acetate ($[Pd(C_2H_3O_2]_3$) has been used in the remediation of chlorinated contaminants such as trichloro-ethane (TCS), trichloro-ethene (TCE) found in soil and ground water (Zhang, 2003). Similar methods were used in the preparation of bimetallic Fe/Ag, Fe/Ni, Fe/Co, Fe/Cu (Xu and Zhang, 2000).

Furthermore, the application of an external magnetic field, problems associated with filtration or phase separation in a conventional solid-liquid system can be easily performed (Giakisikli and Anthemidis, 2013; Herrero-Latorre et al., 2015). Generally, the adsorption process concerning the use of magnetic adsorbents include adsorption separation, magnetic recovery, adsorbent regeneration and reusability, and management of the used adsorbent and spent solution (Gómez-Pastora et al., 2014). Magnetic particles can often be regenerated and reused multiple times without significant loss of performance. The reusability reduces the overall cost and waste associated with the extraction process. The magnetic particles are generally added into the solution and are then stirred continuously to aide contact between the adsorbate and adsorbent for specific period. The magnetic particles are separated by an external magnetic field and immediately eluted in the solution where it losses its magnetic properties and washed with appropriate solvent.

Desorption process will follow the addition of concentrated eluent in the suspension. Desorption is a critical step in magnetic solid phase extraction (MSPE) as it involves releasing the concentrated analytes (metal ions) from the magnetic adsorbent into a suitable solution for subsequent analysis. The choice of desorption method depends on the nature of the metal ions, the properties of the magnetic adsorbent, and the requirements of the subsequent analytical technique. Common solvents could be acidic solutions (HCl, HNO_3), basic solutions (NaOH), organic solvents (methanol, acetonitrile), or a mixture of solvents. Optimizing desorption conditions is crucial to achieve high recovery rates and ensure accurate and reliable analysis.

A. Magnetic particle adsorbent

Magnetic adsorbents can be found naturally or can be prepared in the laboratory (i.e Fe_3O_4). They normally consist of elements such as iron, nickel, cobalt or their oxides and alloys with ferromagnetic, ferrimagnetic or superparamagnetic properties. They can be available in different range of sizes (nano to micro), and different shapes (elongated, round, etc.) which can be controlled carefully during the preparation and synthesis. Methods of preparation or synthesis include chemical coprecipitation (Aphesteguy et al. 2015, Gaviría et al. 2007, Nyirő-Kósa et al. 2012, Shen et al. 2014, Willard et al. 2004), solvothermal (Jean et al. 2012) and just recently, mechanochemical method (Iwasaki et al. 2009). The produced magnetic particles require surface modification (core- shell structure) in order to prevent oxidation, corrosion, and prevents agglomeration. Surface modification also enhances the adsorption capability of the magnetic particle, and increasing the surface contact area thereby increasing the extraction capacity (Ferreira et al. 2010, Lopes et al. 2016, Shen et al. 2014, Singh et al. 2016). The simplicity in preparation and reproducibility of the magnetic particles, their size manipulation, as well as easiness in surface modification, enable them to have a wide range of potential applications in biological, environmental, electronics, and more recently, metal recovery. Among the magnetic particles, the oxides of iron such as magnetite (Fe_3O_4) and maghemite (γFe_2O_3) has gained favourable attention due its small size, high surface area, less sensitivity to oxidation, and superparamagnetic ability thus providing better kinetics and greater extraction capacity towards the desired analytes. Magnetic particle adsorbents reported in the literature which have applications in the extraction of precious metals from aqueous solutions include natural and synthetic magnetite (Alorro et al. 2010), modified or functionalised magnetite (Ferreira et al. 2010, Giakisikli and Anthemidis 2013, Mamani et al. 2013), magnetic carbon nanotubes (Yu et al. 2014), and cobalt ferrite (Kraus et al. 2009).

Activated carbon has been traditionally employed as adsorbent due to its high specific area properties, However, there are many problems encountered such as co-adsorption of other competing base metals such as nickel and copper, small particle size, high regeneration temperature, etc. (Navarro et al., 2007). Therefore, graphitic carbon nanostructures (GCNs) were considered as a promising adsorbent due to its excellent heat resistance, firm, and has high adsorption sites. However, the separation of GCNs from solution would require methods such as centrifugation and/or filtration

which makes the entire process more tedious and complex. A magnetic GCNs synthesized by the authors Wang et al. (2012) which finally resolves the separation process. Since the adsorbent is magnetic, adsorbents can easily separate from the solution using magnets. The synthesized magnetic GCNs was used in the recovery of Ag(I) and Ag(II) with maximum adsorption capacities of 7.88mg/g and 7.92mg/g respectively. A graphene oxide (GO) embedded in polyuerathane foam (GO-PUF) adsorbent also has high adsorption performance for Au, Pd, and Pt. However, it also encounters the similar adsorbent-solution problem with GCNs. Thus, Yoo et al. (2020) fabricated magnetite nanoparticle-graphene oxide (Fe_3O_4-GO) hybrids in aqueous solution with preparation assistance of ultrasonic waves. The introduction of magnetic particle enables the hybrid Fe_3O_4-GO to be easily separated from wastewater. The hybrid recovered Au(III) with maximum capacity of 144.15 mg/g at pH=6.

Chitosan is a deacetylated product of chitin is known to be the most abundant green polymer on earth after cellulose (Zhao et al., 2021). Under acidic conditions, chitosan (as cationic polysaccharide) can be an excellent candidate for metal ions adsorbent from chloride complexes via electrostatic adsorption. A novel magnetic chitosan adsorbent (CDF-CS) prepared by inserting the magnetic particles into a cross-linked compound of chitosan and cystamine was used to adsorbed Au(III) from aqueous solutions. The maximum adsorption capacity of Au(III) onto CDF-CS was 478.47 mg/g which is higher than using raw chitosan as adsorbent (Zhao et al., 2019b). Furthermore, under complex solution systems containing Au(III), Cr(III), Co(III), Mn(II), Sb(III), Cd(II), Mg(II), and As(III), CDF-CS was found to have high affinity for gold, adsorbing almost no other ions except gold.

Magnetite (Fe_3O_4) is an oxide of iron that has been known for so many years. The importance of magnetite is not only for its use as a source of iron but also for its magnetic properties. The ferrimagnetic property of magnetite is formed from the reduction of ferric iron (Fe^{3+}) oxides and the oxidation of iron metal (Fe^0) and ferrous iron (Fe^{2+}). Therefore, the presence of at least 1 unpaired electron in its oxidation states is what makes it strongly attracted to magnets (Parkinson, 2016, Santoyo Salazar et al., 2011). Magnetite is ubiquitous in nature or can be prepared in the laboratory. The studies of Uheida et al. (2006b) and Homchuen et al. (2016) presented the adsorption of PGMs such as Pt, Pd, and Rh from chloride solution using magnetite. Uheida et al. (2006b) used a synthesised 10-nm magnetite particles by dissolving iron salts in NH_3

solution and the precipitated nanoparticles are dispersed in a 0.01M tetramethylammonium hydroxide (TMAOH) aqueous solution, while Homchuen et al. (2016) utilised a commercial grade magnetite characterised by a P_{80} of 6.7 µm in size. Homchuen et al. (2016) initially conducted a precipitation study on PGMs in chloride solution at different pH range and results confirmed that Pt did not precipitate in any pH range while Pd and Rh started to precipitate at pH beyond 6.5 and 4 respectively. Their investigations were then based on this pH where PMs are stable, and results showed a maximum uptake for Pt and Pd at pH 6-7 for 24 hours of 3.0 µmol/g and 2.8 µmol/g respectively while Rh was in equilibrium at pH 3 with a uptake of 4.2 µmol/g. On the other hand, Uheida et al. (2006b) investigated the PGMs adsorption at pH < 3 where the hydroxyl complexes of Pt are not predominant, and the hydrolysis of Pd and Rh have not begun where they achieved maximum uptake for Pd, Rh, and Pt was achieved at pH 3 for 1 hour with 0.103, 0.149, and 0.068 mmol/g respectively. Increasing the chloride concentration slightly increases the uptake for Rh and Pt onto the commercial grade magnetite but decreases on Pd. Meanwhile, PGMs (Pt, Pd, and Rh) uptake onto the synthesised magnetite decreases as chloride concentrations are increased. The decrease in uptake suggests that the presence of Cl^- in the solution may have a backward reaction effect and supress uptake for the PGMs. The adsorbed Pt, Pd, and Rh are subsequently eluted using 0.5 M NHO_3 as eluent with recoveries of 94%, 96%, and 80% respectively.

Alorro et al. (2010) reported that it was possible to recover Au from chloride solutions using synthetic and natural magnetite with recoveries of 86% and 100% respectively at pH 6-7 for 24 hours contact time. Synthetic magnetite was also found to be selective towards Au, Pt, Pd, Cu, and Ni while natural magnetite toward Au only. The detected Au clusters on the surface of the magnetite suggests that $AuCl_4^-$ was reduced to metallic Au by the reaction:

$$AuCl_4^- + 3e^- \leftrightarrow Au^0 + 4Cl^- \quad \text{(Eq 1)}$$

Magnetic particles have been extensively used in many applications. However, pure inorganic magnetic particles are susceptible to oxidation and agglomeration which may affect its magnetic capability (Ferreira et al., 2010). For example, in the typical co-precipitation synthesis of magnetite, the iron (II) can be partially oxidised or the iron (III) can be reduced in alkali solution. Furthermore, ions such as Na^+ and Cl^- in the

solution are easily adsorbed on the surface and are difficult to remove due to its high surface energy resulting a competition on the particles active sites (Chen and Xu, 1998, Ferreira et al., 2010). Hence, surface modification (core-shell) of the magnetic particle is needed with specific active groups to avoid the above limitations. The coating of the magnetic core can be conducted using organic (SiO_2, Al_2O_3, ferrites, MnO, etc.) or inorganic coatings (MIPs, cellulose, alginate, polyacrylamide, etc.). The coating is attached to the magnetic particle as a shell to prevent oxidation, improve its chemical stability, and can be highly selective towards target analyte. In addition, inorganic coatings can be modified by addition of different functional groups (organic or inorganic) to improve its sorption characteristics. Surface modification of magnetic particles are usually prepared by three steps; synthesis of the magnetic particle, coating of the magnetic core, and functionalisation of the resultant core-shell structure according to Figure 2 (Giakisikli and Anthemidis, 2013a).

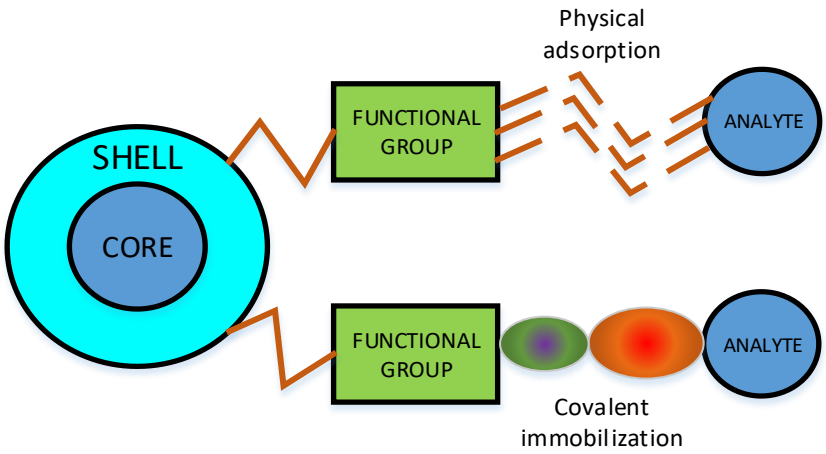

Figure 2. Core-shell structure of the magnetic particle (Giakisikli and Anthemidis, 2013a).

The authors Beata et al. (2015) presented the effects of thermal treatment of uncoated and Ag-coated magnetite nanoparticle at temperatures between 50 °C to 500 °C. A rapid colour transformation was observed on the uncoated magnetite while the Ag-coated magnetite show less pronounced colour changes. This implies that the additional metallic layer partially protects the magnetite core from oxidation. Zhang et al. (2013) developed a thiol-modified Fe_3O_4 nanoparticles and utilised as adsorbents in the recovery of gold from chloride solutions. Fe_3O_4 nanoparticles were initially prepared by co-precipitation method then was coated with SiO_2 through Na_2SiO_3 under

acidic conditions. The synthesised Fe_3O_4-SiO_2 nanoparticles were then activated in an HCl solution in a shaking water bath.

II.3 Preparation and synthesis of magnetic particles

II.3.1 Co-precipitation method

The most common method for the synthesis of iron oxide (Fe_3O_4, Fe_2O_3, etc.) and ferrite (Zn-Mn ferrite, Ni-Zn ferrite, Co-Zn ferrite) is by the addition of alkali to iron salt solutions and keeping the suspensions for ageing. This method is called co-precipitation method. Among the magnetic particles, magnetite and maghemite received high consideration owing to its small size, high surface area, and ferro/ferri-magnetic capability providing better kinetics and high extraction capacity towards analytes (Giakisikli and Anthemidis, 2013a). Magnetite is prepared by combining salts of Fe^{2+} and Fe^{3+} at a certain proportion, then magnetite are being precipitated by the addition of excess ammonia water or sodium hydroxide according to . In this method, oxygen plays an important role in the formation of single phase magnetite thus, media is passed through nitrogen bubbling to eliminate oxygen (Aphesteguy et al., 2015, Gaviría et al., 2007, Nyirő-Kósa et al., 2012, Shen et al., 2014, Xiao et al., 2016)

$$Fe^{2+} + Fe^{3+} + 8OH^- \rightarrow Fe_3O_4 + 4H_2O \qquad \text{(Eq 2)}$$

The synthesis of iron nanoscale was developed in 1996 by the authors Wang and Zhang (1997) using sodium borohydride as reducing agent where ferric iron is reduced by the borohydride according to Eq 3. Excessive borohydride was needed to accelerate the reaction synthesis ensuring uniform growth of nano crystals.

$$4Fe^{3+} + 3BH_4^- + 9H_2O \rightarrow 4Fe^0 + 3H_2BO_3^- + 12H^+ + 6H_2 \qquad \text{(Eq 3)}$$

II.3.2 Hydrothermal and thermal oxidation method

Magnetite can also be prepared using hydrothermal method. This method operates under high temperature and pressure conditions with water as a reaction medium. High temperature improves magnetism while high pressure improves the product purity (Xiao et al., 2016). The reaction of soluble and insoluble substances occurred at high temperature (above 450 °C) and pressure followed by recrystallization of the ideal

product. However, this method always gives a micro-meter sized particles and are not ideal for potential applications such as nano-based catalysts, biomedicine, nanofluids, among others. Thereby, Chen and Xu (1998) presented a low temperature hydrothermal method of synthesising magnetite from iron (II) 2-methoxyethoxides, using 2-methoxyethanol-water-mixed solvent as the medium and produces nano-sized particles. The authors also presented that variation of different reaction conditions such as solvent, temperature, and reaction time have important effects on the ideal products. Solvent-thermal method (solvothermal) is also another way of preparing magnetite. This method is similar to hydrothermal method except that the solvent used is non-aqueous solution. Jean et al. (2012a) prepared magnetite particles using ethylene glycol as solvent and reducing agent. The procedure involves dissolution of $FeCl_3.6H_2O$ in ethylene glycol, then CH_3CO_2Na is added into the mixture with constant agitation for 30 minutes. The mixture was then transferred into a reactor at 200 °C and maintained for 21 h. After cooling, dark precipitates (Fe_3O_4) were then recovered and washed with deionised water and dried.

Maghemite on the other hand, is a product of low temperature oxidation (200 °C to 450 °C) of magnetite. Magnetite is known to oxidise further to form hematite ($\propto Fe_2O_3$), an antiferromagnetic, and a polymorph of hematite known as maghemite (γFe_2O_3 or $\gamma[Fe_2^{3+}]O_3$) and is ferromagnetic Eq 4. Magnetite is transformed to maghemite via topotactic transformation where the electroneutrality, crystalline structure, shape, and the size of the particle is preserved as shown in Figure 3 (Martínez-Mera et al., 2017b, Sidhu et al., 1977).

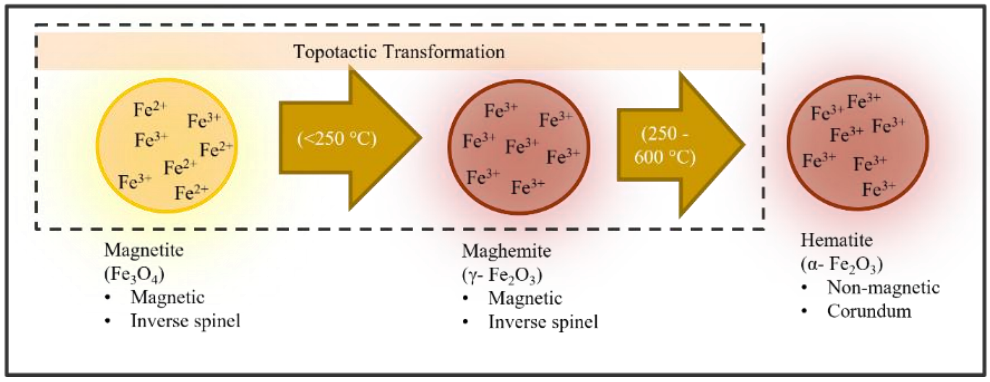

Figure 3. Topotactic transformation of magnetite to maghemite (Martínez-Mera et al., 2017b, Sidhu et al., 1977).

$$3[Fe^{2+}Fe_2^{3+}]O_{4\,(\text{magnetite})} \rightarrow 4[Fe_2^{3+}]O_{3\,(\text{maghemite})} + Fe^{2+} + 2e^- \qquad \text{(Eq 4)}$$

Increasing the temperature further transforms maghemite to hematite and loses its magnetic property. Therefore Hyeon et al. (2002) synthesised a highly crystalline and monodisperse maghemite by thermal decomposition of iron pentacarbonyl in the presence of oleic acid. This method gives several advantages in the preparation of maghemite particles which includes ease of particle size tuning by changing the experimental parameters, can be dispersed further in many hydrocarbons without particle aggregation, and a yield of 80%.

II.3.3 Pyrolysis method

Pyrolysis is a process that involves thermal decomposition of organic materials at elevated temperatures in an inert atmosphere (or vacuum) to produce solid char, liquid bio-oil, and several gases such as hydrogen, carbon monoxide, and methane. Magnetic particles can also be prepared using pyrolysis method. Metal compounds as precursors such as $Fe(acac)_3$, $Fe(CO)_5$, $Co_2(CO)_8$ and $Fe(Cup)_3$, are decomposed under high temperature and are further oxidised to magnetic metal oxide particles. Synthesis of a monodisperse magnetic cobalt nanoparticles was also presented by Sun and Murray (1999) where the growth and stability of the produced nanocrystals are controlled by the combination of oleic and trialkylphosphine. The obtained nanocrystals are then annealed at 300 °C into a common hexagonal-closed-packed crystals. In addition, oleic acid can also be replaced by other acids such as octanoic acid and 5-dodecenoic acid by simple ligand exchange.

II.4 Adsorption isotherms

Adsorption isotherms are graphical representations of the equilibrium relationship between the concentration of a solute in a gas or liquid phase and the concentration of the solute adsorbed onto a solid adsorbent at a constant temperature. These isotherms are important in understanding and describing the behaviours of adsorption process, which are widely encountered in various fields such as chemical engineering, environmental science, and material science. There are several types of adsorption isotherms models, each describing different adsorption behaviours. These models play an important role in understanding process adsorption mechanisms, as well as experimental conditions optimization. The commonly used model includes Langmuir

isotherm and Freundlich isotherm models which only differ in their assumptions. Langmuir model assumes a monolayer adsorption onto a surface adsorbent with no interaction between adsorbed molecules/ions at adjacent sites. The Freundlich model describes a heterogeneous surface with multilayer adsorption and assumes that the adsorption energy decreases with increasing surface coverage.

In this study, the equilibrium data for the sorption of PMs ions onto the magnetic adsorbent is fitted using Langmuir and Freundlich equations (Eq 5 and Eq 6),

$$\frac{C_e}{q_e} = \frac{1}{K_L q_m} + \frac{C_e}{q_m} \quad \text{(Eq 5)}$$

where q_e is the amount of PM adsorbed at equilibrium (mg/g), C_e is the equilibrium PM concentration in solution (mg/L), q_m is the theoretical maximum adsorption capacity of adsorbent (mg/g), and K_L is the Langmuir adsorption constant (L/mg). In addition, the parameter R is calculated to determine the favourability of the adsorption model.

$$R = \frac{1}{1+bC_0} \quad \text{(Eq 6)}$$

where b is the Langmuir constant and C_0 is the initial concentration (mg/L). The R^2 values nearest to 1 indicates favorable adsorption. The linearized form of the Freundlich equation can be expressed as:

$$\ln q_e = \ln K_F + \frac{1}{n} \ln C_e \quad \text{(Eq 7)}$$

where K_F is the Freundlich constant related to the adsorption capacity of the adsorbent, and n is the heterogeneity factor. Both K_F and n can be determined from the slope and intercept of the linear plot of $\log q_e$ vs $\log C_e$.

II.5 Desorption and re-use

The desorption and reuse of adsorbents are critical for the sustainability and cost-effectiveness of adsorption processes. By selecting appropriate desorption methods and carefully managing the regeneration process, adsorbents can be reused multiple times, reducing waste and improving the overall efficiency of the system. Advances in material science and process engineering continue to enhance the regeneration and

reuse capabilities of adsorbents, making them more robust and versatile for various industrial application. Nitric acid (HNO3), hydrochloric acid (HCl), thiourea in nitric acid (HNO3+thiourea), and thiourea in hydrochloric acid solution (HCl+thiourea) at varied concentrations were the common eluent choices (Iqbal et al., 2020).

Adsorbents can lose their capacity after a number of cycles of use due to several factors. Understanding these factors is crucial for improving the longevity and performance of adsorbents in various applications. Adsorbents can accumulate organic and inorganic contaminants that are not easily desorbed. These contaminants can block active sites or pores, reducing the available surface area for adsorption. Some adsorbents can undergo oxidation, which alters their surface properties and reduces adsorption efficiencies. In aqueous environments, hydrolysis reactions can degrade the adsorbent material, especially for organic adsorbents and some metal oxides. Physical abrasion during handling can also cause adsorbent particles to breakdown, leading to a loss of surface area and adsorption capacity. Thermal regeneration methods, if not carefully controlled, can also lead to adsorbent decomposition or their functional groups. Addressing these challenges and continuous research and development in adsorbent technology aim to enhance the durability and performance of adsorbents for suitable and cost-effective applications (Thomas and Crittenden, 1998).

Chapter III

Evaluation of Maghemite-Rich Iron Oxide Composite Prepared from Magnetite as Adsorbent for Gold from Chloride Solutions

This chapter discusses the capability of maghemite-rich adsorbent prepared by thermal oxidation of synthetic magnetite onto gold from chloride solutions. This chapter is published in the Journal of the Minerals, Metals & Materials Society JOM https://doi.org/10.1007/s11837-019-03514-8.

- CALDERON, A. R. M., ALORRO, R. D., TADESSE, B., YOO, K. & TABELIN, C. B. 2019b. Evaluation of Maghemite-Rich Iron Oxide Composite Prepared from Magnetite as Adsorbent for Gold from Chloride Solution. JOM, 71, 4639-4646.

Some part of this chapter was also presented virtually in the Metallurgical Engineering Industry Conference 2022 (MetCon 2022) Philippines, October 20-21,2022.

III.1 Introduction

Iron oxides are ubiquitous in the Earth's crust and are very good candidates for gold adsorption from aqueous solutions. For example, magnetite (Fe_3O_4) has been extensively explored due to its unique magnetic properties and has shown potential as effective adsorbent to recover gold from dilute solutions (Alorro et al., 2010, Ranjbar et al., 2014). Alorro et al. (2010), for example, showed that it was possible to recover 86% of gold using synthetic magnetite from solution with an initial Au concentration of 0.05 mol/m^3 at pH 6-7. A gallic-acid modified magnetite was also demonstrated to recover more than 95% of gold from 25 mg/L $[AuCl_4]^-$ solution at pH 3 (Rahmayanti et al., 2016). Gold is deposited on iron oxides in metallic form in chloride solutions according to the following reduction reaction as in Eq 1.

Iron oxides can be prepared in the laboratory using common chemical reagents by methods such as co-precipitation, solvothermal, and mechanochemical synthesis among others (Aphesteguy et al., 2015, Giakisikli and Anthemidis, 2013b, Jean et al., 2012b, Shen et al., 2014, Iwasaki et al., 2009). Magnetite (Fe_3O_4 or $[Fe^{2+}Fe_2^{3+}]O_4$) contains Fe^{2+} and Fe^{3+} which can be readily oxidised further to hematite ($\propto Fe_2O_3$) ,

which is non-magnetic and maghemite (γFe_2O_3 or $\gamma[Fe_2^{3+}]O_3$), a ferromagnetic polymorph of hematite from Eq 4.

It has been reported that maghemite exhibits remarkable magnetic fluid stability lasting for years in acidic or alkaline medium (Lefebure et al., 1998). Maghemite is a product of an intermediate low temperature oxidation (200 – 450℃) of magnetite (Kalska-Szostko et al., 2015). In this process, all of the Fe^{2+} in the magnetite is oxidised to Fe^{3+} via topotactic transformation reaction where the electroneutrality, crystalline structure, shape, and the size of the particle is preserved (Martínez-Mera et al., 2017a, Sidhu et al., 1977). The increase in oxidation temperature transforms maghemite to hematite and loses its magnetic properties. Thus, appropriate control of oxidation must be performed to avoid such occurrence.

Maghemite is known to be the main gold carrier in the refractory gold bearing ores (Fosu, 2016). In the roasting process of refractory gold ores, it was suggested that high concentrations of gold appear to be occluded in the impenetrable bands of maghemite within iron oxide particles (Paktunc et. al., 2006). These findings strongly suggest that maghemite attracts gold in natural geochemical processes.

It is evident from the literature and from previous studies that magnetic iron oxides, such as magnetite and maghemite, are capable of sorbing gold from aqueous solutions. Aside from their gold adsorption capabilities, these iron oxides can be easily harvested from slurries or separated from mixtures by magnetic separation due to their inherent magnetic properties. In this study, a maghemite-rich iron oxide composite derived from synthetic magnetite via thermal oxidation was used as an adsorbent to recover gold from chloride solution. The capacity and the effectiveness of the material was evaluated and the effects of various parameters, such as pH, contact time, adsorbate concentration, adsorbent dosage, and chloride concentration were investigated.

III.2 Materials and methods

III.2.1 Materials and reagents

Reagent grade sodium chloride (NaCl), sodium hydroxide (NaOH), and hydrochloric acid (HCl) from Sigma Aldrich were used in this study. Gold (III) chloride solution ($AuCl_3$ 1 g/L, Sigma Aldrich) was used as the source of gold ions for the simulated gold solutions of different concentrations. Synthetic magnetite (Fe_3O_4)

powder (>60%, Kara Magnetite Pty. Ltd) was used for the synthesis of iron oxide composite powders.

III.2.2 Preparation and characterisation of the magnetic iron oxide composite

In this chapter, synthetic magnetite powder was roasted to prepare the maghemite-rich iron oxide particles. The synthetic magnetite powder underwent thermal treatment using a furnace (Carbolite, Furnace Industries) at different temperatures at different at certain time intervals. Temperature is crucial in the transformation of magnetite into other iron oxide polymorphs. If the temperature is too high, magnetite loses its magnetic properties and will transform into hematite (Nikiforov et al., 2014b).

The samples collected were examined using X-ray powder diffraction (XRD) to determine its structure and the main phases present. A LASER sizer (Mastersizer 3000, UK) was used for particle size distribution analysis, which indicated an average particle size (d_{50}) of 23.0 µm. The specific surface area and pore size distribution were determined by Brunauer-Emett-Teller (BET) and Barrett-Joyner-Halenda (BJH) methods using N_2 as gas adsorbate (ASAP 2020, Micromeritics Instrument Co., USA). Zeta potential measurements were conducted using a Zetasizer (Malvern Nano Z, UK).

III.2.3 Adsorption and desorption experiments

Batch sorption experiments in single phase were carried out to investigate the adsorption capacity of the maghemite-rich iron oxide composite to recover gold from chloride solution. Gold concentration was derived from e-waste solution (Sun et. al., 2016). Therefore, a fixed 10 mL volume of NaCl solution (0.1–3.0 mol/L) containing 5×10^{-5} mol/L gold concentration was transferred into a 250 mL Erlenmeyer flask. Initial pH was adjusted by adding freshly prepared NaOH and HCl solutions. The iron oxide composite powders were added into the solution at different amounts (0.1–0.5 g). The flask containing the mixture was properly sealed and shaken for various time intervals in a thermostat water bath shaker (ZWY-110×30, Labwit Scientific) at a constant rate of 140 strokes/min and 25 ℃. After a given contact period between the adsorbent and adsorbate, the mixture was then membrane-filtered using 0.45 µm syringe filters. Experiments were repeated with varying pH, contact time, Au concentration, and chloride concentration. The gold content in the filtrate was analysed using inductively coupled plasma optical emission spectrometry (5100 ICP-OES, Agilent).

The gold uptake was calculated using the mass balance shown in Eq 8:

$$\text{Au uptake } \left[\frac{\mu\text{mol}}{\text{g}}\right] = (C_i - C_f) \times \frac{V}{W} \quad \text{(Eq 8)}$$

where C_I is the initial Au concentration, C_f is the residual Au concentration in the filtrate, V is the volume of the sample solution, and W is the weight of the maghemite.

Desorption experiments were conducted to determine the amount of Au that can be recovered from the prepared maghemite-rich composite using different eluant at varied concentrations. Thirty mL solutions with initial concentrations of 0.5mol/L nitric acid, 0.7mol/L thiourea, 0.5mol/L thiourea were used as eluant to dissolve the adsorbed precious metals in 0.1g adsorbent. The pH of the mixture was determined was then shaken at 4h and 24h interval in a water bath shaker and were then syringe filtered. The concentrations of platinum (Au), iron (Fe) and nickel (Ni) in the solution were analysed using Inductively Coupled Plasma – Optical Emission Spectrometry (5100 ICP-OES, Agilent).

III.2.4 Zeta potential measurements

The zeta potential of the maghemite-rich iron oxide composite was measured by dispersing the adsorbent in varied chloride concentrations (0.01 M – 1.0 M NaCl) at different pH at 25°C using a Zetasizer (Malvern NanoZ, UK) with Zeta Nano software application. Initially, 30 mL solution of a known chloride concentration was prepared then the pH was adjusted by adding NaOH or HCl solutions. About 0.03 grams (0.1 w/v %) of the iron oxide composite powders was added and was stirred manually using a glass rod. The mixture was then let to stand without stirring for about a minute. Finally, about 1 mL of the mixture was taken and placed in a capillary cuvette using a syringe and inserted into the Zetasizer. The cuvette was rinsed with deionised water several times followed by the solvent prior to the next measurement.

III.3 Results and discussion

III.3.1 Adsorbent characterization

III.3.1.1 Effect of roasting temperatures

Roasting of synthetic magnetite was initially conducted to determine maximum conversion of magnetite (Fe_3O_4) to maghemite (γFe_2O_3) in a furnace at different temperatures for 24 hours. From the XRD pattern of the roasted synthetic magnetite shown in Figure 4 (a), as the temperature increases, peak angles between 57 and 58 degrees were observed to be deflecting to the right. This peak movement suggests a transformation of magnetite to maghemite and/or hematite which coincided well in the studies of Kim., et. al.2012. Figure 4(b) shows the gradual change in colour as magnetite was transforming to maghemite by roasting.

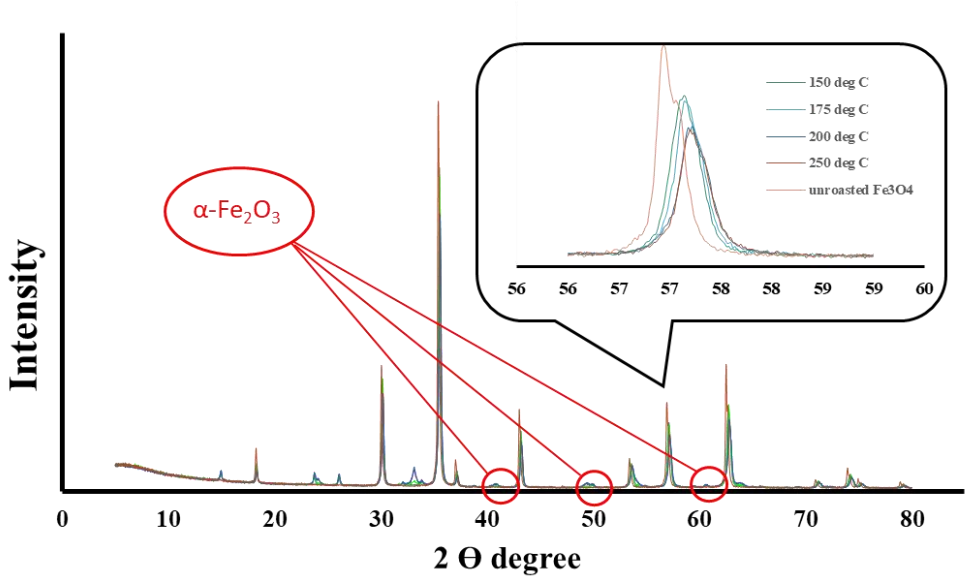

(a)

(b)

Figure 4.(a) XRD Pattern of roasted synthetic magnetite at different temperatures for 24 hours. (b) Samples of roasting products of magnetite in disc prior to XRD analysis.

The amount of converted magnetite at different temperatures were quantified using the XRD's Match!(Crystal Impact) software and are shown in Table 3. Results showed that at 150°C, oxidation of Fe^{2+} to Fe^{3+} has started achieving 8.2% conversion to maghemite. Increasing the roasting temperature of synthetic magnetite to 250°C gradually increases the maghemite conversion but about 8.10% of hematite was formed. Hence, further investigation was done by increasing the roasting temperature to 350°C for 18 hours. The samples collected was then characterised using XRD.

Table 3. XRD Quantitative analysis of roasted synthetic magnetite at different temperatures for 24 hours.

Roasting temp °C	%Fe_3O_4	% γ-Fe_2O_3	% α-Fe_2O_3
0°C (unroasted)	100.00	0.00	0.00
150°C	91.80	8.20	0.00
175°C	95.20	4.80	0.00
200°C	79.90	20.10	0.00
250°C	76.80	15.10	8.10

The XRD pattern of the synthesised maghemite-rich iron oxide composite sample is shown in

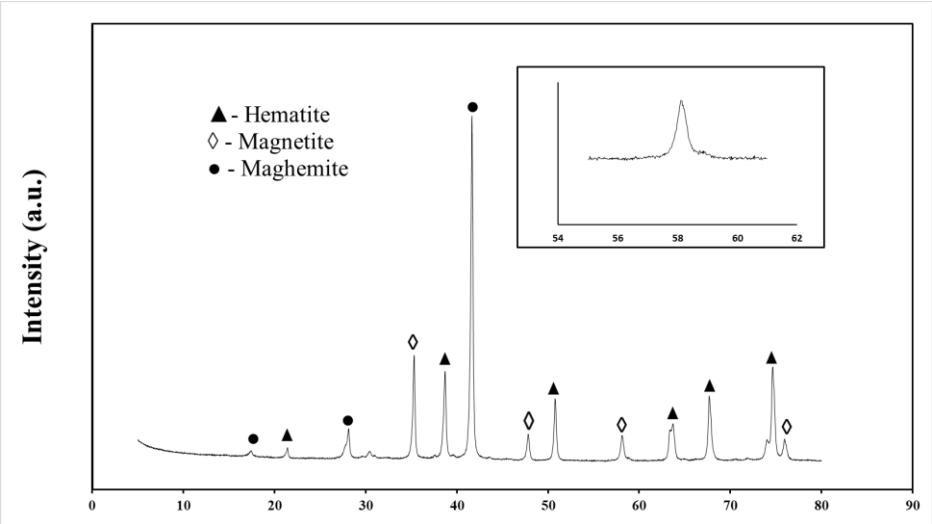

Figure 5. The well peaks clearly indicate a crystalline sample. The synthesised product is composed of magnetite, hematite, and maghemite. The slight deflection to the left of the maghemite peak at angles between 57º and 58º confirms the presence of magnetite in the mixture (Kim et al., 2012). Quantitative XRD analysis show that the thermal treatment of synthetic magnetite resulted in the formation of 44% maghemite with 33% and 23% of hematite and magnetite, respectively. This suggests that at a temperature of 350°C, synthetic magnetite was not completely oxidised into maghemite, while further oxidation to hematite had already begun. When tested using a hand-held permanent magnet, the composite material exhibited ferromagnetic properties confirming the presence of the magnetic forms of iron oxide, magnetite and maghemite, as the major components. Several factors such as particle size, water content and stoichiometry of magnetite prior to oxidation could affect the transformation of magnetite into maghemite (Nikiforov et al., 2014a) but these were not considered in this study. The maghemite-rich particles obtained was used as magentic adsorbent in the succeeding investigations.

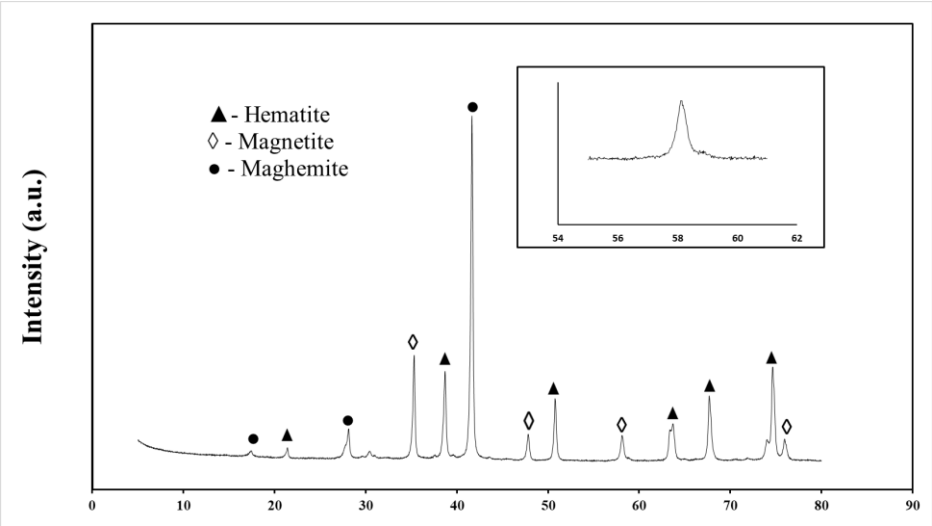

Figure 5. XRD pattern of the maghemite-rich iron oxide composite obtained by roasting synthetic magnetite at 350 °C.

III.3.1. Specific surface area analysis

The specific surface area and the porosity of the prepared maghemite-rich iron oxide samples were determined by two methods: Brunauer-Emmett-Teller (BET) and Barrett-Joyner-Halenda (BJH) analysis using N_2 as the gaseous adsorbate. Adsorption isotherms were obtained by measuring the amount of gas adsorbed across a wide range of relative pressures at a constant temperature (-196.15 °C). Conversely, the desorption isotherms were achieved by measuring the gas removed as the pressure was decreased. The isotherm linear plot of the quantity of gas adsorbed against the absolute pressure for the composite iron oxide sample as shown in Figure 6 indicated a Type II N_2 Adsorption-Desorption Isotherm wherein the flat region in the middle corresponds to a monolayer formation associated with mesopores. The BET and BJH results as showed a specific surface area of 6.2686 m^2/g with an average pore width of 12.5 nm. Mesoporous materials have pore size in the range of 2 to 50 nm.

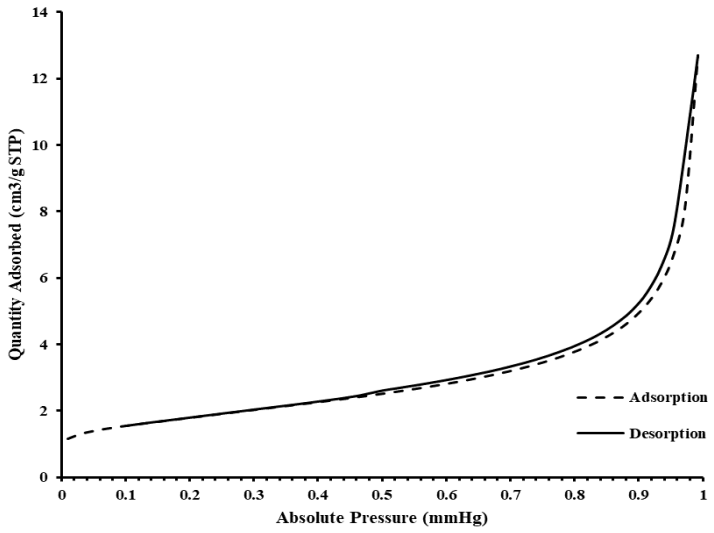

Figure 6. BET-BJH of the prepared maghemite composite adsorbent.

III.3.2. Adsorption performance of maghemite-rich iron oxide composite for Au recovery

To evaluate the capacity of the prepared iron oxide composite to adsorb gold ions in chloride solutions, the effects of solution pH, time, Au concentration, chloride concentration, and adsorbent dosage were investigated. The results are presented in the succeeding sections.

III.3.2.1 Effect of solution pH

Adsorption experiments with varying pH were conducted using an initial Au concentration of 5×10^{-5} mol/L in a 0.1 mol/L NaCl solution, a fixed amount of 0.1 g maghemite-rich iron oxide and 24 hr contact time. Gold does not precipitate in chloride solution at any pH conditions (Alorro et al., 2010), hence, the difference in the initial and the residual Au concentration was considered as the total amount of Au adsorbed (Eq 7). Figure 7(a) shows the influence of pH on Au uptake. In acidic pH region (pH 0–3), only about 15% of Au was recovered. The Au uptake percentage increased with pH reaching a maximum value at a near-neutral pH of about 6.5. At this pH almost complete Au recovery (99.78%) was achieved. Iron dissolution was also observed at the acidic pH region as shown in Figure 7(b). This result is in agreement with the study using synthetic magnetite reported by Alorro et al. (2010), wherein optimum recovery pH was also at 6–7. However, gold uptake and recovery with the prepared iron oxide

composite in the present study were higher compared to that of synthetic magnetite (86% Au recovery) as reported in the previous study (Alorro et al., 2010). Increasing the pH beyond 6.5 resulted in the decrease in Au adsorption.

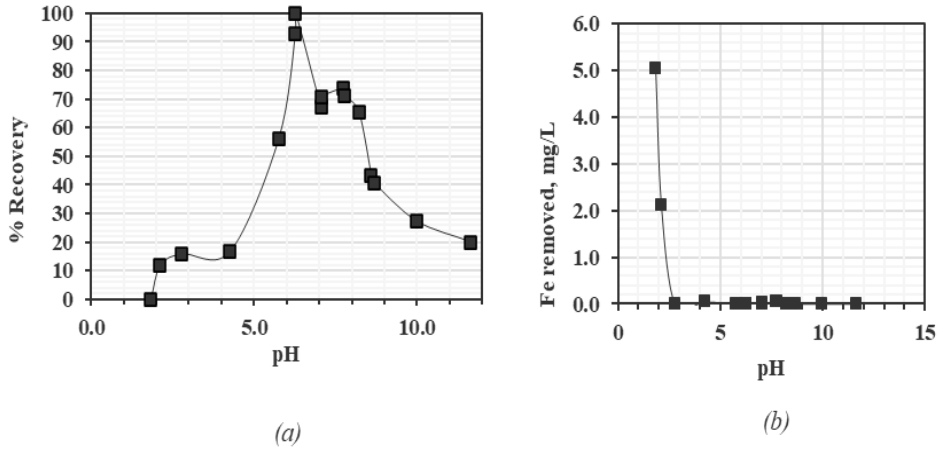

Figure 7. (a) Effect of solution pH on Au uptake onto maghemite-rich iron oxide composite. Average initial Au concentration is 9.0 mg/L; 24 hr contact time; NaCl concentration of 0.1 M; adsorbent dosage is 0.1 g at 25 °C, (b) Effect of pH on Fe dissolution from the iron oxide composite.

III.3.2.2 Zeta potential and chemical speciation

To understand the adsorption mechanism of gold chloride complexes, the zeta potential of the adsorbent particles dispersed in sodium chloride (NaCl) solutions at different pH range was investigated. The stability of the suspension is determined by the magnitude of the surface charge of the particle (zeta potential) and the range of the electrostatic interactions between the particles in the solution (Večeř and Pospíšil, 2012, Lucas et al., 2007). The surface charge of iron oxide composite particle can be positive, neutral or negative depending on the solution pH. High surface charge leads to strong electrostatic repulsion between similar particles and stabilizes the colloidal suspension. As shown in Figure 8, at 4.0<pH<8.0, the maghemite-rich iron oxide composite sample showed a low surface charge density, which suggests that the colloidal particles may be unstable and may consequently flocculate (Lucas et al., 2007). The point of zero charge (PZC) for the adsorbent particles dispersed in 0.01 M, 0.10 M and 1.0 M chloride concentrations was found to occur at about pH 6.25. Below the PZC, increasing NaCl

concentration leads to more negative zeta potential (due to the effects of Cl^- ions), while above the PZC increasing the NaCl leads to less negative zeta potential due to the effects of Na^+ ions.

The PZC coincided well with solution pH of the highest Au uptake shown in Figure 7Figure 7(a). This interesting phenomenon could be explained by electrostatic interactions between the surface of adsorbent and the predominant dissolved Au species in solution. The Eh-pH predominance diagram shown in Figure 9 suggests that between pH 5 and 8, dissolved Au is mainly present as the uncharged $AuOH(H_2O)^0$ oxyanion, which could explain the higher Au uptake as the surface charge of adsorbent approaches zero. Uncharged ions are more easily adsorbed on the surface of a material when its surface charge is close to zero because electrostatic repulsion is minimal. As the surface charge becomes either more positive or more negative, electrostatic repulsion increases between the surface of adsorbent and the uncharged $AuOH(H_2O)^0$ species. This phenomenon has also been noted by several researchers elucidating the sorption behaviour and migration of the uncharged arsenite oxyanion (H_3AsO_3) in iron oxide containing artificial and natural systems (Vlassopoulos and Wood, 1990a, Tabelin et al., 2017d).

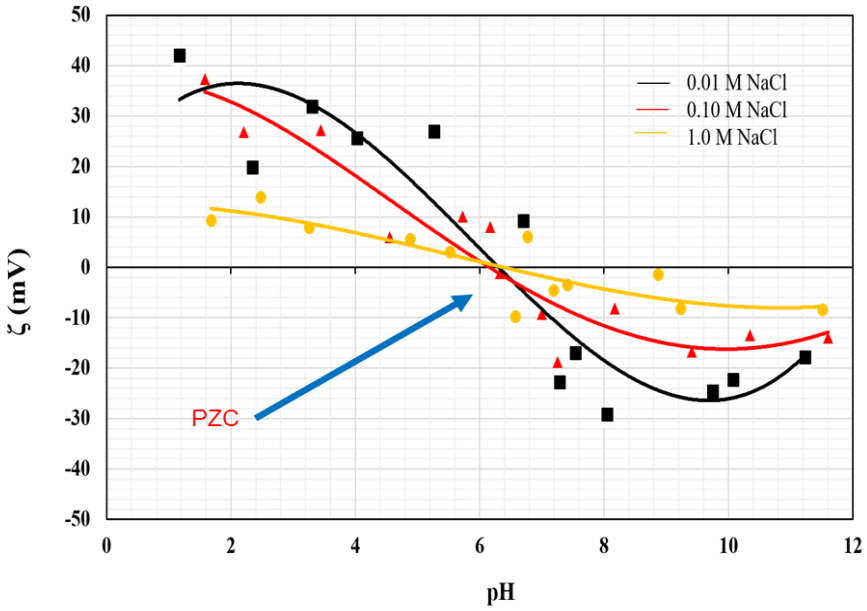

Figure 8. Zeta potential of the maghemite-rich iron oxide composite sample at different pH and NaCl concentrations.

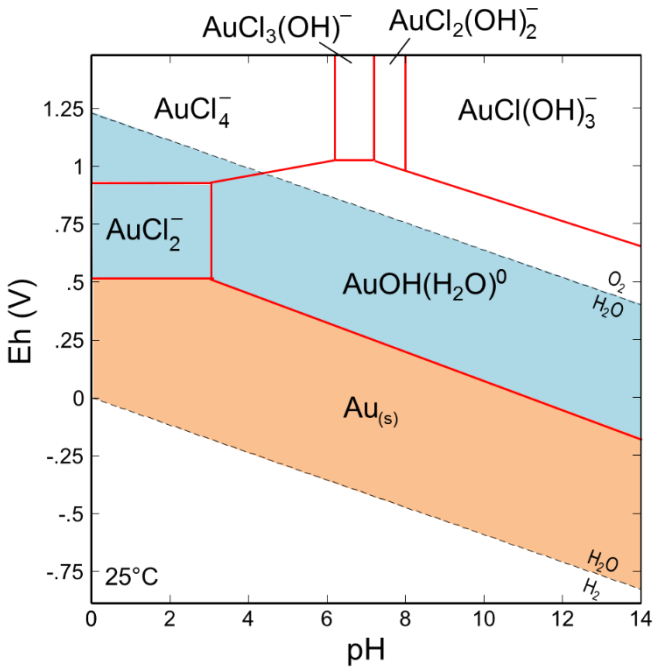

Figure 9. Eh-pH predominance diagram of Au at 25°C, 1.013 bars and activity of Cl^- equal to $10^{-0.25}$ (chemical reactions and thermodynamic constants are based on the work of (Vlassopoulos and Wood, 1990a, Tabelin et al., 2018)).

III.3.2.3 Effect of contact time

To determine the contact time for optimum Au uptake, the shaking time was varied from 1–48 hr with a fixed Au concentration of 5×10^{-5} mol/L, solution pH of 6–8, solid to liquid ratio of 1%, and chloride concentration of 0.10 mol/L.

Figure 10 shows that the adsorption efficiency/capacity of Au increased rapidly with increasing contact time at the initial stage. More than 20% Au recovery was obtained at 6 hr contact time, and it increased further to about 84% at 18 hr. Finally, almost complete recovery was achieved (99.78%) after 24 hr. No significant difference in Au uptake was observed upon increasing the time to 48 hr, suggesting that the surface-active sites for adsorption have reached saturation already. Therefore, 24 hr was considered as the equilibrium adsorption time and was used in the succeeding experiments.

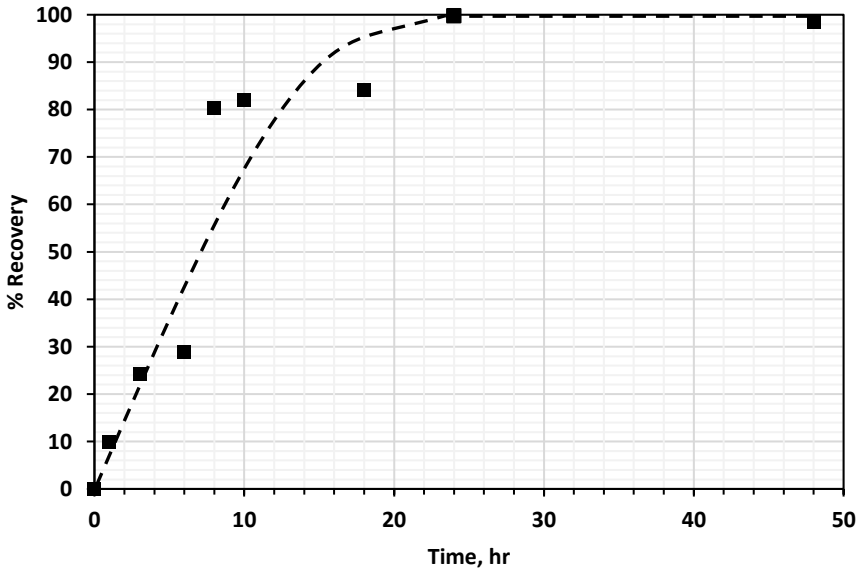

Figure 10. Effect of contact time on Au uptake by maghemite-rich iron oxide composite. Average initial Au concentration: 9 mg/L, NaCl concentration: 0.1 mol/L, pH 6-8, adsorbent amount 0.1 g, shaking speed: 140 rpm, and at 25 °C.

III.3.2.4 Effect of initial Au concentration

The effect of Au concentration on Au adsorption onto maghemite-rich iron oxide composite material was determined by varying the initial Au concentration in the range of 5×10^{-5} mol/L to 5×10^{-4} mol/L. The contact time and amount of adsorbent was fixed at 24 hr and 0.1 g, respectively. The amount of Au adsorbed was determined by the

difference in the initial and the residual gold concentrations. Results are shown in Figure 11 as a plot of Au uptake against the initial gold concentration. Gold uptake increased with increasing initial Au concentration, and it started to level off at 3.5×10^{-4} mol/L initial Au concentration. No significant change in the uptake value was observed when initial Au concentration was increased further. This suggest that the maximum capacity of the maghemite-rich iron oxide composite was reached, and the maximum Au uptake was recorded to be about 11.5 µmol/g.

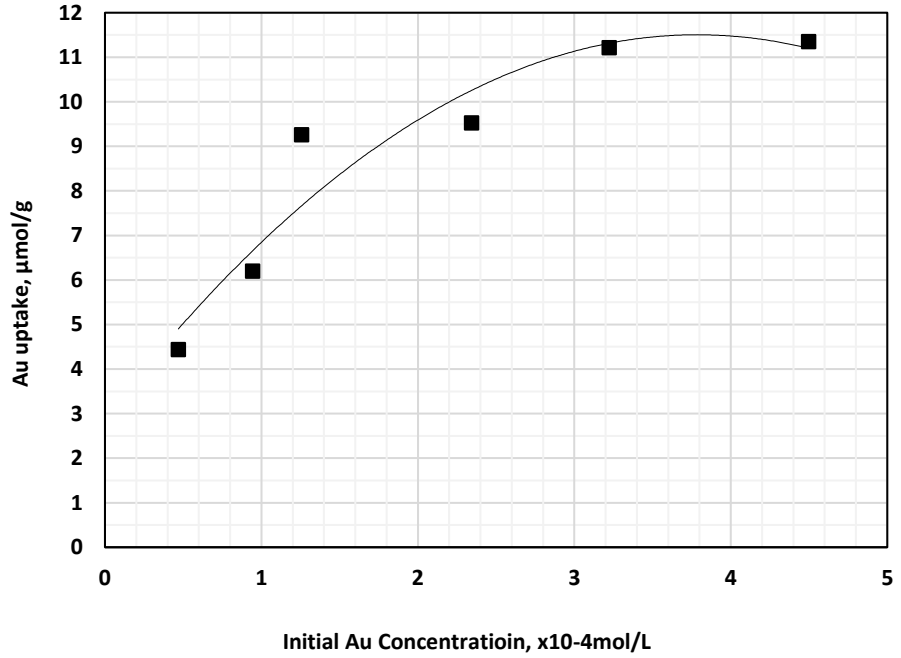

Figure 11. Effect of initial Au concentration on Au uptake onto maghemite-rich iron oxide composite. NaCl concentration: 0.10 M, contact time: 24 h, pH: 6-8, amount of adsorbent: 0.1 g, and temperature 25 ºC.

The maximum adsorption capacity of the maghemite-rich iron oxide composite was calculated by fitting Equations 5 and 7 to the experimental data.

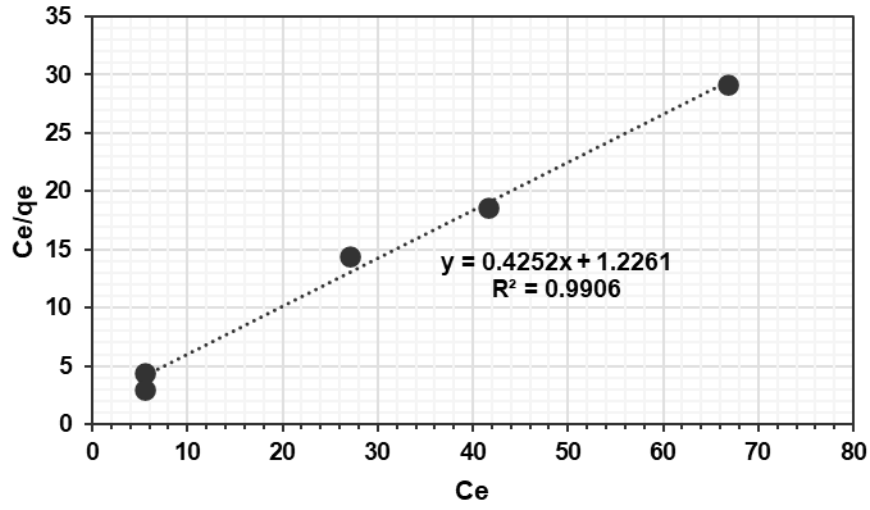

(a)

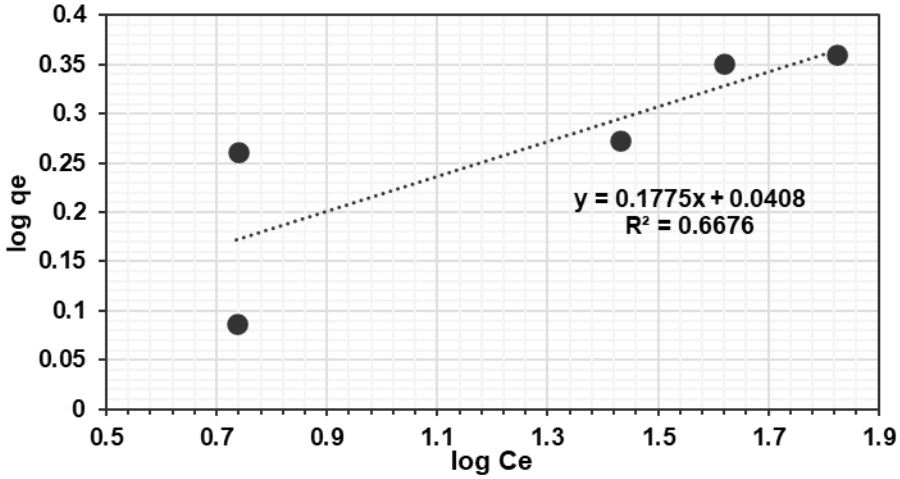

(b)

Figure 12 shows the equilibrium adsorption isotherms for Au adsorption on the iron oxide composite; (a) Langmuir Isotherm and (b) Freundlich Isotherm. The maximum adsorption capacity of the adsorbent (q_m) was about 2.352 mg/g. The Freundlich constant related to the adsorption capacity of the adsorbent (K_F) was calculated as 1.042 L/mg, with n value of 24.51. The R^2 coefficients were determined to be 0.9906 and 0.6676 for the Langmuir and Freundlich isotherms, respectively, which strongly suggest that the experimental results closely fit the Langmuir model. This result also confirms that the adsorption was of monolayer coverage and the interaction of Au ions, and the surface of the maghemite-rich iron oxide composite was characterized by chemisorption mechanism.

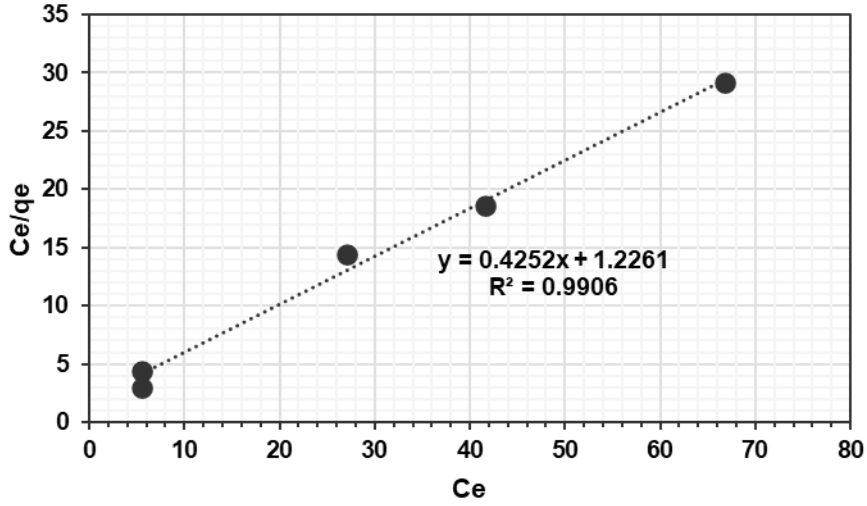

(a)

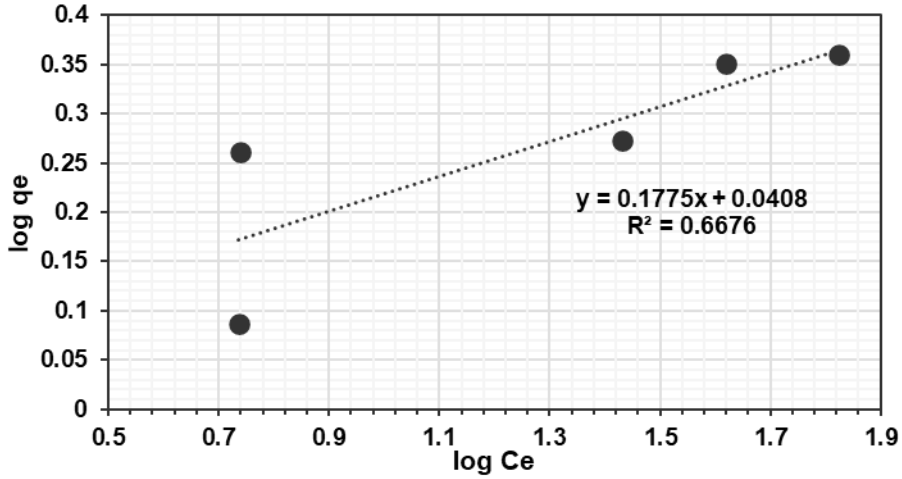

(b)

Figure 12. Equilibrium adsorption isotherms for Au ions onto maghemite-rich iron oxide composite (a) Langmuir Isotherm and (b) Freundlich Isotherm. Initial Au concentration: 5×10^{-5} mol/L to 5×10^{-4} mol/L; Contact time: 24 h, pH: 6-8, adsorbent dosage: 0.1 g, and temperature 25 ºC.

III.3.2.5 Effect of chloride concentration (ionic strength)

The NaCl concentration was varied to investigate the effect of the ionic strength on the adsorption of Au onto maghemite-rich iron oxide composite particles. Varying the Cl^- concentration may affect the Au adsorption process by either affecting the interfacial potential and the activity of the adsorbing species, or through competition of the electrolyte ions and adsorbing ions for available active sites (Hayes et al., 1988).

Figure 13 shows that Au uptake decreased as the chloride concentration is increased. Gold recovery decreased from more than 90% at low NaCl concentrations to below 30% at 3.0M NaCl concentration. This decrease in Au uptake was also observed by Alorro et al., (2010). Chloride ions may adsorb on the surface of the maghemite-rich iron oxide composite particles rendering the surface charge more negative, hence, disturbing the electrostatic approach of gold complexes or species in the solution to the active sites (Hayes et al., 1988).

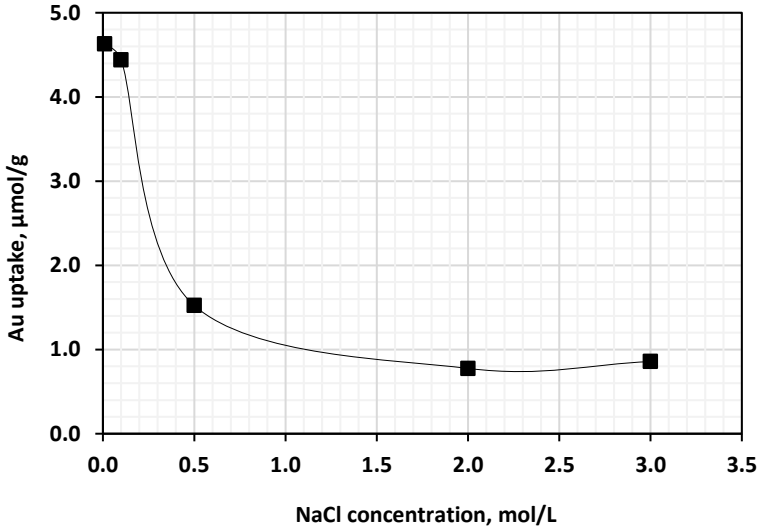

Figure 13. The influence of chloride concentration on the adsorption of Au onto maghemite-rich iron oxide composite. Average initial Au concentration: 9.0 mg/L, pH 6-8, contact time: 24 hr, adsorbent amount: 0.1 g, and at 25 ºC.

III.4 SEM EDX Mapping

SEM analysis is one of the powerful technique to determine the microstructural analysis of the adsorbent which provides information including the morphology, topographic features, crystal structure and orientation as well as image presentation in order to observe and visualise modifications of its structure by physical/chemical treatments (Pellenz et al., 2023). SEM is utilised in this study to determine the deposition of gold after the adsorption process onto the maghemite-rich adsorbent.

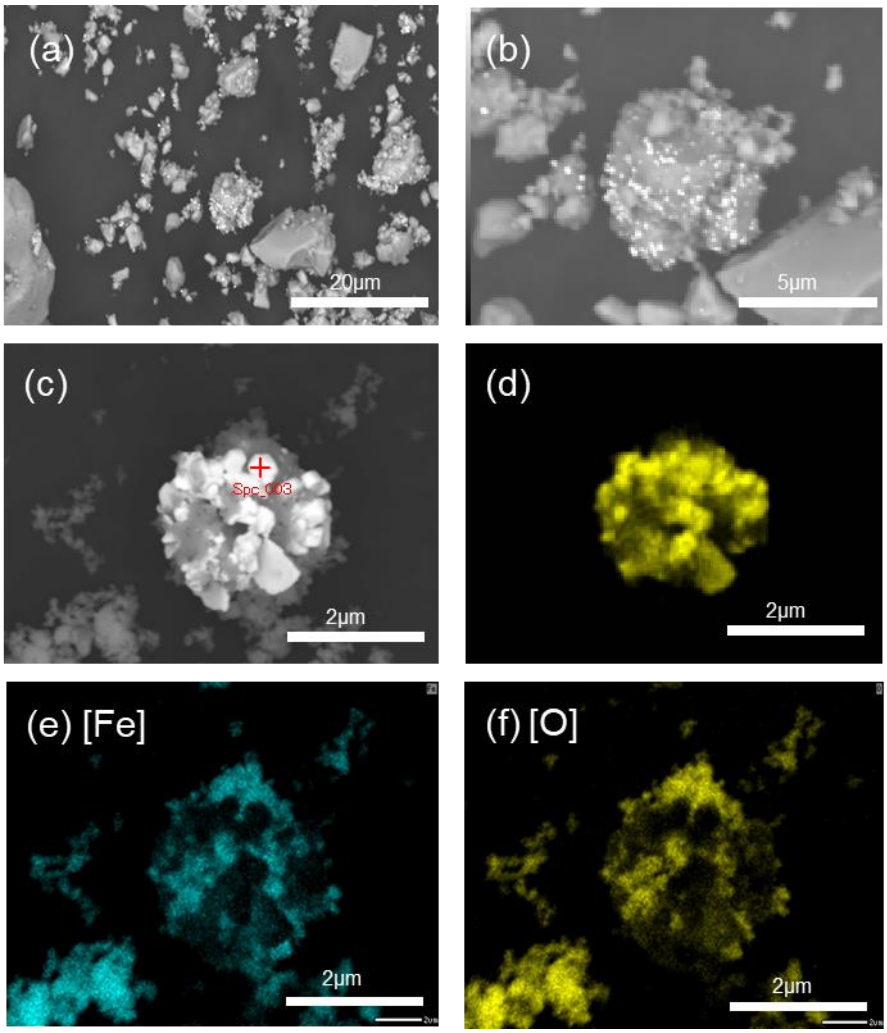
(a)
20µm
(b)
5µm
(c)
Spc_003
2µm
(d)
2µm
(e) [Fe]
2µm
(f) [O]
2µm

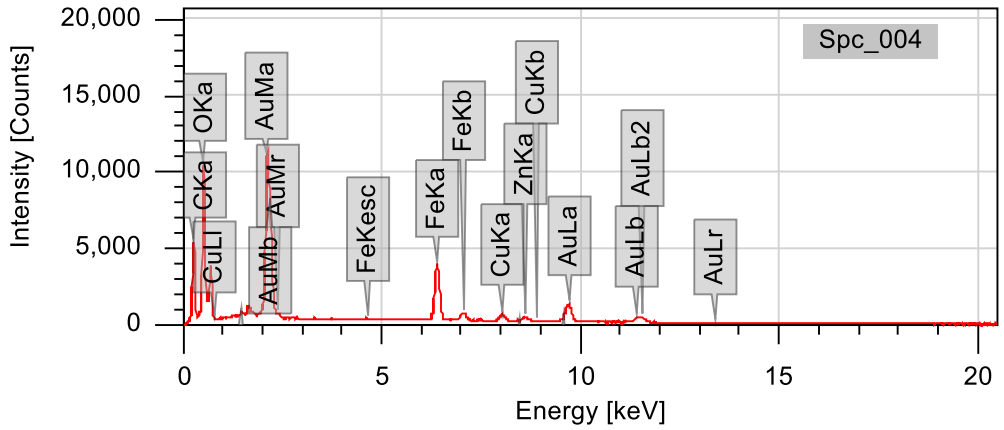
Spc_004
Intensity [Counts]
Energy [keV]
20,000
15,000
10,000
5,000
0
0
5
10
15
20
OKa
CKa
CuLl
AuMa
AuMr
AuMb
FeKesc
FeKa
FeKb
CuKa
ZnKa
CuKb
AuLa
AuLb
AuLb2
AuLr

(g)

Figure 14. (a-g) SEM-EDX mapping of maghemite-rich composite containing Au. Gold concentration: 9.0 mg/L in 0.1M NaCl, pH 6-8, contact time: 24 hr, adsorbent amount: 0.1 g, and at 25 ºC. (2µm at 7000 x magnification, MIRA 3 FE-SEM, Tescan Ltd., Czech Republic).

EDX was also performed along with the SEM analysis to identify the percentage of each element on the surface of the sample. The point of identification was at Sp_003 shown in Figure 14(c) where the metallic gleam was observed. Table 4 presents the EDX result confirms the presence of a reduced metallic gold on the surface of the adsorbent with 82% wt Au and other predominant elements such as Cu, Fe, O, etc. Elemental mapping (

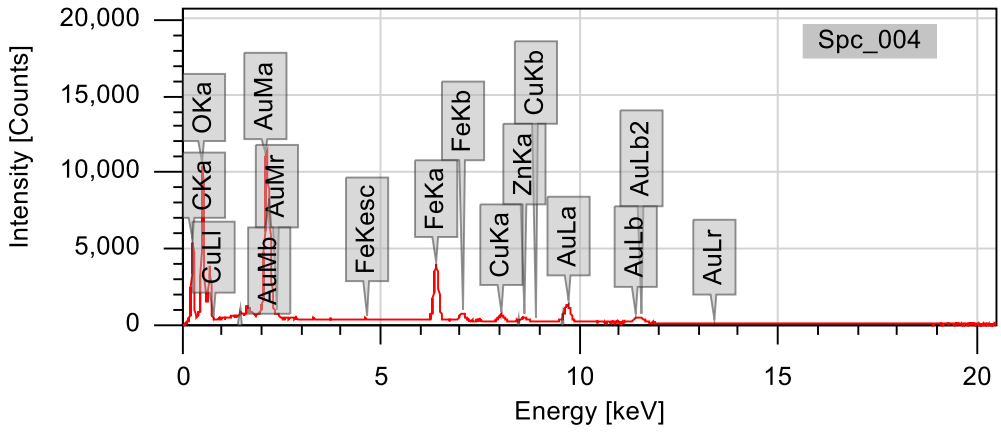

(g)

Figure 14 e-f) show that the reduction of Au is associated with Fe and O. The reduction of Au(III) to metallic Au(0) was achieved by the reaction (Eq 9). Maghemite, on the other hand, underwent partial reduction to release the Fe^{2+} ions as shown in (Eq 10). Overall reaction is described in (Eq11).

$$Au^{3+} + 3e^{-} \rightarrow Au^{0} \qquad \text{(Eq 9)}$$

$$Fe_2O_3 + 2e^{-} + 6H^{+} \rightarrow 2Fe^{2+} + 3H_2O \qquad \text{(Eq 10)}$$

$$2Au^{3+} + Fe_2O_3 + 6H^{+} \rightarrow 2Au^{0} + 2Fe^{2+} + 3H_2O \qquad \text{(Eq 11)}$$

Table 4. EDX results obtained from an SEM-EDX equipment at point Sp_003 showing the Fe, O, C, and Cu percentage on the maghemite-rich adsorbent (2µm at 7000 magnification).

Display name	Standard data	Quantification Method	Result Type
Spc_003	Standardless	ZAF	Metal

Element	Line	Mass%	Atom%
C	K	5.63 ±0.04	39.55 ±0.31
O	K	2.23 ±0.04	11.76 ±0.21
Al	K	0.25 ±0.02	0.78 ±0.05
Fe	K	1.31 ±0.03	1.98 ±0.05
Cu	K	4.89 ±0.08	6.49 ±0.10
Zn	K	3.21 ±0.08	4.14 ±0.10
Au	M	82.47 ±0.24	35.30 ±0.10
Total			100.00
Spc_003			Fitting ratio 0.0166

III.5 Desorption studies

The amount of Au released from the adsorbent surface were determined in the desorption tests. In the results summarized in

Table 5, the acidic pH of 0.5M NH_3 eluant did not desorb Au from the adsorbent rather, dissolving Fe from the maghemite-rich adsorbent. In some cases, gold nanoparticles may interact with the surface of the iron oxides through inter-molecular forces and can readily disrupted using a suitable complexing agent. The authors Birich et al. (2019) elucidated that organic thiourea ($CS(NH_2)_2$) has demonstrated a promising Au complexing agent. At higher pH, thiourea can undergo hydrolysis where amine (-NH_2) and thio (-SH) groups can lose protons leading to breakdown of thiourea into products such as ammonia, urea, or hydrogen sulphide (H_2S) . Therefore, thiourea leaching process is typically performed at a certain pH (~pH1-2) and requires an oxidising agent to form the reactive compound (Li and Miller, 2006, Zhang et al., 2001). In this case, the dissolved iron (Fe^{3+}) has potentially act as oxidant in the formation of formamidine disulphide which subsequently oxidised Au and forms a cationic Au thiourea complex according to the reactions Eq 12 and Eq 13. At pH 8-8.8, thiourea showed an increasing desorption recovery when thiourea concentration was

increased from 0.7M to 1.75M concentration. About 80% Au recovery was achieved after 24 hours contact time using 1.75M thiourea with minimal or no Fe and Ni dissolution.

$$2CS(NH_2)_2 + 2Fe^{3+} \rightarrow C_2S_2(NH)_2(NH_2)_2 + 2Fe^{2+} + 2H^+ \quad \text{(Eq 12)}$$

$$2Au + C_2S_2(NH)_2((NH)_2)_2 + 2CS(NH_2)_2 + 2H^+ \rightarrow 2Au(CS(NH)_2)_2)_2^+ \quad \text{(Eq 13)}$$

Table 5. Dissolution of adsorbed Au from the prepared maghemite-rich magnetic adsorbent.

		Gold		
Eluent	Desorption Time	%Au Desorbed	Fe, ppm	Ni, ppm
0.5 M HNO_3	4	0.00	3.24	0.00
0.7 M thiourea	4	23.05	0.00	0.00
	24	25.79	0.00	0.00
1.0 M thiourea	4	21.68	0.00	0.00
	24	29.77	0.00	0.00
1.75 M thiourea	4	48.33	0.00	0.00
	24	80.17	0.00	0.00

II.6 Summary

In this study, the capacity and effectiveness of a maghemite-rich iron oxide composite consisting of 44% maghemite synthesised by low temperature oxidation of magnetite, were evaluated to recover Au from chloride solution. Batch adsorption experiments were conducted using a simulated gold solution and the prepared adsorbent. The results showed that the composite iron oxide material was more effective than synthetic magnetite for gold recovery in chloride medium. Maximum Au recovery was achieved at pH of about 6.5 and 24 hr contact time with a recovery of 99.78%. The optimum pH was also found to correspond to the point of zero charge (PZC) of the composite iron oxide sample. The Eh-pH predominance diagram also revealed that between pH 5 and 8 where maximum recovery was obtained, dissolved Au is mainly present as the uncharged $AuOH(H_2O)^0$ oxyanion, a form which is more easily adsorbed when the surface charge of the adsorbent is close to zero because electrostatic repulsion is minimal. The Au uptake did not increase significantly when

the contact time was increased beyond 24 hr. High concentrations of chloride ions present in the solution decreased Au uptake. SEM-EDX analysis confirms the reduction of Au on the surface of the adsorbent with 82%wt Au. Desorption process has achieved about 80% Au recovery using 1.75M thiourea as lixiviant for 24 hours contact time with no/minimum Fe and Ni dissolution at pH 8 to pH 8.8.

Chapter 4

Repurposing of Nickeliferous Pyrrhotite from Mine Tailings as Magnetic Adsorbent for the Recovery of Gold from Chloride Solution

This chapter presents the utilization and repurposing of waste materials from mining and minerals industry and used as adsorbents for valuable metals. The ability of magnetic nickeliferous pyrrhotite obtained from nickel sulphide mine tailings in Western Australia as adsorbent for gold from chloride solution was investigated. Investigations and findings discussed in this chapter and have been published in Elsevier Editorial System ™ for Resources, Conservation and Recycling https://doi.org/10.1016/j.resconrec.2020.104971

- CALDERON, A. R. M., ALORRO, R. D., TADESSE, B., YOO, K. & TABELIN, C. B. 2020. Repurposing of nickeliferous pyrrhotite from mine tailings as magnetic adsorbent for the recovery of gold from chloride solution. Resources, Conservation and Recycling, 161.

Some parts of this chapter was presented in the 15th International Symposium on East Asian Resources Recycling Technology (EARTH 2019) at Pyeongchang, Gangwon-do, Korea on October 13-27, 2019.

IV.1 Introduction

Mining and mineral processing industries generate huge quantities of solid wastes, such as waste rocks, overburdens and process tailings, which are disposed near mine or processing sites, and/or managed professionally in designated impoundment areas as a long-term environmental liability. Handling and disposal of massive volume of mine wastes have become one of the main pollution concerns for mining industries and communities, especially in Western Australia, where iron, gold, nickel, and other mining operations are extensive. The disposal of these mine wastes create economic, environmental and legislative burdens for the mining industry (Kuranchie et al., 2013).

Reusing, repurposing or recycling is considered to be the key solution to minimize the environmental impact and to offset the costs of managing mine wastes (Bulut and Yenial, 2016). Depending on their nature or characteristics, mine wastes could be used as raw materials for other industrial applications, with or without pretreatment, such as fill materials (Blight, 2011, Collins and Miller, 1979), bricks and geopolymer production (Ahmari and Zhang, 2013, Kuranchie et al., 2013), concrete and road construction (Ma et al., 2016, Oluwasola et al., 2015, Swami et al., 2007, Wang et al., 2016, Zhao et al., 2014), and adsorbents for wastewater treatment and heavy metals removal (Letina and Letshwenyo, 2018a, Bulut and Yenial, 2016, Sarkar et al., 2017). Including mine wastes in the alternative product life cycle as suggested in the concept of circular economy is very attractive from both environmental and economic perspectives (Bulut and Yenial, 2016). Development of innovative and environmental-friendly technologies that would minimize waste generation in the minerals industry by converting waste materials into useful products for various applications has become indispensable.

Mining and processing of metal-sulphide ores, such as nickel-copper complex sulphides, generate tailings or waste materials rich in iron sulphides. A typical iron sulphide for such ores is pyrrhotite *[$Fe_{(1-x)}S$ with $x = 0 - 0.2$]*, which is nickeliferous in nature. Pyrrhotite is rejected as tails in the beneficiation circuit of Ni sulphide ores primarily to produce high grade concentrates, control circuit throughput, and consequently minimise SO_2 emission during smelting (Garg et al., 2017). Pyrrhotite-rich tailings are reactive, hence, are required to be disposed in properly controlled impoundment areas to prevent acid mine drainage (AMD). AMD is generated when metal-sulphide containing wastes are exposed to oxygen (O_2) and is considered a major environmental concern due to its extremely low pH (< 3) and high concentrations of hazardous heavy metals (Akcil and Koldas, 2006, Garg et al., 2017, Igarashi et al., 2020, Lei and Watkins, 2005, Park et al., 2020, Peek et al., 2011b, Tabelin et al., 2018). About 20% of Ni sulphide mined is rejected as pyrrhotite fraction and dumped as mine waste (Harris et. al., 2010). In Sudbury, Canada, about 50–100 million tons of pyrrhotite tailings have been stockpiled from over 50 years of operation which incur significant cost to manage the risk of AMD formation (Peek et al., 2011b, Garg et al., 2017). Currently, pyrrhotite does not have any specific use but some works have been carried out in the past utilising pyrrhotite-rich tailings as a potential resource for Ni recovery given that they contain about 0.6 – 0.8 wt% Ni (Peek et al., 2011; Harris et.

al., 2010). Peek et al. (2011) have reported several pyrometallurgical and hydrometallurgical processing options for pyrrhotite but evidently, cost effectiveness remains a major challenge. Finding useful applications for pyrrhotite-bearing tails is vital and relevant to make metal-sulphide mining activities more environmentally, economically, and socially sustainable.

Pyrrhotite, along with other sulphide minerals, has reported to be excellent in adsorbing heavy metals (mercury, lead, zinc and cadmium) (Jean and Bancroft, 1986), and was found to play important roles in the deposition of gold complexes, particularly gold(I) hydrosulphide, in natural systems and geochemical processes (Widler and Seward, 2002, Jean and G. Michael, 1985). Although limited, these studies have demonstrated the potential of pyrrhotite as effective adsorbent for metal ions for heavy metal pollution abatement or recovery of precious metals from aqueous solution. Since pyrrhotite, depending on its form, could possess relatively strong magnetic properties [monoclinic pyrrhotite (Fe_7S_8), mackinawite (tetragonal FeS) and greigite (cubic inverse spinel Fe_3S_4)] (Beal et al., 2012, Sagnotti et al., 2007), it can be easily collected from mine tailings by magnetic separation and utilized as magnetic adsorbent. The utilization of pyrrhotite from mine waste as a magnetic adsorbent for precious metals, especially gold (Au) from aqueous solutions, is a novel and a very attractive alternative application for pyrrhotite-rich tailings.

The application of magnetic particles as adsorbents has been considered as one of the most promising technologies in separation and purification of valuable metals from aqueous solutions (Aghaei et al., 2017a, Giakisikli and Anthemidis, 2013b). Magnetic adsorbents are particles composed of Fe, Ni, Co, and/or their oxides and alloys which can be sourced naturally, such as in the case of pyrrhotite and magnetite (Fe_3O_4) minerals, or can be prepared or synthesized in the laboratory (Aghaei et al., 2017a, Gómez-Pastora et al., 2014). The authors have studied previously the use of naturally-occurring and synthetic magnetic particles, such as, magnetite (Alorro et al., 2010, Homchuen et al., 2016) and maghemite-rich composite (Calderon et al., 2019b), as adsorbents for gold and other precious metals from aqueous solution. The main advantage of using magnetic adsorbents in the separation and purification of precious metals aside from high adsorption capacity and selectivity, is their response to external magnetic field rendering solid-liquid separation easy and less complicated (Aghaei et al., 2017a, Herrero-Latorre et al., 2015a, Giakisikli and Anthemidis, 2013b). Although

various types of magnetic adsorbents have been reported in the literature (Aghaei et al., 2017a, Giakisikli and Anthemidis, 2013b), some have limited large scale applications due to the complexity or high cost of synthesis and material modification. Cheaper but effective alternatives, such as the nickeliferous pyrrhotite from mine wastes, are envisaged to offer a cost-effective and eco-friendly solution.

The present research work has attempted the repurposing and utilization of nickeliferous pyrrhotite from mine wastes as magnetic adsorbent for the recovery of gold from chloride solution. The recovery of gold from aqueous solutions and waste effluents, especially solutions or leachates generated by recycling and secondary processing, has always been a matter of interest due to its high economic value and numerous applications. The pyrrhotite samples collected from mine tailings by magnetic separation were prepared by crushing, grinding and sieving, and characterized using various analytical techniques. Adsorption experiments using the pyrrhotite adsorbent were conducted and the influences of different process variables, such as pH, contact time, metal concentration, and chloride concentration on Au adsorption were investigated.

IV.2 Materials and Methods

IV.2.1 Characterization of magnetic nickeliferous pyrrhotite samples

The nickeliferous pyrrhotite samples were collected using a handheld magnet from the waste rock stockpile of a nickel sulphide mine located in the Goldfields region of Western Australia (Figure 15). The sample was crushed manually and then pulverized (C+PB, Rocklabs 2012) to reduce the particle size. The particle size distribution was determined using a laser sizer (Mastersizer 3000, Malvern) while the specific surface area and the porosity were quantified by Brunauer-Emmett-Teller (BET)-N2 and Barrett-Joyner-Halenda (BJH) methods (ASAP 2020, Micromeritics Instrument Co., USA). The zeta potential of the sample was determined using a Zetasizer (Nano Z, Malvern Corporation, UK) at pH 1–12 and different chloride concentrations (0.01–1.0 mol/L). The chemical and mineralogical compositions of the sample were analysed by X-ray Diffraction (XRD, PANAnalytical, UK) and X-ray Flourescence (XRF, PANAnalytical, UK).

(a) (b)

Figure 15. Nickeliferous pyrrhotite obtained from waste mine tailings in Kambalda, WA. (a) Pile of waste rocks. (b) Waste rock obtained.

IV.2.2 Adsorption and desorption experiments

Reagent grade Gold (III) chloride ($AuCl_3$) from Sigma Aldrich were used as source of gold ions for simulated solutions. The sodium chloride (NaCl), hydrochloric acid (HCl), and sodium hydroxide (NaOH), nitric acid (HNO_3), sulfuric acid (H_2SO_4) and thiourea (CH_4N_2S) from Sigma Aldrich and Chem Supply were all of reagent grades.

Adsorption analyses were conducted in batch operation to investigate the capability of the magnetic iron sulphide, which primarily contains pentlandite and pyrrhotite, to recover Au from chloride solutions. Gold concentration was derived from e-waste solution (Sun et. al., 2016). Therefore, a fixed 10 mL volume of sodium chloride (NaCl) solution at 0.1 mol/L containing 5×10^{-5} mol/L Au concentration was transferred into a 250 mL Erlenmeyer flask. Initial pH was adjusted by adding freshly prepared HCl and NaOH solutions. The magnetic iron sulphide powder was then added in the mixture at an initial solid/liquid ratio of 1%. The prepared mixture was then shaken at certain time intervals in a water bath (ZWY-110x30, Labwit Scientific) at a constant rate of 140 strokes per minute and 25 °C. After a given contact period the mixture was membraned filtered using 0.20 µm syringe filters.

The concentrations of gold (Au), iron (Fe), and nickel (Ni) in the aqueous phase were analysed using Inductively Coupled Plasma – Optical Emission Spectrometry (5100 ICP-OES, Agilent). The solid particles were collected after adsorption, washed twice with deionised water, and oven dried for 4 hours. The dried particles were then

examined to check the presence of Au on the surface using scanning electron microscope (MIRA 3 FE-SEM, Tescan Ltd., Czech Republic).

Desorption experiments were also conducted to determine the amount of gold that can be recovered from the loaded magnetic iron sulphide adsorbent using different eluant at varied concentrations. Initial concentrations of 0.5mol/L nitric acid, 0.7mol/L thiourea, 0.5mol/L thiourea in 0.5mol/L sulphuric acid, and 0.5 mol/L glycine were used as eluant to dissolve the adsorbed precious metals. The prepared solution was then shaken at 4h and 24h interval in a water bath shaker and then syringe filtered.

The concentrations of platinum (Pt), palladium (Pd), iron (Fe) and nickel (Ni) in the solution were analysed using Inductively Coupled Plasma – Optical Emission Spectrometry (5100 ICP-OES, Agilent).

IV.2.3 Open circuit potential

An open-circuit potential was also investigated using WaveNow Potentiostat/Galvanostat System with AfterMath software. The natural magnetic iron sulphide (pyrrhotite based) obtained from Kambalda, WA was used as the working electrode while the reference electrode was an KCl saturated Ag/AgCl electrode. Firstly, the sample was cut to about 1 x 1 cm with 0.5 cm thickness. The sample was then connected to a silver wire to the digital multimeter. A silver paste was placed in the point of connection to ensure connection between the sample and the silver wire. Finally, the sample and silver wire were placed inside a plastic tube and established by a cold-curing resin as illustrated in Figure 16.

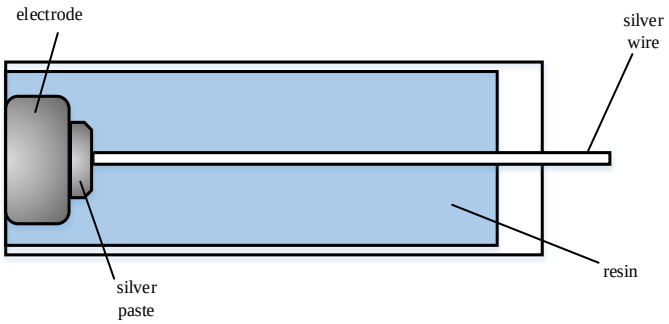

Figure 16. Natural magnetic iron sulphite (pyrrhotite based) working electrode.

The open-circuit potential voltammetry measurements were investigated at room temperature (25°C) in 0.1M NaCl concentrations at five different pH values: 2, 3, 5, 9, and 11. The potential difference between the prepared electrode with regards to the reference electrode was recorded immediately after submerging the electrode into the solution and at 5 minutes interval until the resulting potential was constant. The part of the electrode exposed to the solution was polished by an abrasive paper until a flat surface was obtained and rinsed with deionised water to after every use. Freshly prepared 1M HCl and 1M NaOH were used to set the acidic and alkaline pH respectively.

IV.3 Results and discussion

IV.3.1 Adsorbent characterization

The XRD pattern of the iron sulphide ore sample from Kambalda, Western Australia is presented in Figure 17(a). The polycrystalline sample is composed of 65% pyrrhotite, 32% pentlandite, and 3% other impurities. The chemical composition as determined by XRF consisted of 49.15% Fe, 26.9% S, 12.2% Ni and other components. The particle size of the milled magnetic nickeliferous pyrrhotite sample used in the adsorption experiments was characterized by a D75 of 86.36 µm. The specific surface area and average pore width of the milled sample as measured by BET and BJH methods, were 1.00 m2 /g and 14.08 nm, respectively, which correspond to characteristics of a mesoporous material (Figure 17b).

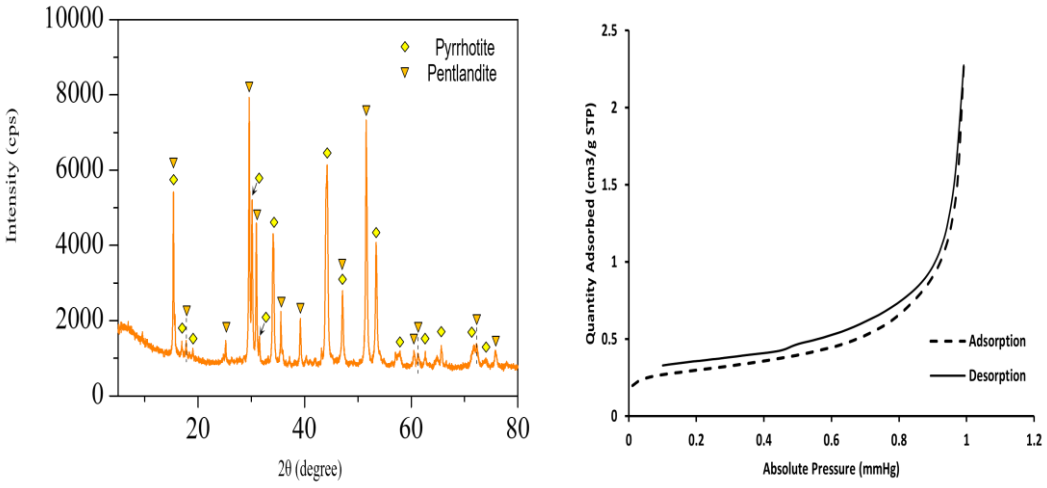

Figure 17. (a) XRD spectra of natural iron sulphide ore from Kambalda, WA, and (b) BET and BJH results

IV.3.2 Effects of pH

Adsorption experiments were conducted at different pH with fixed initial Au concentration of 5×10-5 mol/L in 0.1 mol/L NaCl solution and dosage (0.1 g). Gold chloride adsorption on magnetic nickeliferous pyrrhotite as a function of pH is presented in Figure 18. Complete Au recovery (100%) was achieved between pH 1.8 and 5.5, signifying that Au adsorption efficiency is high at acidic pH range. This is equivalent to Au uptake amount of 4.70 µmol/g. Gold recoveries started to decrease at pH >5.5 and were at a minimum at alkaline pH ranges. Gold adsorption on magnetic nickeliferous pyrrhotite was also associated with Fe dissolution as shown in Figure 19. About 300 mg/L of Fe was detected at acidic pH regions where Au recoveries were at a maximum. The concentrations of released Fe decreased with increasing pH values with none detected at alkaline pH.

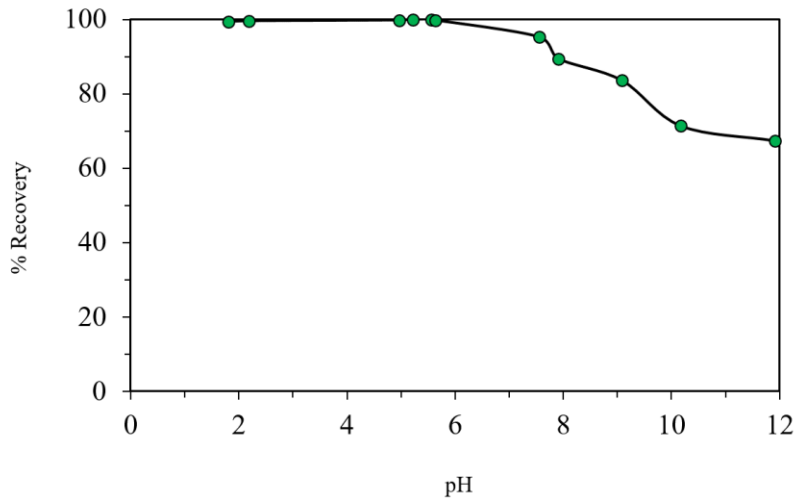

Figure 18. Gold Recovery as a function of pH. (Cl^- concentration: 0.10 M, contact time: 24 H, adsorbent dosage: 0.10 g, and temperature: 25 °C).

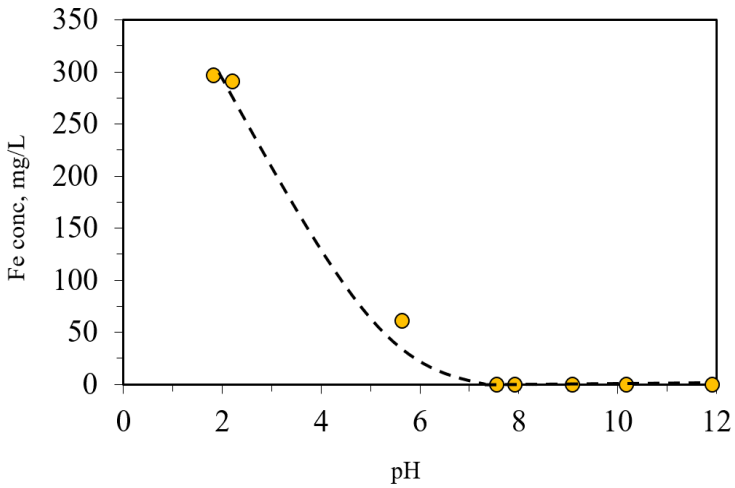

Figure 19. Dissolved Fe concentration as a function of pH (Cl^- concentration: 0.10 M, contact time: 24 H, adsorbent dosage: 0.10 g, and temperature: 25 °C).

The zeta potential of the magnetic nickeliferous pyrrhotite sample was measured at different pH values and NaCl concentrations to help explain the adsorption results shown in Figure 18. The point of zero charge (PZC) of the adsorbent dispersed in 0.1 M NaCl solution was determined to be around pH 3.8 as depicted in Figure 20. In the Eh-pH predominance diagram shown in Figure 21, the dissolved Au present between pH 1 and 3 mainly exist as $AuCl_2^-$, which means that this negatively charged Au complex is attracted to the positively charged surface of adsorbent. From Figure 18, above pH 3.5, the surface charge on the magnetic sulphide adsorbent becomes less positive but because dissolved Au also speciates into the uncharged $AuOH(H_2O)^0$ oxyanion, Au uptake remained high. Adsorption of the uncharged Au oxynanion was promoted when the surface charge of adsorbents approaches the PZC because electrostatic repulsion becomes minimal. A similar phenomenon was recently reported by the authors on the uptake of dissolved Au by maghemite in Cl^- solution (Calderon et al., 2019a). Moreover, a similar behavior was noted by several researchers on the sorption of the uncharged arsenite oxyanion (H_3AsO_3) on iron oxides (Tabelin et al., 2017b, Tabelin et al., 2017a, Vlassopoulos and Wood, 1990b).

Iron sulphides such as mackinawite and pyrrhotite were known to have high solubility factors at low pH and readily oxidise during sample preparation and measurements (Davison, 1991, Fornasiero et al., 1992). The high solubility and often rapid dissolution rates of the iron sulphides make an accurate determination of the PZC

almost impossible. The PZC of iron sulphides are difficult to accurately measure because they readily oxidize during sample preparation and measurements. Fornasiero et al. (1992), for example, carefully measured the PZC of pyrite by eliminating dissolved oxygen in their experiments using various techniques and concluded that it was almost impossible to prevent pyrite's partial oxidation during preparation and measurement. They estimated that the PZC of pyrite lies around pH 1.5 and the more positive values reported by various authors could be explained by the formation of iron oxyhydroxides/oxides. More recently, Tabelin et al. (2017c) reported that partially oxidised pyrite exhibited two PZCs in between 1 and 4, which was related to the formation of iron-oxyhydroxides on the surface of the mineral. The presence of these two PZCs was also observed in the zeta potential results in 0.01 and 0.1 M NaCl (Figure 20). Increasing the Cl^- species in the solution decreases the surface potential of colloids, which are in agreement with the electrokinetic studies for iron sulphides of Bebie et al. (1998) and J. Dekkers and A.A. Schoonen (1994).

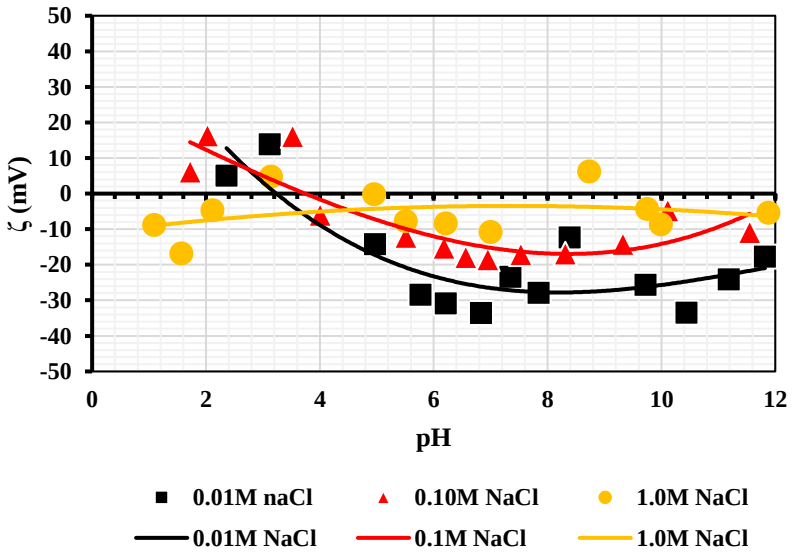

Figure 20. Zeta potential of natural iron sulphide at different pH and NaCl concentrations.

IV.3.3 Effects of contact time

The effect of contact time on Au adsorption on magnetic nickeliferous pyrrhotite was studied by varying the shaking time from 15 min – 24 h while keeping the initial

Au concentration constant at 5 × 10−5 mol/L, pH at 2–3, adsorbent dosage at 0.1 g, and temperature at 25 °C. As shown in Figure 21, 100% Au recovery was achieved even at contact time of 15 min and remained virtually constant with longer adsorption time beyond 1 h A contact time of 1 h was considered for the subsequent experiments. Visual inspection of the adsorption process confirmed the success of Au recovery as shown in Figure 22(2) and (3). The stock solution containing gold chloride complexes was initially pale yellow in colour and after the addition of magnetic nickeliferous pyrrhotite adsorbent and contact time of 1 h, the solution turned clear or colourless, indicating the absence of Au chloride ions. The results of time experiments signified that the kinetics of Au adsorption using magnetic nickeliferous pyrrhotite was very fast. Kinetically, it's superior than Au adsorption using magnetic iron oxide adsorbents reported in previous studies with 24 h as the considered optimum contact time (Alorro et al., 2010, Calderon et al., 2019b)

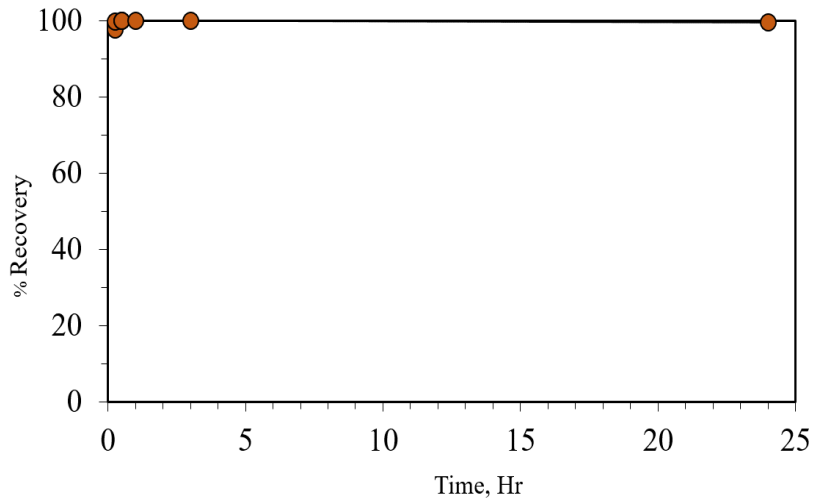

Figure 21. Effect of time on Au uptake by pentlandite-pyrrhotite ore. Chloride concentration: 0.10 M, pH 2-3, 0.1 g adsorbent, and at 25 °C.

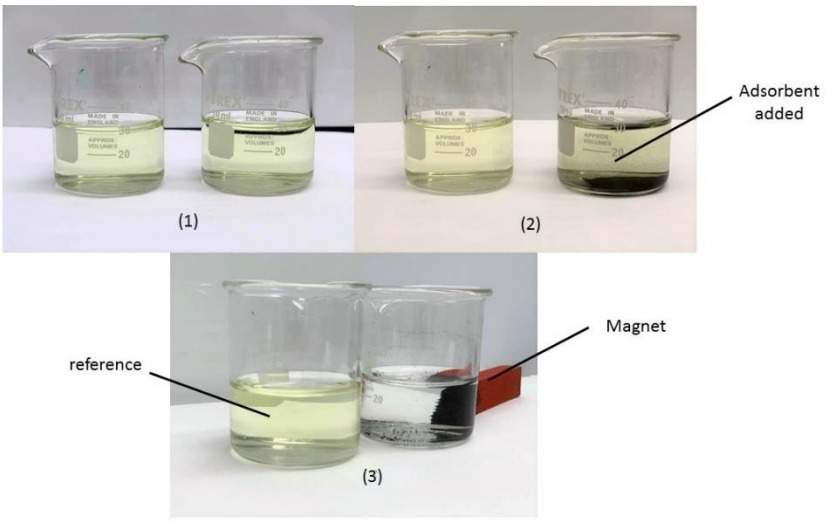

Figure 22.(1) as is sample; Au conc: $5x10^{-5}$ mol/L; (2) and (3) photos of the gold chloride solutions before and after adsorption using magnetic nickeliferous pyrrhotite as adsorbent (contact time: 1hr).

IV.3.4 Effects of initial Au concentration

The effect of initial Au concentration on Au adsorption on magnetic nickeliferous pyrrhotite was studied by varying the initial Au concentration in the range of 5 × 10−5 mol/L to 5 × 10−4 mol/L. Gold recoveries were at 100% at all levels of Au concentrations investigated and were independent of Au concentrations Figure 23(a). The gold uptake amount as a function of initial Au concentration presented in Figure 23(b) revealed that Au uptake increased linearly with increasing initial Au concentration. This observation can be associated to linear adsorption isotherm model or adsorption which obeys the Henry's law Eq 14 below.

$$q = kc \qquad \text{(Eq 14)}$$

where q refers to the amount of adsorbate at equilibrium, k is the Henry's adsorption constant, and c is the equilibrium concentration of the adsorbate on the adsorbent. Henry-type adsorption isotherm is applicable when residual adsorbate concentration is very low and unoccupied sorption sites are readily available (Maurya et al., 2006, Nimibofa et al., 2017). The above results could also mean that the maximum loading capacity for the magnetic nickeliferous pyrrhotite adsorbent was not reached yet, and the material can still uptake more Au. To check this, experiments involving reuse of loaded magnetic nickeliferous pyrrhotite were conducted wherein the same adsorbent

was added to fresh solutions containing known concentration of Au (5 × 10−5 mol/ L) and the step was repeated several times with solid-liquid separation and washing stages in between. The results are shown in Figure 24. Up to 8 times re-use steps were performed and for each step, 100% Au recovery was achieved. After the 8th re-use step, the magnetic adsorbent has accumulated about 35 µmol/g (about 6.9 mg Au/g adsorbent) of Au. These results indicated the excellent Au loading capacity of the magnetic nickeliferous pyrrhotite adsorbent.

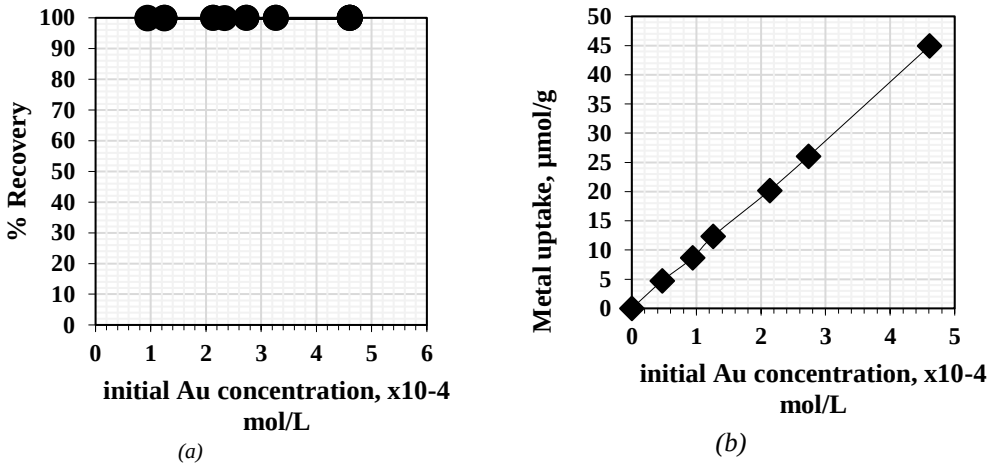

(a) *(b)*

Figure 23. Effects of initial Au concentration on Au adsorption to the magnetic sulphide sample (Cl- concentration: 0.10 M, pH: 2-3, contact time: 1 hr, adsorbent dosage: 0.1 g, and temperature: 25°C): (a) Au recovery as a function of initial Au concentration, and (b) Au uptake as a function of initial Au concentration.

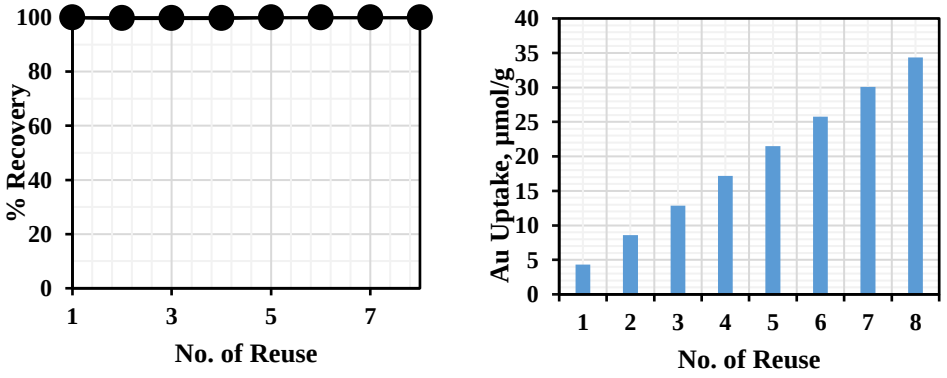

(a) *(b)*

Figure 24. Effect of adsorbent reuse on Au recovery/uptake on magnetic nickeliferous pyrrhotite (Cl- concentration: 0.10M, pH 2-3, contact time: 1 hr, adsorbent dosage:0.1g, and temperature: 25ºC): (a) Au recovery as a function of number of adsorbent reuse, and (b) Au uptake as a function of adsorbent reuse.

IV.3.5. Effects of chloride concentration

The effect of chloride concentration on Au adsorption on magnetic nickeliferous pyrrhotite sample was investigated by varying Cl− concentrations from 0.01–3.0 mol/L and using a fixed initial Au concentration of 5 × 10−5 mol/L. The zeta potential data presented in Figure 20 suggests that the zeta potential (mV) shifted from a positive to a negative value with high chloride concentrations. This observation was elucidated by Figure 25, which shows the results on Au adsorption at different NaCl concentrations. It can be seen from the figure that at higher Cl− concentrations, a significant decrease in Au adsorption was observed. This decrease in uptake under acidic conditions could be explained via two mechanisms: (1) backward reaction effects in which adsorbed/cemented Au to the adsorbent is redissolved because of the presence of excess Cl- in solution (please see Eq 1), and (2) limited formation of metal oxyhydroxides on the surface of the sample. As explained previously, better sorption occurred when more positively charged oxyhydroxides are formed on the magnetic nickeliferous pyrrhotite sample because of electrostatic attraction. At very high Cl− concentrations under acidic conditions, formation of metal-oxyhydroxides/oxides are suppressed due to the formation of high solubility metal-chloride complexes in solution and on the surface of sulphide minerals (Lehmann et al., 2000, Huyen et al., 2019, Park et al., 2018).

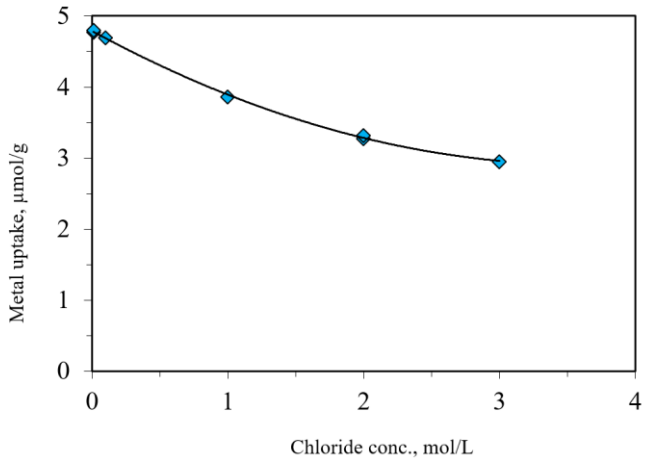

Figure 25. Effect of chloride concentration on the Au uptake of magnetic iron sulphide. Solution pH 2-3, 0.1 g adsorbent, 1 hr contact time, and at 25 °C.

The impact of Cl^- concentration on Au adsorption on the surface of the magnetic iron sulphide was further investigated by measuring the open circuit potential (OCP) of the adsorbent. Results are reported with respect to the standard hydrogen electrode (SHE) by adding 0.22249 V to the measured potential with respect to the Ag/AgCl electrode. The related potentials for 0.1M electrolyte versus pH is shown in Figure 26 where it showed a decrease in the potential (mV) as pH of solution increases. It was previously reported by the authors Moslemi et al. (2011) that the pyrrhotite open circuit potentials with respect to standard hydrogen electrode at pH 2, 4, 6, 8, 10, and 12 were 516.7, 389.5, 323.7, 221.9, 131.4, and 36.2mV respectively, whereas in this study, the presence of sodium chloride at pH 2, 3, 5, 9, and 11 gave a circuit potentials of 324.3, 323.8, 321.5, 91.6 and 72.0mV respectively. This means that the presence of sodium chloride in the solution decreases the potential due to the presence of H^+ and OH^- in the acidic and alkaline regions that causes different electrochemical reactions (Moslemi et al., 2011). This result agrees with the adsorption result shown in Figure 18 where the presence of OH^- in the alkaline region causes the formation of iron hydroxides that covers the electrode surface hindering the attachment of gold chloride complex.

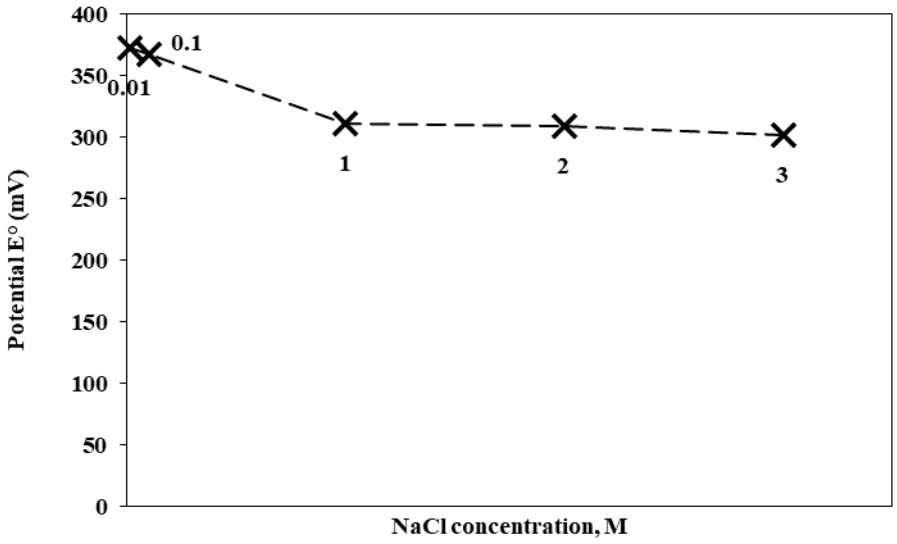

Figure 26. Open circuit potential of magnetic iron sulphide ore against Ag|AgCl (sat.) reference electrode varied NaCl concentration.

IV.3.6. SEM Analysis

The XRD result shown in Figure 17(a) confirmed that the magnetic nickeliferous pyrrhotite adsorbent used in this study was mainly composed of pentlandite and pyrrhotite. SEM analysis of the loaded adsorbent and EDX mapping of Fe, Ni, S and Au was conducted to determine which of the two main components (pentlandite or pyrrhotite) was responsible for Au uptake. As shown in Figure 27 (a-b), elemental mapping revealed that Au distribution appears to be closely associated with the distribution of Ni and S in the adsorbent. Galvanic interactions is one possible explanation for the preferential uptake of Au to pentlandite rather than to pyrrhotite as shown in Figure 28. Because pentlandite and pyrrhotite are semiconductive materials, they could easily form galvanic cells when in close contact to each other in solution similar to those observed by Seng et al. (2019) on pyrite and zero-valent iron and zero-valent aluminium. According to Bozkurt et al. (1998), pentlandite has a higher rest potential than pyrrhotite so when they are both present in solution, a galvanic cell is formed where pentlandite acts as the cathode while pyrrhotite becomes the anode. The sorption and subsequent reductive deposition of dissolved Au likely occurred on the cathode (pentlandite) while the anode (pyrrhotite) was dissolved. A similar phenomenon was observed by Jeon et al. (2018) between metallic copper and aluminium in their studies on Au extraction from crushed printed circuit boards in thiosulfate solutions. Galvanic interactions of pentlandite and pyrrhotite could also explain the observed high dissolved Fe concentrations measured in solution for adsorption experiments at acidic pH shown in Figure 19. Figure 27 (b) shows a metallic characteristic of gold on the iron sulphide adsorbent.

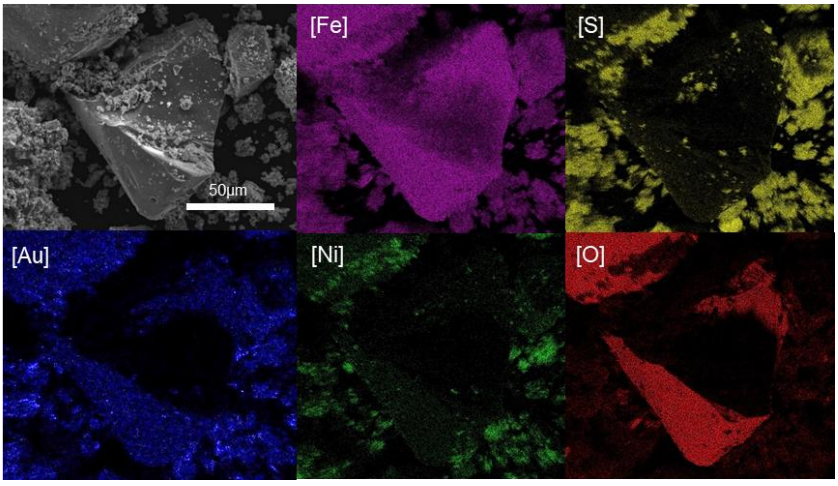

(a)

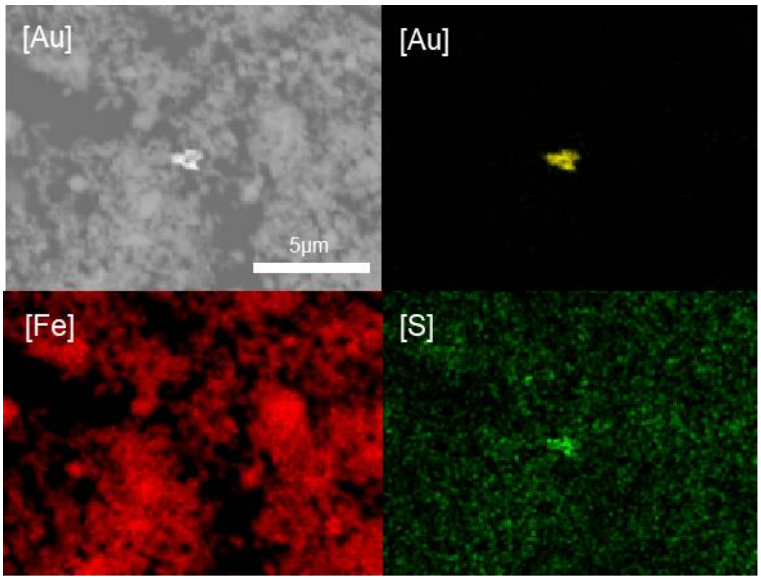

(b)

Figure 27. (a) SEM photomicrograph of magnetic sulphide sample, and the elemental maps of Au, Fe, Ni, S and O after adsorption at 50µm. (b) Elemental maps of Au, Fe, and S at 5µm at 4000x magnification.

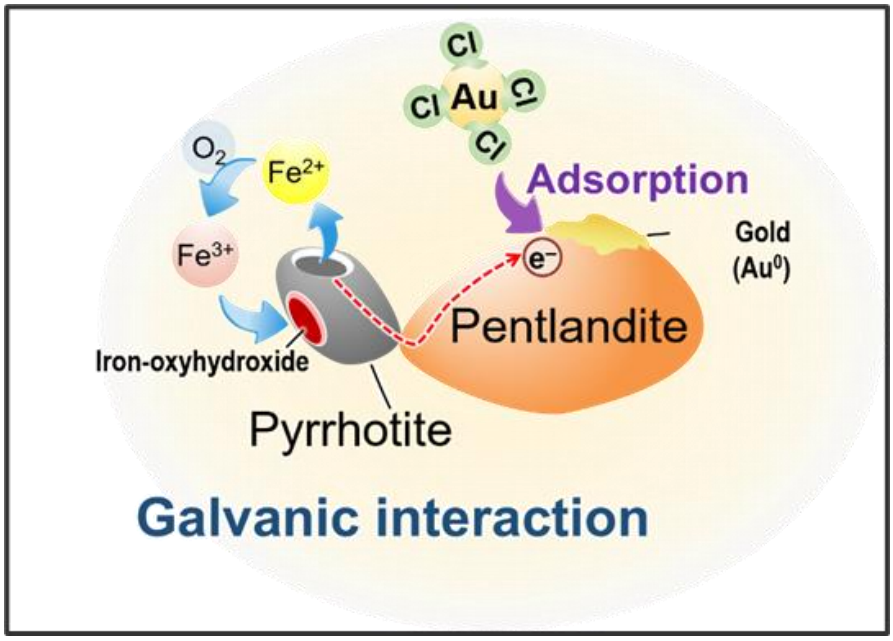

Figure 28. Reductive deposition of dissolved Au onto the pyrrhotite-pentlandite adsorbent via galvanic interaction.

IV.3.7. XPS Analysis

To further explore the primary mechanisms of Au recovery by the magnetic nickeliferous pyrrhotite adsorbent, Au speciation after adsorption was quantified by XPS. Figure 29 depicts the narrow scan spectrum of Au 4f orbital of the loaded magnetic nickeliferous adsorbent where a doublet in the spectrum was observed due to spin-orbit coupling. These doublets (i.e., two consecutive peaks) dominated the Au spectrum and were centered at 83.84 eV ($Au4f_{7/2}$) and 89.0 eV ($Au4f_{5/2}$). This high-resolution narrow scan Au spectrum was deconvoluted using a true Shirley background and 80%-20% Gaussian-Lorentzian peak model.

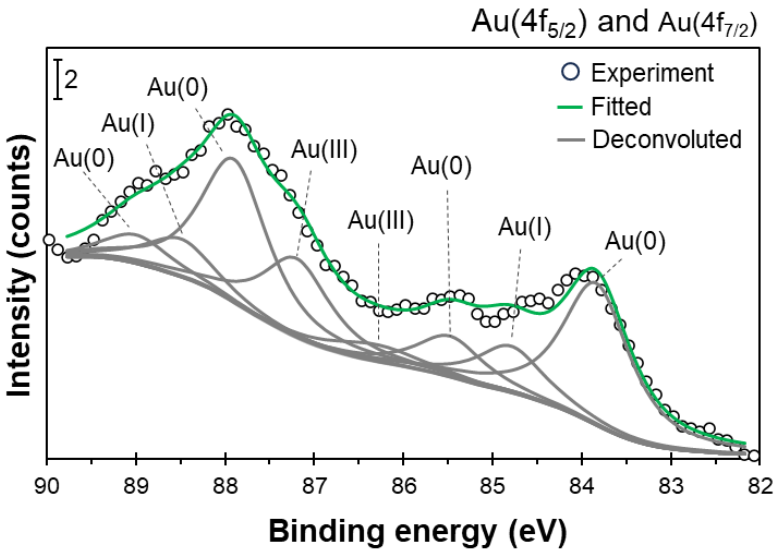

Figure 29. XPS narrow scan spectrum of pyrrhotite after the adsorption experiments with Au.

The deconvolution results identified three oxidation states of Au on the loaded adsorbent (Table 6): (i) Au(III) (87.2 and 86.32 eV) (Liu et al., 2021; Odio et al., 2014), (ii) Au(I) (88.5 and 84.8 eV) (Odio et al., 2014), and (iii) Au(0) (89.0, 87.9, 85.48 and 83.84 eV) (Odio et al., 2014). The presence of Au(III) on the loaded adsorbent could be attributed to direct adsorption of Au(III)-Cl complexes, the dominant Au species used in the adsorption experiments. Meanwhile, the detection of Au(I) and Au(0) by XPS suggests that reduction of Au(III) was another important Au recovery mechanism

by the adsorbent. By calculating the area of each deconvoluted curve, the relative abundances of the three Au oxidation states on the loaded adsorbent could be estimated. The results show that ~65% of recovered Au was in its elemental form or native state (Au(0)), suggesting that the magnetic nickeliferous pyrrhotite adsorbent recovered the majority of Au ions via reductive precipitation or cementation. This ability of the adsorbent to reduce Au(III) into Au(0) could be explained by galvanic interactions between pyrrhotite and pentlandite as explained earlier (Figure 28).

Table 6. XPS data and chemical states of Au on pyrrhotite after adsorption experiments.

Spectral Peak	Binding Energy (eV)		FWHM (eV)		% Abundance	Chemical State	Reference
	This study	Reference	This study	Reference			
Au(4f7/2)	83.84	84	0.9	-	26.1	Au(0)	Odio et al. (2014)
Au(4f7/2)	84.8	84.8	0.9	-	8.6	Au(I)	Odio et al. (2014)
Au(4f7/2)	85.48	85.4	0.9	-	7.6	Au(0)	Odio et al. (2014)
Au(4f7/2)	86.32	86.7	1.22	-	4.4	Au(III)	Liu et al. (2021)
Au(4f5/2)	87.2	87.4	0.9	-	14.6	Au(III)	Odio et al. (2014)
Au(4f5/2)	87.9	87.9	0.9	-	26.5	Au(0)	Odio et al. (2014)
Au(4f5/2)	88.5	88.5	0.9	-	7.0	Au(I)	Odio et al. (2014)
Au(4f5/2)	89.0	89	0.9	-	5.3	Au(0)	Odio et al. (2014)

Note: "-" means not reported

IV.3.8 Desorption studies

Different eluants were used in the desorption of Au from the loaded magnetic particles including HNO_3, thiourea, H_2SO_4, and glycine at 4 h and 24 h contact time as summarized in Table 7 below. In the acidic environment, 0.5M HNO_3 eluant did not desorb Au but rather, the adsorbent may undergo oxidation resulting in the dissolution of Fe and Ni. As discussed in the previous chapters, thiourea at lower pH has proven to have strong affinity to Au in the solution where Fe^{3+} acts as oxidant in the formation of cationic Au-thiourea complex as shown in Eq 12 and Eq 13 (Li and Miller, 2006). At varied concentrations of thiourea, from 0.7M to 1.75M at pH 7 to pH 8.5, Au recovery was found to be at 33.0%Au to 33.69% which are about similar and within experimental error at. Higher %Au recovery obtained from the mixture of 1.0M thiourea in 1.0M H2SO4 at pH<1 where 36.36%Au was achieved. This result coincided with the studies of Li et. al., where the optimum pH for thiourea leaching was at the range of pH 1-2. However, dissolution of Fe and Ni was also observed in this condition at 461.34ppm and 5.72 ppm respectively and may affect adsorbent's adsorption capacity and reusability. This phenomenon can be eliminated by surface modification which is not included in this study. Surface modification can be conducted by coating of the magnetic core with the use of silica, alumina, or other metal oxides as well as organic polymers/non-polymers followed by modification or functionalization (Giakisikli, et.al. 2013). Silica gel coating is the most prominent coating material for magnetite because of its mechanical and chemical stability as well as thermal resistance under various conditions (C.F.Poole, 2003). Silica-Fe_3O_4 nanoparticles functionalized with Tris(2-aminoethyl) amine (TREN) was prepared after the activation of iron oxide surface with NaOH solution and subsequent reaction with silane agents. The prepared TREN-Fe_3O_4 were used in selective extraction of trace elements such as Ag(I) and Au(III) from natural waste water streams (Zhad, H.R., et. al.,2003). Moreover, the authors presented the use of 2 mol/L HCl and 0.1mol/L thiourea in 1 mol/L H_2SO_4 were the best eluents for silver gold ions with a preconcentration factors of 142 and 125 for silver and gold respectively.

Table 7. Desorption of gold from nickeliferous pyrrhotite adsorbent.

Eluent	Desorption Time, hr	pH	Gold		
			%Au Desorbed	Fe, ppm	Ni, ppm
0.5 M HNO_3, 4h	4	0.98	0.00	35.04	5.54
0.7 M thiourea, 4h	4	7.78	31.15	0.00	0.30
0.7 M thiourea, 24h	24	7.05	33.42	0.00	0.50
1.0 M thiourea, 4h	4	7.68	33.69	0.00	0.60
1.0 M thiourea, 24h	24	8.48	33.08	0.34	0.50
1.75 M thiourea, 2h	4	8.22	33.20	0.00	0.28
1.75 M thiourea, 24h	24	7.33	33.38	3.24	0.56
0.5 M thiourea in 0.5 M H_2SO_4, 4h	4	1.14	36.36	400.96	5.02
1.0 M thiourea in 1.0 M H_2SO_4, 4h	4	0.86	35.28	461.34	5.72
0.5 M glycine, 24h	24	5.89	0.00	5.84	8.76
1.0 M glycine, 24h	24	6.04	0.00	10.20	4.50

IV.4 Summary

Recycling, reuse and repurposing of waste materials generated by mining and minerals industry are considered to be eco-friendly and cost-effective solutions for managing mining wastes. One of the most promising routes is the utilization of mine wastes as adsorbent material for the recovery of gold and other precious metals from aqueous solutions. This work investigated the potential of a magnetic nickeliferous pyrrhotite recovered from the tailings of a nickel sulphide mine to adsorb Au from chloride solutions. XRD and XRF results indicated that the sample was composed of about 65% pyrrhotite and 32% pentlandite with other impurities. Adsorption experiments using a simulated gold chloride solution were conducted to study the effects of pH, contact time, initial Au concentration and Cl− concentrations on Au adsorption. The results showed that Au uptake was very fast, achieving 100% Au recovery after 15 min of contact time at pH <5.5. The results also elucidated that the magnetic nickeliferous pyrrhotite adsorbent has excellent Au loading capacity with complete Au recovery attained even after several re-use. The presence of pyrrhotite and pentlandite in the adsorbent was believed to be beneficial for Au recovery. Galvanic

interaction was discussed as the possible mechanism for Au uptake. This finding is supported by further examination using XPS analysis where Au(III) was detected as direct adsorption while Au(I) and Au(0) are reduced or cemented onto the magnetic particle. The mixture of thiourea and H_2SO_4 was the promising eluant in the desorption of Au from the loaded adsorbent that recovered about 36.36% Au. The results strongly demonstrate the potential of the magnetic nickeliferous pyrrhotite from mine wastes as an effective and low-cost adsorbent for Au.

Chapter 5

Magnetic Adsorbent from Mine Tailings for the Recovery of Platinum Group Metals (PGMs) from Chloride Solution

This chapter discusses the effectiveness of magnetic iron sulphide from mine tailings to recover platinum group metals such as platinum, palladium, and rhodium from chloride solution using magnetic solid phase extraction (MSPE) method.

V.1. Introduction

Platinum Group Metals consists of platinum, palladium, and rhodium are highly valuable and economically significant elements due to their unique physical properties, chemical reactivity, and potential applications in catalysis (Kim et al., 2010, Karim and Ting, 2021, Nikoloski and Ang, 2013, Syed, 2012, Aghaei et al., 2017a). PGMs excellent corrosion resistance and very stable to oxidation at high temperatures makes them indispensable in a wider range of applications(Ramesh et al., 2008, Rao and Reddi, 2000, Safarzadeh et al., 2018, Taninouchi et al., 2017, Uheida et al., 2006a, Zhao and Dai, 2014). For example, in an industrial automotive catalysis, platinum, palladium and rhodium were widely consumed to reduce or eliminate the production of harmful gases such as carbon monoxide and nitrous oxides (Lengke et al., 2006). The continuing demand for PGMs that is driven by their unique properties, coupled with limited resources available to satisfy the current practices may result a total depletion of these precious metals in the near future. Therefore, methods on the recovery and separation of precious metals from secondary sources such as electronic wastes (E-wastes), spent catalysts, etc. are required. For example, Au, Pt and Pd were recovered from spent catalysts and waste PCBs by cementation (Kim et al., 2010, Park and Fray, 2009). However, some metal impurities such as Cu, Fe, and Ni also co-precipitated which render the process more tedious and labour intensive. Solvent extraction method was also reported to recover Pt and Pd from waste PCBs and spent alumina catalysts (Paiva et al., 2017, Zhang and Zhang, 2014a). However, these methods are complicated and appropriate equipment handling must be ensured to avoid solute and reagent losses. Solid phase extraction (SPE) using magnetic particles as adsorbent such as magnetite was also investigated to recover precious metals from chloride solutions (Alorro et al., 2010, Calderon et al., 2019a, Homchuen et al., 2016, Uheida et al., 2006b) This method

is highly preferred and offers several advantages such as ease of preparation and operation, low environment impact, and low cost (Aghaei et al., 2017b, Giakisikli and Anthemidis, 2013a, Herrero-Latorre et al., 2015b). However, due to the complexity and overlapping properties, slow kinetics on precious metals uptake were observed. In addition, magnetite (synthetic) has limited application because of high cost of synthesis and modification. This means that cheaper, readily available and highly selective adsorbents with faster adsorption kinetics are needed for the application of magnetic adsorbent technology in an industrial scale.

Pyrrhotite, for instance, depending on its form could possess a relatively strong magnetic properties (Sagnotti, 2007). Pyrrhotite associated with other minerals such as pentlandite, chalcopyrite, and other sulphides are commonly found in waste rocks dumped along mine sites and of no value (Letina and Letshwenyo, 2018b, Peek et al., 2011a, Ritcey, 2005). From our previous work, we reported the effectiveness of mining waste iron sulphides, pyrrhotite-pentlandite magnetic adsorbent, which recovered 100% Au from chloride solution. Galvanic interaction was the potential adsorption mechanism where Au deposition occurred in cathode (pentlandite) while the anode (pyrrhotite) dissolves (Calderon et al., 2020). Hence in this work, a natural magnetic iron sulphide primarily consists of pyrrhotite-pentlandite from nickel-mine waste rocks was evaluated for its ability in the recovery of precious metals from chloride solutions. Recoveries were examined under various parameters such as pH, contact time, precious metals concentration, and chloride concentrations.

V.2 MATERIALS AND METHODS

V.2.1 Adsorbent Characterization

The magnetic iron sulphide adsorbent used in this study has been introduced/discussed in Chapter IV. The particle was obtained from a waste stockpile of a nickel sulphide mine located in Kambalda WA using a handheld magnet. Crushing and pulverization (C+PB, Rocklabs 2012) were conducted to reduce the particle size. The particle size distribution was determined using a laser sizer (Mastersizer 3000, Malvern) while the specific surface area and the porosity were quantified by Brunauer-Emmett-Teller (BET)-N2 and Barrett-Joyner-Halenda (BJH) methods (ASAP 2020, Micromeritics Instrument Co., USA). The zeta potential of the sample was determined

using a Zetasizer (Nano Z, Malvern Corporation, UK) at pH 1–12 and different chloride concentrations (0.01–1.0 mol/L). The chemical and mineralogical compositions of the sample were analysed by X-ray Diffraction (XRD, PANAnalytical, UK) and X-ray Flourescence (XRF, PANAnalytical, UK).

V.2.2 Precipitation, adsorption and desorption method

Reagent grade Platinum ($PtCl_3$), Palladium ($PdCl_2$) and Rhodium ($RhCl_2$) from Sigma Aldrich were used to prepare Pt, Pd, And Rh ions for simulated solutions. The sodium chloride (NaCl), hydrochloric acid (HCl), and sodium hydroxide (NaOH), nitric acid (HNO_3), sulfuric acid (H_2SO_4) and thiourea (CH_4N_2S) from Sigma Aldrich and Chem Supply were all of reagent grades.

Precipitation test was initially carried out to determine the degree of solubility of the prepared synthetic precious metals solution at different pH without adsorbent addition. Adsorption tests were conducted in batch mode to investigate the capability of the magnetic iron sulphide, which primarily contains pentlandite and pyrrhotite, to recover PGMs such as Pt, Pd, and Rh from chloride solutions. Platinum, palladium and rhodium concentrations were derived from e-waste solution (Sun et. al., 2016). A fixed 10 mL volume of sodium chloride (NaCl) solution at 0.1 mol/L containing single component of 5×10^{-5} mol/L PGMs concentration was transferred into a 250 mL Erlenmeyer flask. Solution pH was adjusted by the addition of freshly prepared HCl and NaOH solutions. The magnetic iron sulphide powder was then added in the mixture at 1% initial solid/liquid ratio. The prepared mixture was then shaken at a certain time interval in a water bath (ZWY-110x30, Labwit Scientific) at a constant rate of 140 strokes per minute and 25 °C. After a given contact period the mixture was membraned filtered using 0.20 µm syringe filters.

The solid particles were collected after adsorption, washed twice with deionised water, and oven dried for 4 hours. The dried particles were then examined to check the presence of PGMs on the surface using scanning electron microscope (MIRA 3 FE-SEM, Tescan Ltd., Czech Republic) and x-ray photoelectron spectroscopy.

Desorption experiments were conducted by preparing 30-mL of different eluents at initial concentrations of 0.5mol/L nitric acid, 0.7mol/L thiourea, 0.5mol/L thiourea in 0.5mol/L sulphuric acid, and 0.5 mol/L glycine. One gram of PM-loaded magnetic

particle was then added to the prepared solution was then shaken at 4h and 24h interval in a water bath shaker and then syringe filtered.

The concentrations of platinum (Pt), palladium (Pd), iron (Fe) and nickel (Ni) in the solution were analysed using Inductively Coupled Plasma – Optical Emission Spectrometry (5100 ICP-OES, Agilent).

V.3. RESULTS AND DISCUSSION

V.3.1 Adsorbent Characterization

The physical and chemical characteristics of the magnetic sulphide adsorbents were discussed in Chapter IV. Various characterization techniques were conducted such as XRD, XRF, BET, among others and are discussed further in Chapter IV.4.1. Using an XRF laser scan, the magnetic adsorbent was found to have 65% pyrrhotite, 32% pentlandite, and 3% other impurities with 49.15% Fe, 26.9% S, 12.2% Ni, and others. A particle size of D_{80} 86.36 µm and a specific surface area of 14.08nm was obtained using a laser sizer and BET-BJH method respectively.

V.3.2 Effect of Solution pH

V.3.2.a Precipitation Analysis

Initially, precipitation tests were conducted to determine the stability of platinum-group metals (PGMs) in chloride solution at different pH ranges. A 5×10^{-5} mol/L of PGMs in 0.10M NaCl solution was shaken for 24hours at different pH. As shown in Figure 30, platinum appeared to be stable and did not precipitate at any pH range while palladium and rhodium started to precipitate at pH 4 and 3.5 respectively. These results coincided well with the studies of Alorro et al. (2010) in the adsorption of gold, platinum, palladium, and rhodium at varied pH onto the synthetic and naturally-occurring magnetite adsorbent. It was also noted that Au is stable at any pH range and that the adsorption recovery is mainly determined by the difference of the initial and final Au solution concentration. Using the pH tests as the basis, the pH used in the succeeding tests in the adsorption of platinum, palladium, and rhodium in the simulated single component systems were pH <12, <4, and <3.5 respectively.

Palladium and rhodium in chloride solution typically form a complex such as $PdCl_4^{2-}$, $RhCl_6^{3-}$, etc.. When pH is raised by adding a base, hydroxide ions (OH^-) can replace

the chloride ligands leading to precipitation as palladium hydroxide and rhodium hydroxide. Precipitation reaction described by the following Equations 15 and 17. At higher temperatures or strong basic conditions, the formed palladium and rhodium hydroxides can undergo dehydration process by the equations 16 and 18:

$$PdCl_4^{2-} + 4OH^- \rightarrow Pd(OH)_{2(s)} + 4Cl^- \quad \text{(Eq 15)}$$

$$Pd(OH)_2 \rightarrow Pd(O)_{(s)} + H_2O \quad \text{(Eq 16)}$$

$$RhCl_6^{3-} + 6OH^- \rightarrow Rh(OH)_{3(s)} + 6Cl^- \quad \text{(Eq 17)}$$

$$2Rh(OH)_3 \rightarrow Rh_2O_{3(s)} + 3H_2O \quad \text{(Eq 18)}$$

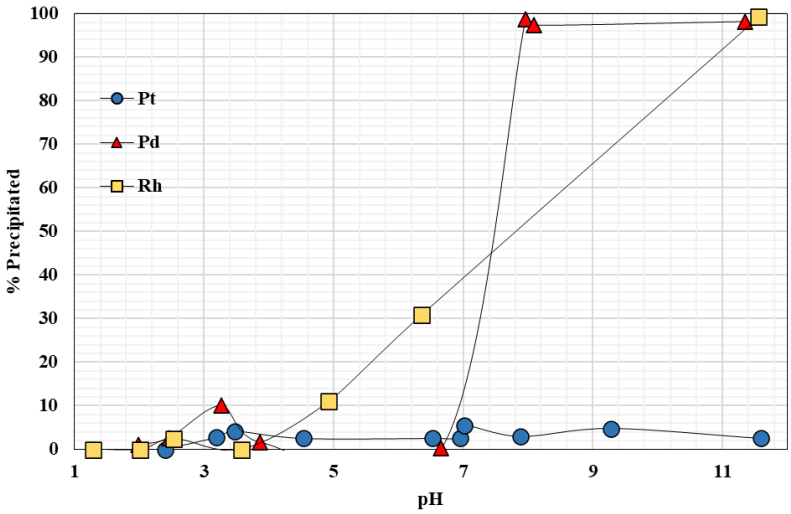

Figure 30. Precipitation analysis of PMs at different pH. Initial PMs concentration of 5×10-5 mol/L in 0.1 mol/L NaCl at 24h shaking time.

V.2.3.b Adsorption Tests

Adsorption experiments were conducted at different pH range with an initial Pt, Pd, and Rh concentration of 5×10-5 mol/L in 0.1 mol/L NaCl solution and adsorbent (magnetic iron sulphide) dosage of 0.1g. Figure 31 (a) presented the effects of solution pH on the adsorption of Pt, Pd, and Rh at pH<12, pH<4, and pH<3.5 respectively for 24 hours. Platinum showed an increasing recovery at lower pH and reached 100% at

pH 4 and plateaued to pH 12. The point of zero charge of iron sulphide dispersed in 0.1M NaCl as shown in the previous chapter (Figure 20) was at pH3.8. This suggests that the negatively charged platinum chloride complex ($PtCl_4^{2-}$) from Figure 32 is attracted to the positively charged adsorbent as pH approaches PZC. Complete recovery (100%) for palladium at pH 1-4, which means that the extraction efficiency of Pd is high in acidic conditions. The prepared adsorbent has an initial Fe content of 49.16% Fe (XRD assay results) equivalent to 491600 ppm. Therefore, the highest dissolution of Fe at low pH from Figure 31(b) during adsorption process was at a range of 0.7%-1.0% Fe.

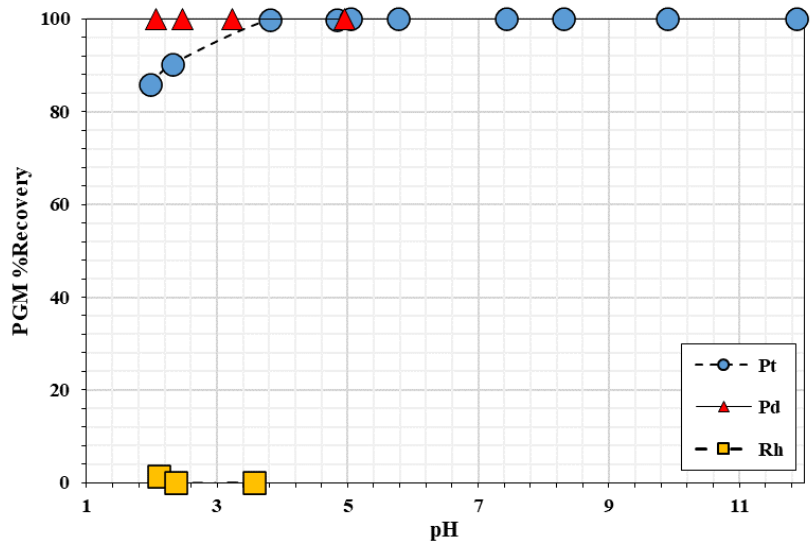

(a)

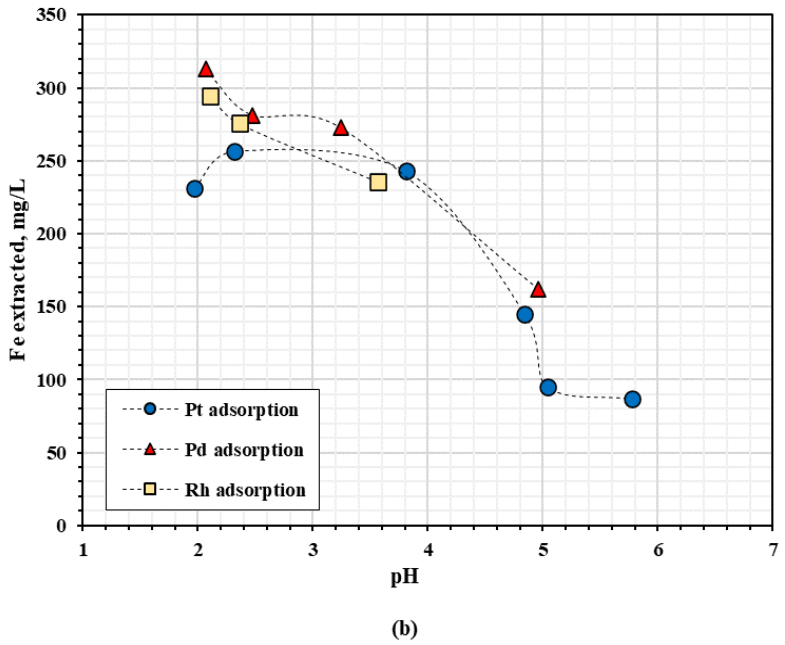

Figure 31. (a) Effect of solution pH on the recovery of PGMs from 0.1M chloride solution. (b) Amount of Fe removed. Conditions: 0.1M chloride, initial 10 ppm PMs, 24H contact time, 0.1g pyrrhotite.

The Eh-pH diagram shown in Figure 32 shows the graphical representation of the thermodynamic stability of PGM-chloride species in solution at 25°C. In the acidic environment (low pH), the PGMs may form various chloride complexes depending on their oxidation states such as $PtCl_6^{2-}$, $PdCl_4^{2-}$, $PdCl_6^{2-}$, and $RhCl_6^{3-}$. As the pH increases (becomes more alkaline), chloride may start to be replaced by hydroxide ions (OH^-) as the coordination environment around the PGM ions changes leading to the formation of hydroxy complexes and are often more stable compared to their chloro- counterparts. These hydroxy ions will tend to compete with chloride ions to complex with PGMs in solution making the charge more positive (Mahmoud, 2003). Therefore, the high recovery of Pt and Pd at lower pH can be attributed by this phenomenon where hydroxy ions present in the solution are minimal. Rhodium on the other hand, showed very low recovery. According to the studies of (Morisada et al., 2012, Cozzi and Pantani, 1958, Benguerel et al., 1995), in order to achieve a more negative Rh-chloride complex, it needs to create a higher Cl-ligands which can be done by increasing chloride concentration in the solution (>0.1M). Thus, in this study, 0.1M chloride concentration may not be enough to create a desirable rhodium-chloride complex for adsorption at lower pH to occur.

The high amount of iron removed from the magnetic iron sulphide adsorbent in the acidic region as shown in Figure 31 (b) is attributed to the oxidative dissolution of Fe. This suggests that Fe is extremely soluble at pH 1-2 followed by a slower dissolution until it reached a stable dissolution plateau as shown in Figure 31(b) on Pt adsorption. Similar oxidative dissolution of Fe dust samples where the dissolution kinetics of Fe may depend on the degree of weathering the mineral composition of Fe particles (Shi et al., 2011).

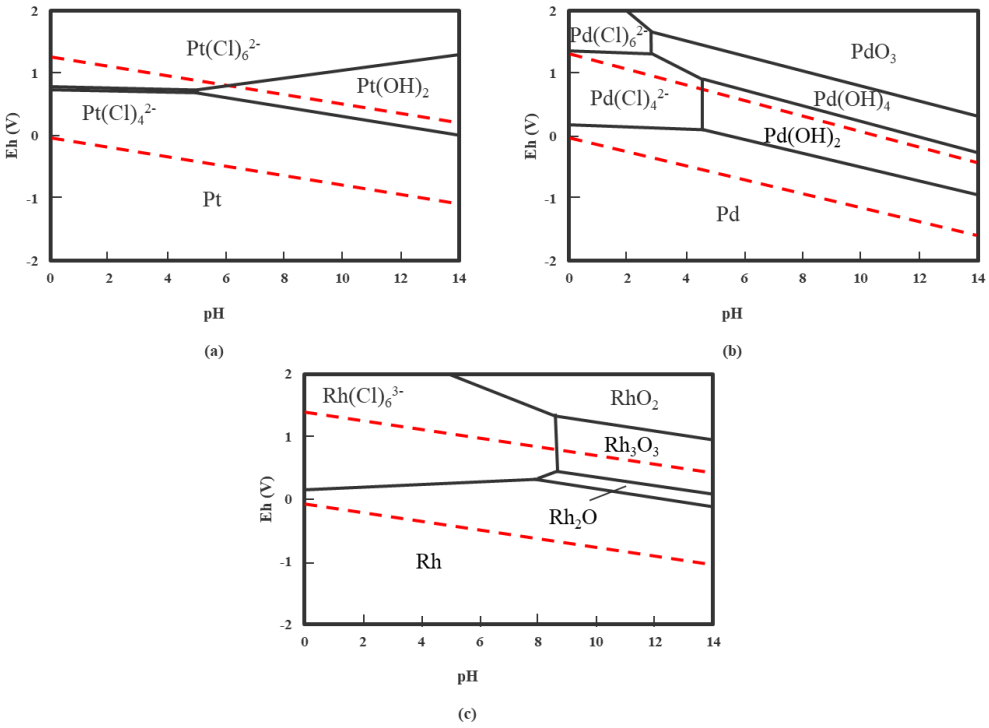

Figure 32. Eh-pH diagram of (a) Pt-Cl-H_2O and (b) Pd-Cl-H_2O systems. Metal concentration 10^{-5} M, Cl- concentration 10^{-1} M, at 25°C (Mahmoud, 2003).

V.3.3 Effect of adsorption time

The effect of adsorption time was investigated at an initial concentration of $5x10^{-5}$ mol/L of Pt, Pd, and Rh in 0.1M NaCl with 0.1g of the magnetic iron sulphide adsorbent at pH 1-12, pH<4, and pH<3.5 respectively and were shaken at varied contact time intervals.

Figure 33 showed that palladium uptake was fast, reaching 100% recovery after 1 h. At lower pH, the adsorbent may have a surface charge that interacts favorably with Pd-Cl complex leading to faster adsorption. Although slower compared to palladium, platinum adsorption occurred at an increasing rate achieving 100% recovery after 24 h contact time. Pt-Cl onto adsorbent may have a slower kinetics of complex formation, and the adsorbent surface may become saturated with chloride ions thereby reducing the availability of adsorption sites for platinum. Rhodium on the other hand, indicated a very low recovery of only about 10.6% after 72 hours contact time which can be attributed to low chloride concentration as discussed previously. Since rhodium showed very low recovery, the succeeding investigations were only focused on platinum and palladium.

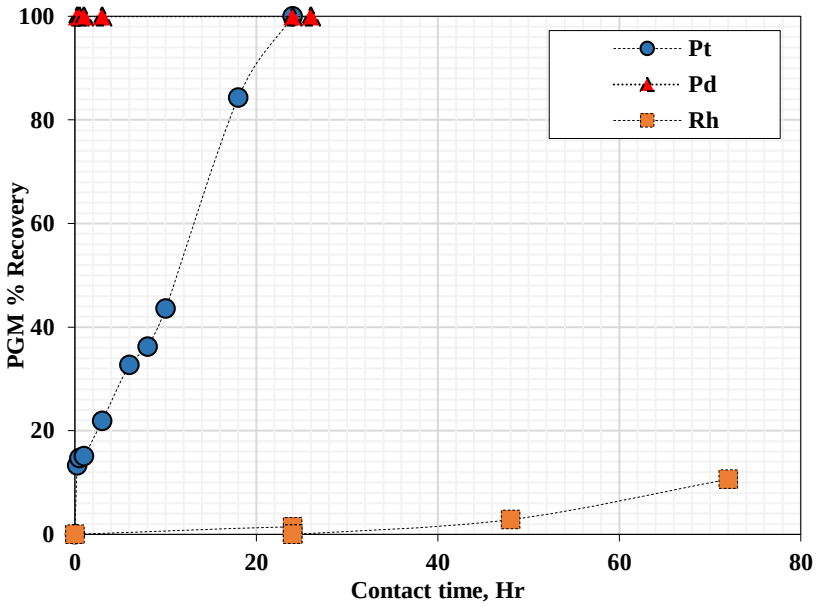

Figure 33. Effect of contact time. Conditions are: 0.1 M NaCl, initial $5x10^{-5}$ mol/L PMs, pH <5, 0.1g of the prepared magnetic iron sulphide adsorbent.

V.3.4 Effect of Initial PMs Concentration

The effect of initial PGMs concentration in the adsorption capacity was examined by varying the Pt and Pd concentration in the solution at the range of $5x10^{-5}$ mol/L to $5x10^{-4}$ mol/L in 0.1M HCl solution at pH<5 with the addition of 0.1g magnetic iron sulphide. The contact times considered for adsorption tests were the ones giving 100% recovery – 24 hours for Pt and 1 hour for Pd. At 100% recovery, the maximum uptake of Pt was 11.7µmol/g (2.3 mg Pt/mg) after 24 H contact time, while Pd was 23.66µmol/g (2.5 mg Pd/g) after 1 H contact time as shown in

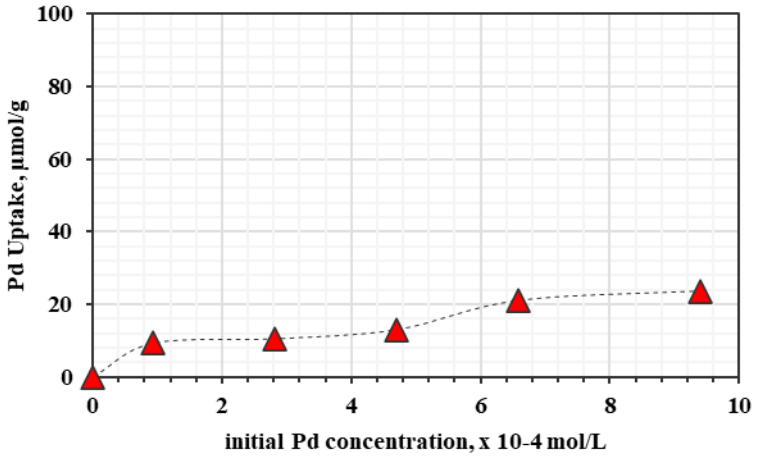

(b)

Figure 34 (a-b).

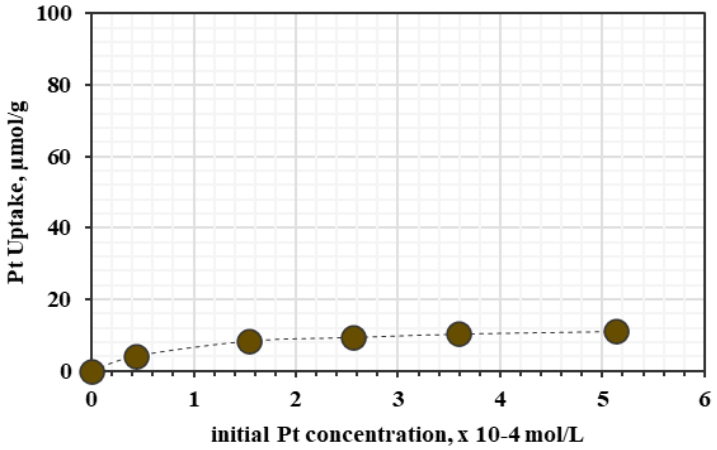

(a)

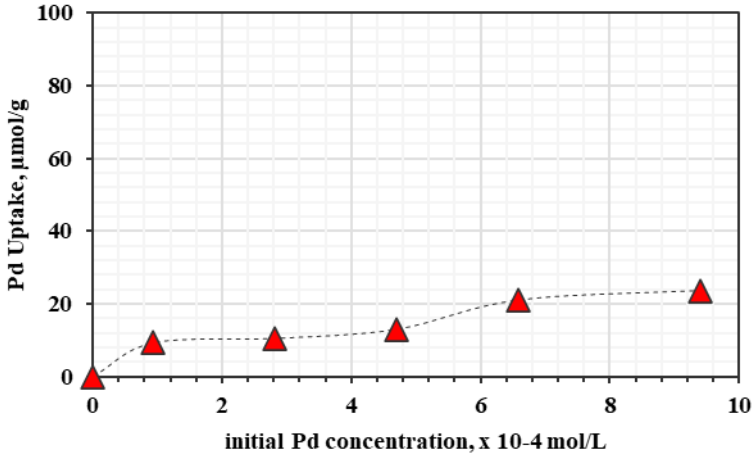

(b)

Figure 34. (a) Effect of initial Pt concentration (0.10 M NaCl, pH <5, 0.1g pyrrhotite, 24H contact time). (b) Effect of initial Pd concentration (0.10 M NaCl, pH <5, 0.1g pyrrhotite, 1 H contact time).

The adsorption isotherms are known through specific constants values. The obtained constants indicate the surface features of the adsorbent and their tendency towards it. Langmuir and Freundlich isotherm models express the adsorption of the precious metal's molecules on surfaces of the nickeliferous pyrrhotite adsorbent follows the homogenous and heterogenous approaches respectively. Under optimized conditions, the correlation coefficient (R^2) of Freundlich model was higher than the correlation coefficient (R^2) for the Langmuir model for Pd uptake (0.90 vs 0.82). This suggests that the adsorption occurs through a series of layers of adsorbate molecules on the surface, rather than just a monolayer. The heterogenous surface properties of the magnetic adsorbent such as surface charge and surface area, can influence the interaction between the adsorbent and Pd that contributes to the non-linear adsorption behavior. In this study, palladium adsorption onto the magnetic iron sulphide adsorbent could potentially be characterized by a multilayer adsorption mechanism with a maximum adsorption capacity of 4.64 mg/g. On the other hand, Pt uptake favors the Langmuir isotherm and signifies a monolayer adsorption characteristic with a maximum adsorption capacity of 2.14mg/g as shown in Table 8.

Table 8. Equilibrium adsorption isotherms for Pd and Pt ions onto nickeliferous pyrrhotite. Initial Pd and Pt concentration: 5×10^{-5} mol/L to 5×10^{-4} mol/L; Contact time: 4 h for Pd, and 24 h for Pt, pH: <5, adsorbent dosage: 0.1 g, and temperature 25 ºC.

Analyte	Langmuir			Freundlich		
	qm (mg/g)	*KL (L/mg)*	*R2*	*n*	*KF (L/mg)*	*R2*
Pt	2.14	1.06	0.99	9.60	1.11	0.96
Pd	4.62	0.02	0.82	1.37	2.08	0.90

V.3.5 Effect of Chloride Concentration

The presence of chloride ions can have a significant effect on the adsorption of platinum and palladium onto the prepared iron sulphide magnetic particle. The behavior depends on various factors including the nature of the magnetic particles, oxidation states of Pt and Pd, and the specific experimental conditions. In this study, the effect of chloride concentrations is carried out by varying the initial chloride concentration between 0.01M NaCl, $5x10^{-5}$ mol/L Pt/Pd, pH<5 with 1.0g adsorbent added in the solution at shaking times; 24 h for Pt and 1h for Pd. Results showed a decrease in Pt and Pd recovery as amount of chloride concentration increases which suggests that the chloride concentration may alter the overall solution chemistry including changes in redox potential. These changes can impact the solubility and speciation of Pt and Pd, influencing their low adsorption behavior (

Figure 35). Moreover, iron sulphide magnetic particle may have a limited number of active sites available for adsorption. As chloride ions increases, the available sites may become saturated with chloride ions, reducing the sites for Pt and Pd adsorption

(Mahmoud, 2003). This findings coincide well with our previous work where Au(II) uptake decreases as Cl^- ions increases in the solution (Calderon et al., 2020).

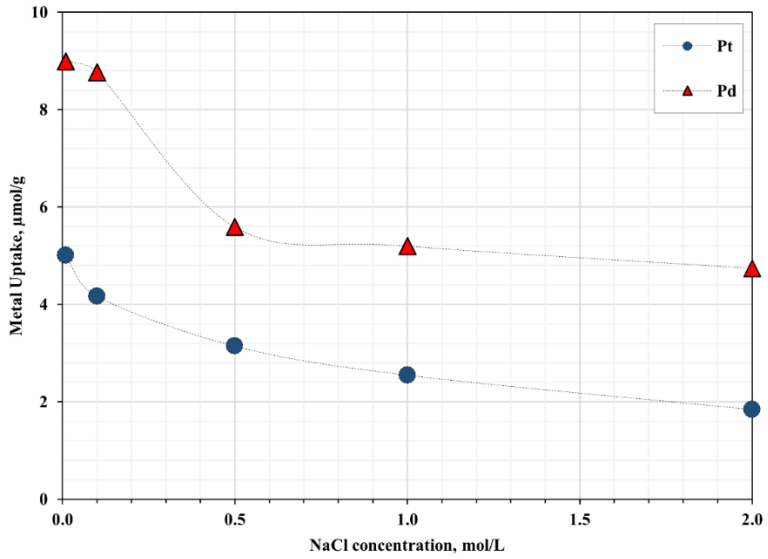

Figure 35. Effect of chloride concentration on Pt and Pd uptake onto the magnetic pyrrhotite adsorbent (Pt: 0.1g adsorbent, pH<5, 24 hr contact time; Pd: 0.1g adsorbent, pH<5, 1hr contact time)

V.3.6 SEM Analysis

SEM analysis and EDX elemental mapping of the PGM-loaded adsorbent after adsorption were conducted to determine the details of the surface morphology and the elemental association of platinum and palladium onto the magnetic iron sulphide at 50µm resolution. From the XRD report in Chapter IV, the prepared magnetic iron sulphide consists primarily of pentlandite and pyrrhotite. The elemental mapping distribution of Pt and Pd shown in Figure 36 (a-b) revealed that both are strongly associated with Ni, S, and Fe which suggests a galvanic interaction. The same observation was observed in the adsorption of Au discussed from the previous chapter where the deposition of dissolved gold occurred on the cathode (pentlandite) while the anode (pyrrhotite) is dissolved as shown in Figure 28.

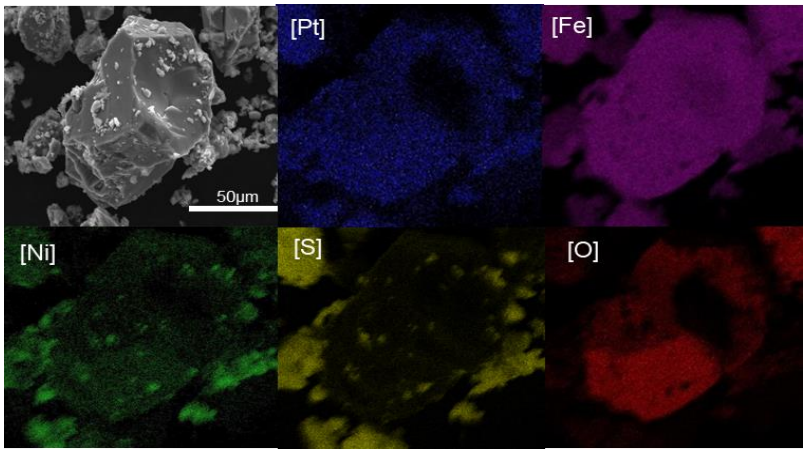

(a)

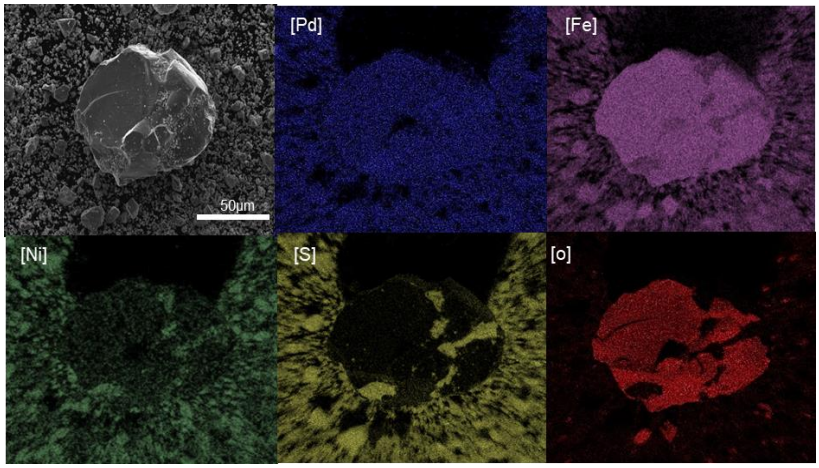

(b)

Figure 36. SEM photomicrograph of magnetic sulphide sample, and the elemental maps of (a) Pt, (b) Pd, with Fe, Ni, and S after adsorption.

V.3.6 XPS Studies

To further support the adsorption mechanism of Pt and Pd recovery by the magnetic iron sulphide, a quantification of species by XPS after adsorption was conducted. A high-resolution scan of Pt and Pd was deconvoluted using a true Shirley background and 80%-20% Gaussian-Lorentzian peak model. Results are discussed in the following sub section.

V.3.6.a XPS of Platinum loaded adsorbent

The deconvoluted plots identified three oxidation states of Pt as shown in Figure 37 and Table 9 which includes (i) Pt(IV) (78.7 and 75.4 eV) (Lengke et al., 2006), (ii) Pt(II) (76.7 and 73.4 eV) (Lengke et al., 2006), and Pt(0) (75.0 and 71.7 eV) (Lengke et al., 2006). The presence of Pt(IV) (as the initial Pt species in the adsorption experiments) could be attributed to direct adsorption of Pt(IV)-Chloride complexes on the magnetic adsorbent. Meanwhile, the identification of Pt(II) and Pt(0) suggests a reduction of Pt(IV) before adsorption. The relative abundance of each oxidation state was determined by calculating the area of their corresponding deconvoluted curves, and the results indicate that ~15% of the recovered Pt was in its elemental form Pt(0) while ~60% was the result of reduction of Pt(IV) to Pt(II) followed by adsorption. These results suggest that the recovery of Pt ions by the magnetic adsorbent was controlled by both adsorption and reductive precipitation or cementation. The XPS findings are also supported by the adsorption results (see Table 8); that is Pt recovery by the magnetic adsorbent was dominated by adsorption. For the reduction of Pt (IV) to Pt(II) and Pt(0), one possible mechanism to explain this phenomenon is galvanic interaction between pyrrhotite and pentlandite (Calderon et al., 2020).

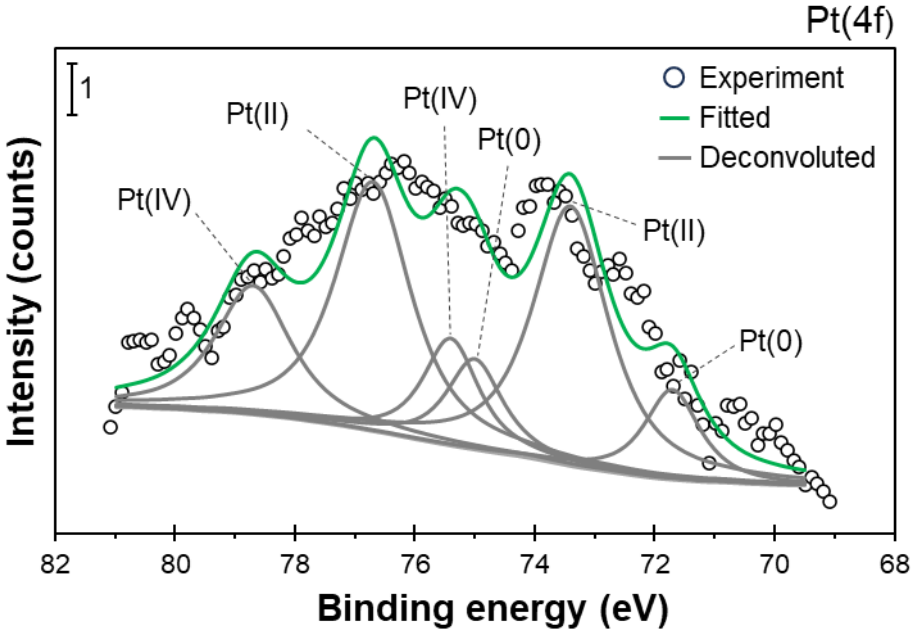

Figure 37. XPS narrow scan spectrum of magnetic iron sulphide after the adsorption experiments with platinum.

Table 9. XPS data and chemical states of Pt on magnetic iron sulphide after adsorption experiments.

Spectral Peak	Binding Energy (eV)		FWHM (eV)		% Abundance	Chemical State	Reference
	This study	Reference	This study	Reference			
Pt(4f)	71.7	71.7	1.1	1.1	7.7	Pt(0)	Lengke et al. (2006)
Pt(4f)	73.4	73.4	1.5	1.5	30.6	Pt(II)	Lengke et al. (2006)
Pt(4f)	75	75	1.1	1.1	7.8	Pt(0)	Lengke et al. (2006)
Pt(4f)	75.4	75.4	1.1	1.1	9.3	Pt(IV)	Lengke et al. (2006)
Pt(4f)	76.7	76.7	1.5	1.5	29.4	Pt(II)	Lengke et al. (2006)
Pt(4f)	78.7	78.7	1.5	1.5	15.2	Pt(IV)	Lengke et al. (2006)

V.3.6.b XPS analysis of palladium-loaded adsorbent

A doublet was observed in the narrow scan spectrum of Pd 3d orbital and was found to be centered at 335.7 eV ($Pd3d_{3/2}$) and 342.7 eV ($Pd3d_{5/2}$) shown in Figure 38. The deconvoluted results identified three oxidation states of Pd which include: (i) Pd(IV) (338.3 and 343.45 eV) (Li et al., 1997), (ii) Pd(II) (337.9 and 339.2 eV) (Hyland and Bancroft, 1990), and (iii) Pd(0) (335.7 and 342.7 eV) (Li et al., 1997). The detection of Pd(IV), Pd(II) and Pd(0) on the surface of magnetic adsorbent suggest that both adsorption and cementation contributed to the recovery of Pd similar to the phenomenon observed with Pt.

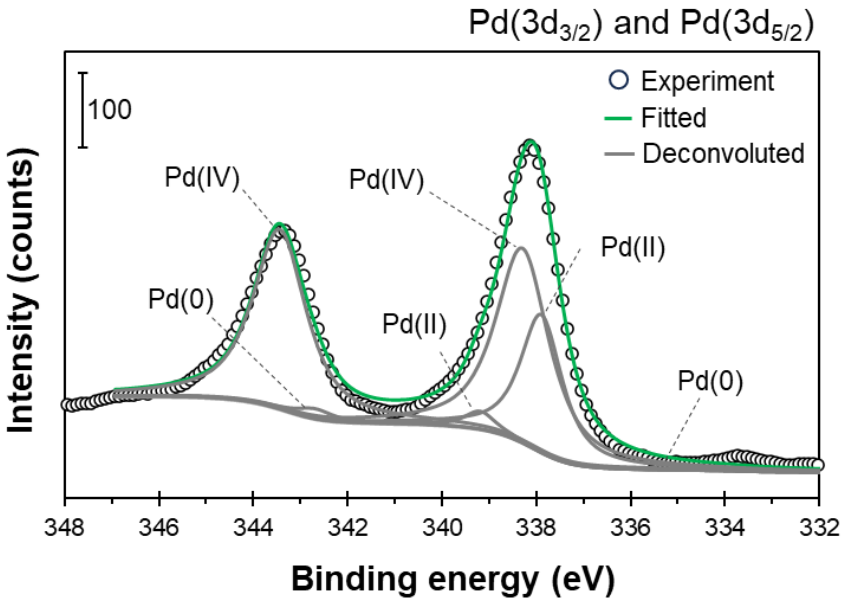

Figure 38. XPS narrow scan spectrum of magnetic iron sulphide after the adsorption experiments with palladium

Table 10. XPS data and chemical states of Pd on magnetic iron sulphide after adsorption experiments.

Spectral Peak	Binding Energy (eV)		FWHM (eV)		% Abundance	Chemical State	Reference
	This study	Reference	This study	Reference			
Pd(3d3/2)	335.7	335.5	0.9	-	0.01	Pd(0)	Li et al. (1997)
Pd(3d3/2)	337.9	337.9	1.06	-	21.7	Pd(II)	Hyland and Bancroft (1990)
Pd(3d3/2)	338.3	338.3	1.35	-	39.1	Pd(IV)	Li et al. (1997)
Pd(3d3/2)	339.2	339.2	0.77	-	2.02	Pd(II)	Hyland and Bancroft (1990)
Pd(3d5/2)	342.7	342.7	0.9	-	1.32	Pd(0)	Li et al. (1997)
Pd(3d5/2)	343.45	343.3	1.35	-	35.9	Pd(IV)	Li et al. (1997)

Note: "-" means not reported

V.4 Desorption studies

Desorption experiments were conducted to determine the effectiveness of different reagents to releaseadsorbed platinum and palladium from the loaded magnetic iron sulphide adsorbent. 30mL of different eluents like nitric acid (HNO_3), thiourea in sulfuric acid (H_2SO_4 + thiourea), and glycine solutions at varied concentrations from 0.5mol/L to 1.75 mol/L with different contact time (2h and 4h only) were used to study possible maximum recovery of selected precious metals. Uheida and company presented the use of HNO_3 as successful in eluting all metal ions. However, 0.5 M HNO_3 as eluant showed very minimal or no recovery for Pt and Pd (Table 11). Thiourea as eluant was used at different concentrations. The 0.5M thiourea in 0.5M H_2SO_4 eluant at 4h contact time eluted about ~11% of platinum however, at very low pH, significant amount of Fe and Ni dissolution occurred. The same scenario appeared when using 1.0M thiourea in 1.0M H_2SO_4 (Figure 39). The promising eluant for Pt desorption was found to be 1.0 M thiourea, not much difference between 4h and 24h contact time, where 6.71-6.8%Pt desorbed with very minimal Fe and Ni dissolution. The best desorption efficiency of Pd was when 1.75M thiourea was used where 15.63%Pd was desorbed. Glycine, which is known to speed up leaching of gold-copper ores during cyanidation (Oraby et al., 2017), showed very minimal desorption for Pt (~0.38%) and no Pd. It is noted that the desorption aspect in this study requires further investigation and optimization. The high PGM with high Fe and Ni dissolution from the loaded particle at lower pH suggests that the naturally occurring magnetic particle has high susceptibility to oxidation hence, surface modification is needed i.e. coating with organic/inorganic functional groups, to improve sorption capacity which is not included in this study.

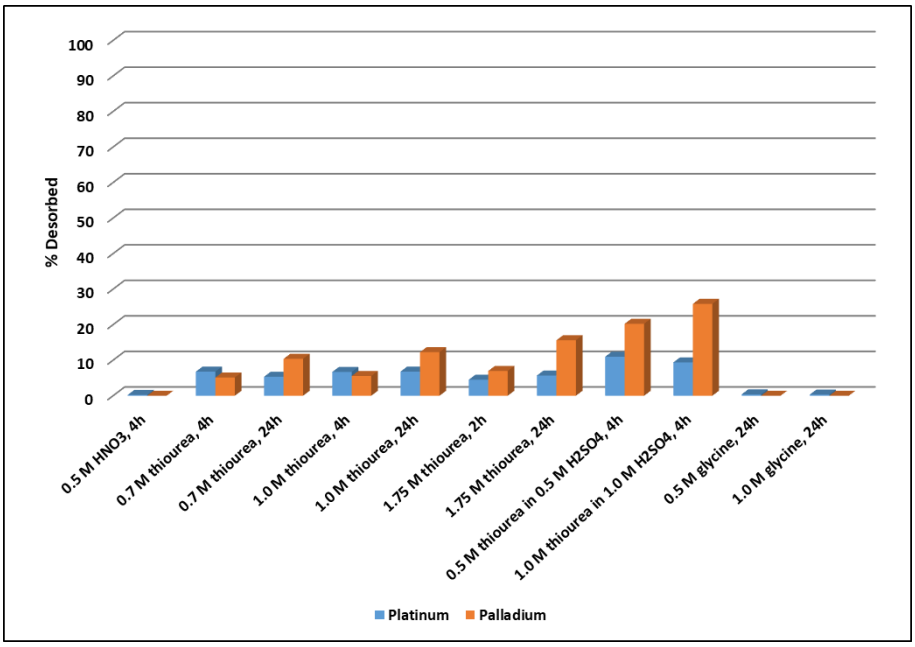

Figure 39. Amount of Pt and Pd desorbed using different eluents after 4h and 24 h contact time (30mL eluant, 1.0g loaded adsorbent).

Table 11. Desorption of platinum and palladium from loaded nickeliferous pyrrhotite adsorbent.

Eluent	Desorption Time	Platinum			Palladium		
		%Pt Desorbed	Fe, ppm	Ni, ppm	%Pd Desorbed	Fe, ppm	Ni, ppm
0.5 M HNO_3	4	0.23	24.67	1.03	0.00	65.96	7.48
0.7 M thiourea	4	6.79	0.00	0.04	5.13	0.00	0.90
	24	5.36	1.06	1.02	10.39	0.00	0.18
1.0 M thiourea	4	6.71	0.00	0.06	5.57	0.00	1.02
	24	6.80	0.00	0.20	12.27	0.00	0.24
1.75 M thiourea	4	4.51	0.00	1.32	6.98	0.00	0.50
	24	5.70	0.00	0.28	15.63	0.00	0.26
0.5 M thiourea in 0.5 M H_2SO_4	4	10.99	335.12	3.78	20.26	411.88	5.90
1.0 M thiourea in 1.0 M H_2SO_4	4	9.39	412.04	4.40	25.87	562.60	7.70
0.5 M glycine	24	0.38	3.64	1.44	0.00	1.12	1.36
1.0 M glycine	24	0.34	11.24	1.58	0.00	2.32	1.76

V.4 Summary

Platinum and palladium are very important metals in this modern fast-changing era. This study investigated a method of recovering these platinum group metals from aqueous solution via MSPE process using a magnetic adsorbent derived from wmine wastes. Pyrrhotite-based magnetic adsorbent obtained from mine tailings t was utilized as adsorbent to achieve an environment-friendly solution in handling mine waste products. Using XRF and XRD, the obtained particle composed of 56% pyrrhotite, 32% pentlandite, and 3% other impurities. Particle size was found to be D80 86.36 µm with a specific surface area of 14.08nm. Palladium uptake was fast with 100% recovered after 30 minutes contact time at pH<3 with maximum uptake of 23.66µmol/g of adsorbent. Although slower than palladium, platinum reached maximum recovery after 24h contact time with maximum uptake of 11.7µmol/g. XPS studies suggests that the recovery of both Pt and Pd by the magnetic iron sulphide adsorbent were attributed by adsorption. Finally, the reduction of Pt(IV) to Pt(0) and Pd(IV) to Pd(0) can be explained by galvanic interaction between pyrrhotite and pentlandite (Calderon et al., 2020). Platinum achieved 6.71% - 6.8% recovery using 1.0M thiourea as eluant, while Pd recovered 15.63%. Desorption results in this study are suggested to undergo further investigation and optimization. The high Fe and Ni dissolution during desorption is attributed to the dissolution of metals at lower pH which can be eliminated by adsorbent functionalization or surface modification which is beyond the scope of this study.

Chapter 6

VI.1 General Conclusions and Recommendations

Magnetic solid phase extraction (MSPE) is a versatile technique that enhances the efficiency and accuracy of analytical processes across various fields. This method combines with the principles of solid-phase extraction (SPE) and is used in analytical chemistry for isolating and concentrating analytes from complex matrices. The main principle of MSPE is the utilization of magnetic particles (i.e. magnetite, functionalised magnetite, etc.) to selectively bind the target analytes. After the sorbents capture the analytes from the sample matrix, a magnetic field is applied to separate the sorbents (with bound analytes) from solution. The bound analytes are then eluted (desorbed) from the sorbents using an appropriate solvent for further analysis. The magnetic separation process in MSPE is quick and straightforward, reducing the time needed for sample preparation.

MSPE has wider applications such as in environmental analysis (pollutant detection, water quality monitoring, etc.), food and beverage testing (residue analysis, nutrient analysis, etc.), and other industrial applications. In this study, MSPE method is used as separation and purification technique in the recovery of precious metals such as Au, Pt, Pd, and Rh from aqueous solutions, and the effects of various parameters such as pH, contact time, PMs initial concentrations, chloride concentrations were investigated. This study also attempted to utilise mine tailings materials as adsorbents aiming to develop a more environment friendly and cost-effective process in the recovery of noble metals from solutions promoting circular economy, reduces the need for new resources and minimizes environmental impacts.

This thesis comprised of six chapters which details the purpose of this research and outcomes of the investigations. In chapter I, it presented the background of the study, its significance, and the objectives. This chapter discusses how precious metals such as Au, Ag, Pt, Pd, and Rh have played a significant role in human history and continue to be important in various aspects in modern life such as in electronics, automotive catalysis, medical applications, aerospace, among others. Significant increase in population coupled with urbanization and modernization resulted in the high demand of these precious metals. For example, frequent mobile phone updates generate massive amounts of end-of-life e-wastes. These e-wastes contains precious metals that are

higher than their respective ores. The high production of e-wastes poses environmental and health risks and therefore, proper management of wastes, including recycling and safe disposal, is highly recommended.

Several methods were proposed (or techniques already established) in the extraction and recovery of precious metals from e-wastes which includes physical, pyrometallurgical, hydrometallurgical, bio-hydrometallurgical, etc. Among these methods, hydrometallurgical is preferred due to extraction efficiency, highly selective to target analytes, reduced energy consumption, and environmental reasons such as minimal waste generation and low gas emissions.

In Chapter II, various hydrometallurgical process of separation and purification of precious metals and their processing drawbacks were presented. Precipitation, solvent-extraction, ion-exchange, and solid-phase extraction (SPE) were among the methods that have been successful at a certain degree in the recovery of precious metals from solutions. Solid phase extraction (SPE) was found to be more attractive over the other methods due to several advantages such simpler and faster operation, high capacity, less environmental impact, ease of preparation/handling, and lower cost. Solid Phase Extraction (SPE) has wide applications in several industries including hydrometallurgical processing, water treatment, biotechnology, and analytical systems. This method is carried out by allowing the target analyte to adhere onto the surface of the adsorbent either by ion exchange or chelating mechanism. SPE using magnetic particle as adsorbents (which are composed of Ni, Fe, Co, and/or their oxides), method known as MSPE, and its effectiveness in the recovery/removal precious metals from solutions/wastewater were also discussed. The interest in using magnetic particles in the removal/recovery of metal ions from aqueous solutions is related to their unique characteristics, such as very large surface area and high surface reactivity, excellent metal-binding, and selective adsorption properties with ease of phase separation, and problems associated with phase separation in conventional separation techniques can be resolved.

Magnetic adsorbents can be naturally occurring or can be prepared in the laboratory using different techniques such as co-precipitation, hydrothermal, thermal oxidation, pyrolysis, among others. In addition, the prepared magnetic adsorbents can be functionalized (surface-modification) with specific ligands or functional groups to facilitate higher affinity and maximum adsorption capacity. This chapter also presented

a summary of various studies on different types of magnetic particle adsorbents and their effectiveness in the recovery of precious metals from solutions.

In Chapter III, a maghemite-rich iron oxide composite was synthesized and used as adsorbent for gold from chloride solutions. Maghemite, a polymorph of magnetite, exhibits a remarkable fluid stability in both acidic and alkaline medium. Maghemite is a product of intermediate low temperature oxidation of maghemite wherein the electroneutrality, crystal structure, shape, and size are preserved via a process called topotactic transformation. Temperature was crucial in this process because of the potential formation of hematite, the other polymorph of magnetite, but non-magnetic. Maghemite-rich iron oxide adsorbent was prepared by low temperature (350°C) oxidation or roasting of synthetic magnetite for 18 hours and produced a maghemite-rich composite that has 44% maghemite, 33% hematite, and 23% magnetite using quantitative XRD analysis. The result suggests that at 350°C, magnetite was not fully oxidised to maghemite while formation of hematite has already begun. Specific surface area and the porosity of the prepared magnetic adsorbent were determined by Brunauer-Emmett-Teller (BET) and Barreett-Joyner-Halenda (BJH) analysis using N_2 gas as adsorbate. Results revealed that the mahemite-rich adsorbent has a specific surface area of 6.286 m^2/g with an average pore width of 12.5nm which corresponds to a mesoporous material.

Experimental results showed that gold recovery reached 99.78% with maximum adsorption capacity of 2.352mg/g at pH 6.5 and 24 hr contact time. This suggests that the maghemite-rich iron oxide composite was more effective than using unroasted synthetic magnetic magnetite in the chloride medium with only 86%Au (Alorro et. Al. 2010). The obtained optimum pH was also found to correspond to the point of zero charge (PZC) of the composite iron oxide sample. The Eh-pH predominance diagram also revealed that between pH 5 and 8, where maximum recovery was obtained, dissolved Au is mainly present as the uncharged $AuOH(H_2O)^0$ oxyanion, a form which is more easily adsorbed when the surface charge of the adsorbent is close to zero because electrostatic repulsion is minimal. Experimental result was closely fit the Langmuir adsorption isotherm model that corresponds to a monolayer coverage and the interaction between Au ions and the surface of the prepared adsorbent was characterised by chemisorption mechanism. High concentrations of chloride ions present in the solution decreased Au uptake mainly due to the unavailability of adsorbent's active

sites. SEM-EDX analysis of the loaded iron oxide adsorbent confirmed the presence of the metallic (reduced) Au on the surface of the adsorbent with 82% wt. Desorption process has achieved about 80% Au recovery using 1.75M thiourea as lixiviant for 24 hours contact time with minimum iron and nickel dissolution.

From the natural geological settings, maghemite can be the main gold carrier in the refractory gold ores (Fuso B., 2016). Synthesizing maghemite and use as adsorbents to recover precious metals from solutions can be a good replacement of carbon in a typical recovery process. Results in this chapter suggests that synthetic maghemite obtained from synthetic magnetite by thermal oxidation can be applied in metal recovery method from industrial waste streams, mining tailings, and electronic wastes, and other wastewater streams, contributing to environmental remediation efforts.

In Chapter IV, a naturally-occurring magnetic iron sulphide obtained from mine tailings in Western Australia was utilised in the recovery of Au from chloride solutions via MSPE method. Magnetic iron sulphides are group of minerals that contain (Fe) and sulphur (S) and exhibit magnetic properties. These minerals are of interest in geology and material science due to their magnetic properties and their role in processes like magnetism in rocks and mineral beneficiation. Repurposing of overburdens or waste materials generated by mining and minerals industry are considered eco-friendly and cost-effective solutions for managing mining wastes. One of the most promising routes is the utilization of mine wastes as adsorbent material for the recovery of gold and other precious metals from aqueous solutions. This work investigated the potential of a magnetic nickeliferous pyrrhotite recovered from the tailings of a nickel sulphide mine to adsorb Au from chloride solutions. XRD and XRF results indicated that the obtained magnetic sample was composed of about 65% pyrrhotite and 32% pentlandite with other impurities. SEM-EDX image and elemental mapping conforms that the nickeliferous pyrrhotite sample primarily contains Fe (50.49 wt%), S (20.43 wt%), and Ni (26.32%) with some traces of Al and O impurities. Using the BET-BJH method, average particle size of the material after grinding was 0.106µm with average pore width and specific surface area of 14.08nm and 0.9993m^2/g respectively. The prepared adsorbent showed a magnetic characteristic upon introducing handheld magnet.

Adsorption experiments using a simulated gold chloride solution were conducted to study the effects of pH, contact time, initial Au concentration and Cl^- concentrations on Au adsorption. Experimental results showed that Au uptake was very fast, achieving

100% Au recovery after 15 min of contact time at pH <5.5. Gold maximum adsorbent capacity reached 6.9 mg/g. The results also elucidated that the magnetic nickeliferous pyrrhotite adsorbent has excellent Au loading capacity with complete Au recovery attained even after several re-use. The presence of pyrrhotite and pentlandite in the adsorbent was believed to be beneficial for Au recovery. Galvanic interaction was discussed as the possible mechanism for Au uptake where the reductive deposition of dissolved Au occurred in the cathode (pentlandite) while the cathode dissolves (pyrrhotite). SEM-EDX revealed the metallic characteristic of Au on the surface of the magnetic nickeliferous pyrrhotite adsorbent. This finding was supported by further examination using XPS analysis where Au(III) was detected as direct adsorption while ~15.6%Au(I) and ~65.5%Au(0) are reduced or cemented onto the magnetic particle. The mixture of 0.5M thiourea in 0.5M H_2SO_4 was the promising eluant in the desorption of Au from the loaded adsorbent that recovered about 36.36% Au. The results strongly demonstrated the potential of the magnetic nickeliferous pyrrhotite from mine wastes as an effective and low-cost adsorbent for Au.

In Chapter V, the prepared magnetic nickeliferous pyrrhotite adsorbent discussed in chapter IV was utilized to recover platinum-group metals (PGMs) such as platinum, palladium, and rhodium from chloride solutions. Physical and chemical characteristics of the magnetic adsorbent were discussed in chapter IV. Precipitation experiments was initially conducted in single component systems to determine the stability of PGMs at different pH ranges. Platinum was found to be stable at any pH while palladium and rhodium started to precipitate at pH 4 and 3.5 respectively. The obtained pH was used as basis in the actual PGM adsorption. Palladium adsorption kinetics was fast with 100% recovered after 30 minutes contact time at pH<3 with maximum uptake of 23.66 µmol/g of adsorbent. Although slower than palladium, platinum reached maximum recovery (100%) after 24h contact time with maximum uptake of 11.7 µmol/g. The high uptake of Pt and Pd at lower pH was mainly because the presence of minimal hydroxy ions in the solution. The low uptake of Rh on the other hand can be attributed to low rhodium chloro-ligand formation at lower pH and was therefore excluded in the succeeding investigations. The high amount of Fe and Ni removed from the magnetic adsorbent is mainly due to the high oxidative dissolution at lower pH. The SEM-EDX analysis showed that Pt and Pd were both strongly associated with Ni, S, and Fe suggesting a galvanic interaction. The same phenomenon from the previous chapter where the deposition of the PGMs occurred in the cathode (pentlandite) while the anode

(pyrrhotite) dissolves. By plotting the relative abundance of each oxidation state in the XPS analysis, it was revealed that ~15% of Pt(0) was reduced on the surface of the adsorbent while ~60% was the result of the reduction of Pt(IV) to Pt(II) followed by adsorption. Similar to Pt, both adsorption (75%Pd(IV), 23.7% Pd(II)) and cementation (1.33%Pd(0)) also contributed in the recovery of Pd. In the desorption process, Pt and Pd recovery achieved ~6.8% and 15.63% respectively using 1.0M thiourea as eluant. The high Fe and Ni dissolution during desorption is attributed to the oxidative dissolution of these metals at lower pH.

VI.2 Recommendations

Roasting optimization is recommended to achieve maximum conversion of synthetic magnetite to maghemite. This can be done by considering different temperature and heat treatment time profiles. Detailed characterization of converted materials should also be conducted. Gold and other precious metals adsorption should also be investigated.

The major challenge in achieving maximum adsorption capacity and reusability of the prepared magnetic adsorbent is the stability of the adsorbent. Adsorbent functionalization can be one of the best options. The obtained magnetic nickeliferous pyrrhotite adsorbent has proven the capacity for gold, platinum, and palladium recovery from solutions. Hower, un-modified adsorbent can be susceptible to oxidation and may further lead to adsorbent degradation and can affect adsorption capabilities. Therefore, surface modification, methods previously discussed, to enhance adsorption capacity.

Developing efficient methods to desorb precious metals from magnetic adsorbent particles and re-use them without degradation of their performance remains an area of research. In the desorption studies, thiourea was found to be one of the best eluant for gold, platinum, and palladium without no or minimal dissolution of nickel and/or iron. It is recommended to evaluate suitable eluant using thiourea, either by higher concentration (economic practically required) or a mixture of thiourea and other reagents.

REFERENCES

<Surface_charge_density_I._T._LUCAS.pdf>.

<Utilisation of copper mine tailings asroad construction materials through geopolymerization.pdf>.

ADHIKARI, B. B., GURUNG, M., ALAM, S., TOLNAI, B. & INOUE, K. 2013. Kraft mill lignin – A potential source of bio-adsorbents for gold recovery from acidic chloride solution. *Kraft mill lignin – A potential source of bio-adsorbents for gold recovery from acidic chloride solution,* 231**,** 190-197.

AGHAEI, E., ALORRO, R., ENCILA, A. & YOO, K. 2017a. Magnetic Adsorbents for the Recovery of Precious Metals from Leach Solutions and Wastewater. *Metals,* 7.

AGHAEI, E., ALORRO, R. D., ENCILA, A. & YOO, K. 2017b. Magnetic Adsorbents for the Recovery of Precious Metals from Leach Solutions and Wastewater. *Metals,* 7.

AHMARI, S. & ZHANG, L. 2013. Utilization of cement kiln dust (CKD) to enhance mine tailings-based geopolymer bricks. *Construction & building materials,* 40**,** 1002-1011.

AKCIL, A., ERUST, C., GAHAN, C. S., OZGUN, M., SAHIN, M. & TUNCUK, A. 2015. Precious metal recovery from waste printed circuit boards using cyanide and non-cyanide lixiviants--A review. *Waste Manag,* 45**,** 258-71.

AKCIL, A. & KOLDAS, S. 2006. Acid Mine Drainage (AMD): causes, treatment and case studies. *Journal of cleaner production,* 14**,** 1139-1145.

AKTAS, S., GOZUAK, B., ACMA, H., REHA OZALP, M. & ACMA, E. 2011. Gold recovery from chloride solutions using fallen leaves. *Environmental chemistry letters,* 9**,** 47-53.

AKTAS, S. & MORCALI, M. H. 2011. Gold uptake from dilute chloride solutions by a Lewatit TP 214 and activated rice husk. *International Journal of Mineral Processing,* 101**,** 63-70.

ALORRO, R. D., HIROYOSHI, N., KIJITANI, H., ITO, M. & TSUNEKAWA, M. 2010. On the Use of Magnetite for Gold Recovery From Chloride Solution. *Mineral Processing and Extractive Metallurgy Review,* 31**,** 201-213.

AMPHLETT, J. T. M., OGDEN, M. D., FOSTER, R. I., SYNA, N., SOLDENHOFF, K. & SHARRAD, C. A. 2018. Polyamine functionalised ion exchange resins: Synthesis, characterisation and uranyl uptake. *Chemical engineering journal (Lausanne, Switzerland : 1996),* 334**,** 1361-1370.

APHESTEGUY, J. C., KURLYANDSKAYA, G. V., DE CELIS, J. P., SAFRONOV, A. P. & SCHEGOLEVA, N. N. 2015. Magnetite nanoparticles prepared by co-precipitation method in different conditions. *Materials Chemistry and Physics,* 161**,** 243-249.

ASSADIAN, M., IDRIS, M. H., SHAHRI, S. M. G. & GHOLAMPOUR, B. 2013. Gold Recovery from WEEE by Chlorine System. *Applied Mechanics and Materials,* 330**,** 123-125.

BAI, F., YE, G., CHEN, G., WEI, J., WANG, J. & CHEN, J. 2013. Highly selective recovery of palladium by a new silica-based adsorbent functionalized with macrocyclic ligand. *Separation and purification technology,* 106**,** 38-46.

BARAKAT, M. A., MAHMOUD, M. H. H. & MAHROUS, Y. S. 2006. Recovery and separation of palladium from spent catalyst. *Applied Catalysis A: General,* 301**,** 182-186.

BEAL, J. H. L., ETCHEGOIN, P. G. & TILLEY, R. D. 2012. Synthesis and characterisation of magnetic iron sulfide nanocrystals. *Journal of Solid State Chemistry,* 189**,** 57-62.

BEATA, K.-S., URSZULA, W., DARIUSZ, S. & PER, N. 2015. Thermal treatment of magnetite nanoparticles. *Beilstein Journal of Nanotechnology,* 6**,** 1385-1396.

BEBIE, J., SCHOONEN, M. A. A., FUHRMANN, M. & STRONGIN, D. R. 1998. Surface charge development on transition metal sulfides: An electrokinetic study. *Geochimica et Cosmochimica Acta,* 62**,** 633-642.

BENGUEREL, E., COTE, H, G., LAUTIE, H, A., DEMOPOULOS & H, G. 1995. Characterization of extracted complexes in liquid-liquid extraction of rhodium with Kelex 100 in the presence of SnCl\+v\2\-v. *Journal of chemical technology and biotechnology (1986),* 62**,** 380-384.

BENSON, M., BENNETT, C. R., HARRY, J. E., PATEL, M. K. & CROSS, M. 2000. The recovery mechanism of platinum group metals from catalytic converters in spent automotive exhaust systems. *Resources, Conservation & Recycling,* 31**,** 1-7.

BIRICH, A., STOPIC, S. & FRIEDRICH, B. 2019. Kinetic Investigation and Dissolution Behavior of Cyanide Alternative Gold Leaching Reagents. *Scientific reports,* 9**,** 7191-7191.

BLIGHT, G. 2011. Mine Waste. *Waste.*

BOZKURT, V., XU, Z. & FINCH, J. A. 1998. Pentlandite/pyrrhotite interaction and xanthate adsorption. *International journal of mineral processing,* 52**,** 203-214.

BULUT, G. & YENIAL, Ü. 2016. Effects of major ions in recycled water on sulfide minerals flotation. *Minerals & Metallurgical Processing,* 33**,** 137-143.

CALDERON, A. R. M., ALORRO, R. D., TADESSE, B., YOO, K. & TABELIN, C. B. 2019a. Evaluation of Maghemite-Rich Iron Oxide Composite Prepared from Magnetite as Adsorbent for Gold from Chloride Solution. *JOM***,** <xocs:firstpage xmlns:xocs=""/>.

CALDERON, A. R. M., ALORRO, R. D., TADESSE, B., YOO, K. & TABELIN, C. B. 2019b. Evaluation of Maghemite-Rich Iron Oxide Composite Prepared from Magnetite as Adsorbent for Gold from Chloride Solution. *Jom,* 71**,** 4639-4646.

CALDERON, A. R. M., ALORRO, R. D., TADESSE, B., YOO, K. & TABELIN, C. B. 2020. Repurposing of nickeliferous pyrrhotite from mine tailings as magnetic adsorbent for the recovery of gold from chloride solution. *Resources, Conservation and Recycling,* 161.

CHAND, R., WATARI, T., INOUE, K., KAWAKITA, H., LUITEL, H. N., PARAJULI, D., TORIKAI, T. & YADA, M. 2009. Selective adsorption of precious metals from hydrochloric acid solutions using porous carbon prepared from barley straw and rice husk. *Minerals engineering,* 22**,** 1277-1282.

CHEN, D. & XU, R. 1998. Hydrothermal synthesis and characterization of nanocrystalline Fe 3O 4 powders. *Materials Research Bulletin,* 33**,** 1015-1021.

COLLINS, R. J. & MILLER, R. H. 1979. Utilization of mining and mineral processing wastes in the United States. *Minerals and the Environment,* 1**,** 8-19.

COZZI, D. & PANTANI, F. 1958. The polarographic behaviour of rhodium(III) chlorocomplexes. *Journal of inorganic & nuclear chemistry,* 8**,** 385-398.

CRUNDWELL FRANK, K., DAVENPORT WILLIAM, G., RAMACHANDRAN, V., ROBINSON TIMOTHY, G. & MOATS MICHAEL, S. 2011. Platinum-Group Metals, Production, Use and Extraction Costs. Elsevier.

CUI, J. & ZHANG, L. 2008. Metallurgical recovery of metals from electronic waste: A review. *Journal of Hazardous Materials,* 158**,** 228-256.

DAVIS, G. & HERAT, S. 2008. Electronic waste: The local government perspective in Queensland, Australia. *Resources, conservation and recycling,* 52**,** 1031-1039.

DAVISON, W. 1991. The solubility of iron sulphides in synthetic and natural waters at ambient temperature. *Research across Boundaries,* 53**,** 309-329.

DEMOPOULOS, G. P. 1986. Solvent Extraction in Precious Metals Refining. *JOM (1989),* 38**,** 13-17.

FENG, B., YAO, C., CHEN, S., LUO, R., LIU, S. & TONG, S. 2018. Highly efficient and selective recovery of Au(III) from a complex system by molybdenum disulfide nanoflakes. *Chemical engineering journal (Lausanne, Switzerland : 1996),* 350**,** 692-702.

FERREIRA, R., PEREIRA, I., CAVALCANTE, L., GAMARRA, L., CARNEIRO, S., AMARO, E., FABRIS, J., DOMINGUES, R. & ANDRADE, A. 2010. Synthesis and characterization of silica-coated nanoparticles of magnetite. *Hyperfine Interactions,* 195**,** 265-274.

FORNASIERO, D., EIJT, V. & RALSTON, J. 1992. An electrokinetic study of pyrite oxidation. *Colloids and Surfaces,* 62**,** 63-73.

FOSU, B. 2016. *Experimental investigation of recovering gold from maghemite-rich magnetic concentrates by roasting.* ProQuest Dissertations Publishing.

FOTOOHI, B. & MERCIER, L. 2015. Some insights into the chemistry of gold adsorption by thiol and amine functionalized mesoporous silica in simulated thiosulfate system. *Hydrometallurgy,* 156**,** 28-39.

GARG, S., JUDD, K., MAHADEVAN, R., EDWARDS, E. & PAPANGELAKIS, V. G. 2017. Leaching characteristics of nickeliferous pyrrhotite tailings from the Sudbury, Ontario area. *Canadian metallurgical quarterly,* 56**,** 372-381.

GAVIRÍA, J. P., BOHÉ, A., PASQUEVICH, A. & PASQUEVICH, D. M. 2007. Hematite to magnetite reduction monitored by Mössbauer spectroscopy and X-ray diffraction. *Physica B: Condensed Matter,* 389**,** 198-201.

GIAKISIKLI, G. & ANTHEMIDIS, A. N. 2013a. Magnetic materials as sorbents for metal/metalloid preconcentration and/or separation. A review. *Analytica Chimica Acta,* 789**,** 1-16.

GIAKISIKLI, G. & ANTHEMIDIS, A. N. 2013b. Magnetic materials as sorbents for metal/metalloid preconcentration and/or separation. A review. *Anal Chim Acta,* 789**,** 1-16.

GOLEV, A., SCHMEDA-LOPEZ, D. R., SMART, S. K., CORDER, G. D. & MCFARLAND, E. W. 2016. Where next on e-waste in Australia? *Waste Management,* 58**,** 348-358.

GÓMEZ-PASTORA, J., BRINGAS, E. & ORTIZ, I. 2014. Recent progress and future challenges on the use of high performance magnetic nano-adsorbents in environmental applications. *Chemical Engineering Journal,* 256**,** 187-204.

GURUNG, M., ADHIKARI, B. B., KAWAKITA, H., OHTO, K., INOUE, K. & ALAM, S. 2012. Selective Recovery of Precious Metals from Acidic Leach Liquor of Circuit Boards of Spent Mobile Phones Using Chemically Modified Persimmon Tannin Gel. *Industrial & engineering chemistry research,* 51**,** 11901-11913.

GURUNG, M., ADHIKARI, B. B., KHUNATHAI, K., KAWAKITA, H., OHTO, K., HARADA, H. & INOUE, K. 2011. Quaternary Amine Modified Persimmon Tannin Gel: An Efficient Adsorbent for the Recovery of Precious Metals from Hydrochloric Acid Media. *Separation science and technology,* 46**,** 2250-2259.

HAYES, K. F., PAPELIS, C. & LECKIE, J. O. 1988. Modeling ionic strength effects on anion adsorption at hydrous oxide/solution interfaces. *Journal of colloid and interface science,* 125**,** 717-726.

HERRERO-LATORRE, C., BARCIELA-GARCIA, J., GARCIA-MARTIN, S., PENA-CRECENTE, R. M. & OTAROLA-JIMENEZ, J. 2015a. Magnetic solid-phase extraction using carbon nanotubes as sorbents: a review. *Anal Chim Acta,* 892**,** 10-26.

HERRERO-LATORRE, C., BARCIELA-GARCÍA, J., GARCÍA-MARTÍN, S., PEÑA-CRECENTE, R. M. & OTÁROLA-JIMÉNEZ, J. 2015b. Magnetic solid-phase extraction using carbon nanotubes as sorbents: A review. *Analytica Chimica Acta,* 892**,** 10-26.

HOMCHUEN, P., ALORRO, R. D., HIROYOSHI, N., SATO, R., KIJITANI, H. & ITO, M. 2016. A Study on the Utilization of Magnetite for the Recovery of Platinum Group Metals from Chloride Solution. *Mineral Processing and Extractive Metallurgy Review,* 37**,** 246-254.

HU, C., XU, W., MO, X., LI, H., ZHOU, S., ZHANG, P. & TANG, K. 2018. Efficient adsorption toward precious metal from aqueous solution by zeolitic imidazolate framework-8. *Adsorption : journal of the International Adsorption Society,* 24**,** 733-744.

HUYEN, D. T., TABELIN, C. B., THUAN, H. M., DANG, D. H., TRUONG, P. T., VONGPHUTHONE, B., KOBAYASHI, M. & IGARASHI, T. 2019. The solid-phase partitioning of arsenic in unconsolidated sediments of the Mekong Delta, Vietnam and its modes of release under various conditions. *Chemosphere (Oxford),* 233**,** 512-523.

HYEON, T., LEE, S. S., PARK, J., CHUNG, Y. & NA, H. B. 2002. ChemInform Abstract: Synthesis of Highly Crystalline and Monodisperse Maghemite Nanocrystallites Without a Size-Selection Process. *ChemInform,* 33**,** no-no.

HYLAND, M. M. & BANCROFT, G. M. 1990. Palladium sorption and reduction on sulphide mineral surfaces: An XPS and AES study. *Geochimica et cosmochimica acta,* 54**,** 117-130.

IGARASHI, T., HERRERA, P. S., UCHIYAMA, H., MIYAMAE, H., IYATOMI, N., HASHIMOTO, K. & TABELIN, C. B. 2020. The two-step neutralization ferrite-formation process for sustainable acid mine drainage treatment: Removal of copper, zinc and arsenic, and the influence of coexisting ions on ferritization. *The Science of the total environment,* 715**,** 136877-136877.

IQBAL, A., JAN, M. R., SHAH, J. & RASHID, B. 2020. Dispersive solid phase extraction of precious metal ions from electronic wastes using magnetic multiwalled carbon nanotubes composite. *Minerals engineering,* 154**,** 106414.

IWASAKI, T., KOSAKA, K., YABUUCHI, T., WATANO, S., YANAGIDA, T. & KAWAI, T. 2009. Novel mechanochemical process for synthesis of magnetite nanoparticles using coprecipitation method. *Advanced powder technology : the international journal of the Society of Powder Technology, Japan,* 20**,** 521-528.

J. DEKKERS, M. & A.A. SCHOONEN, M. 1994. An electrokinetic study of synthetic greigite and pyrrhotite. *Geochimica et Cosmochimica Acta,* 58**,** 4147-4153.

JEAN, G. E. & BANCROFT, G. M. 1986. Heavy metal adsorption by sulphide mineral surfaces. *Geochimica et cosmochimica acta,* 50**,** 1455-1463.

JEAN, G. E. & G. MICHAEL, B. 1985. An XPS and SEM study of gold deposition at low temperatures on sulphide mineral surfaces: Concentration of gold by adsorption/reduction. *Geochimica et cosmochimica acta,* 49**,** 979-987.

JEAN, M., NACHBAUR, V. & LE BRETON, J.-M. 2012a. Synthesis and characterization of magnetite powders obtained by the solvothermal method: Influence of the Fe3+ concentration. *Journal of Alloys and Compounds,* 513**,** 425-429.

JEAN, M., NACHBAUR, V. & LE BRETON, J.-M. 2012b. Synthesis and characterization of magnetite powders obtained by the solvothermal method: Influence of the Fe.sup.3+ concentration. *Journal of alloys and compounds,* 513**,** 425.

JEON, S., TABELIN, C. B., TAKAHASHI, H., PARK, I., ITO, M. & HIROYOSHI, N. 2018. Interference of coexisting copper and aluminum on the ammonium thiosulfate leaching of gold from printed circuit boards of waste mobile phones. *Waste management (Elmsford),* 81**,** 148-156.

KALSKA-SZOSTKO, B., WYKOWSKA, U., SATULA, D. & NORDBLAD, P. 2015. Thermal treatment of magnetite nanoparticles. *Beilstein J Nanotechnol,* 6**,** 1385-96.

KARIM, S. & TING, Y.-P. 2021. Recycling pathways for platinum group metals from spent automotive catalyst: A review on conventional approaches and bio-processes. *Resources, conservation and recycling,* 170**,** 105588.

KIM, C. 2000. Recovery of platinum-group metals from recycled automotive catalytic converters by carbochlorination. *Industrial and Engineering Chemistry Research (USA),* 39**,** 1185-1192.

KIM, M.-S., KIM, E.-Y., JEONG, J., LEE, J.-C. & KIM, W. 2010. Recovery of Platinum and Palladium from the Spent Petroleum Catalysts by Substrate Dissolution in Sulfuric Acid. *Materials Transactions,* 51**,** 1927-1933.

KIM, W., SUH, C. Y., CHO, S. W., ROH, K. M., KWON, H., SONG, K. & SHON, I. J. 2012. A new method for the identification and quantification of magnetite-maghemite mixture using conventional X-ray diffraction technique. *Talanta,* 94**,** 348-52.

KURANCHIE, F. A., SHUKLA, S. K. & HABIBI, D. 2013. Mine Wastes in Western Australia and Their Suitability for Embankment Construction. *Geo-Congress 2013.*

KYRIAKAKIS, G. 2005. *Extraction of gold from platinum group metal (PGM) ores*.

LAM, K. F., FONG, C. M., YEUNG, K. L. & MCKAY, G. 2008. Selective adsorption of gold from complex mixtures using mesoporous adsorbents. *Chemical engineering journal (Lausanne, Switzerland : 1996),* 145**,** 185-195.

LEFEBURE, S., DUBOIS, E., CABUIL, V., NEVEU, S. & MASSART, R. 1998. Monodisperse magnetic nanoparticles: Preparation and dispersion in water and oils. *Journal of materials research,* 13**,** 2975-2981.

LEHMANN, M. N., STICHNOTH, M., WALTON, D. & BAILEY, S. I. 2000. Effect of chloride ions on the ambient electrochemistry of pyrite oxidation in acid media. *Journal of the Electrochemical Society,* 147**,** 3263-3271.

LEI, L. & WATKINS, R. 2005. Acid drainage reassessment of mining tailings, Black Swan Nickel Mine, Kalgoorlie, Western Australia. *Applied geochemistry,* 20**,** 661-667.

LENGKE, M. F., FLEET, M. E. & SOUTHAM, G. 2006. Synthesis of Platinum Nanoparticles by Reaction of Filamentous Cyanobacteria with Platinum(IV)−Chloride Complex. *Langmuir,* 22**,** 7318-7323.

LETINA, D. & LETSHWENYO, W. M. 2018a. Investigating waste rock, tailings, slag and coal ash clinker as adsorbents for heavy metals: Batch and column studies. *Physics and Chemistry of the Earth, Parts A/B/C,* 105**,** 184-190.

LETINA, D. & LETSHWENYO, W. M. 2018b. Investigating waste rock, tailings, slag and coal ash clinker as adsorbents for heavy metals: Batch and column studies. *Physics and Chemistry of the Earth,* 105**,** 184-190.

LI, F., ZHANG, B., DONG, S. & WANG, E. 1997. A novel method of electrodepositing highly dispersed nano palladium particles on glassy carbon electrode. *Electrochimica acta,* 42**,** 2563-2568.

LI, H., FENG, X., GUO, Y., CHEN, D., LI, R., REN, X., JIANG, X., DONG, Y. & WANG, B. 2014. A malonitrile-functionalized metal-organic framework for hydrogen sulfide detection and selective amino acid molecular recognition. *Scientific reports,* 4**,** 4366-4366.

LI, J. & MILLER, J. D. 2006. A REVIEW OF GOLD LEACHING IN ACID THIOUREA SOLUTIONS. *Mineral processing and extractive metallurgy review,* 27**,** 177-214.

LI, J., SAFARZADEH, M. S., MOATS, M. S., MILLER, J. D., LEVIER, K. M., DIETRICH, M. & WAN, R. Y. 2012. Thiocyanate hydrometallurgy for the recovery of gold. Part I: Chemical and thermodynamic considerations. *Hydrometallurgy,* 113-114**,** 1-9.

LIN, S., KUMAR REDDY, D., BEDIAKO, J. K., SONG, M.-H., WEI, W., KIM, J.-A. & YUN, Y.-S. 2017. Effective adsorption of Pd(ii), Pt(iv) and Au(iii) by Zr(iv)-based metal–organic frameworks from strongly acidic solutions. *Journal of materials chemistry. A, Materials for energy and sustainability,* 5**,** 13557-13564.

LIN, S., ZHAO, Y., BEDIAKO, J. K., CHO, C.-W., SARKAR, A. K., LIM, C.-R. & YUN, Y.-S. 2019. Structure-controlled recovery of palladium(II) from acidic aqueous solution using metal-organic frameworks of MOF-802, UiO-66 and MOF-808. *Chemical engineering journal (Lausanne, Switzerland : 1996),* 362**,** 280-286.

LIU, Z., HÖFFT, O. & ENDRES, F. 2021. Disproportionation Reaction of Gallium during Electrodeposition from an Ionic Liquid, Monitored by In Situ Electrochemical XPS. *Journal of physical chemistry. C,* 125**,** 24589-24595.

LUCAS, I. T., DURAND-VIDAL, S., DUBOIS, E., CHEVALET, J. & TURQ, P. 2007. Surface Charge Density of Maghemite Nanoparticles: Role of Electrostatics in the Proton Exchange. *Journal of physical chemistry. C,* 111**,** 18568-18576.

MA, B.-G., CAI, L.-X., LI, X.-G. & JIAN, S.-W. 2016. Utilization of iron tailings as substitute in autoclaved aerated concrete: physico-mechanical and microstructure of hydration products. *Journal of Cleaner Production,* 127**,** 162-171.

MACHIDA, M., MOCHIMARU, T. & TATSUMOTO, H. 2006. Lead(II) adsorption onto the graphene layer of carbonaceous materials in aqueous solution. *Carbon (New York),* 44**,** 2681-2688.

MAHMOUD, M. H. H. 2003. Leaching platinum-group metals in a sulfuric acid/chloride solution. *JOM (1989),* 55**,** 37-40.

MAMANI, J. B., COSTA-FILHO, A. J., CORNEJO, D. R., VIEIRA, E. D. & GAMARRA, L. F. 2013. Synthesis and characterization of magnetite nanoparticles coated with lauric acid. *Materials Characterization,* 81**,** 28-36.

MARINHO, R. S., DA SILVA, C. N., AFONSO, J. C. & DA CUNHA, J. W. 2011a. Recovery of platinum, tin and indium from spent catalysts in chloride medium using strong basic anion exchange resins. *J Hazard Mater,* 192**,** 1155-60.

MARINHO, R. S., SILVA, C. N. D., AFONSO, J. C. & CUNHA, J. W. S. D. D. 2011b. Recovery of platinum, tin and indium from spent catalysts in chloride medium using strong basic anion exchange resins. *Journal of Hazardous Materials,* 192**,** 1155-1160.

MARTÍNEZ-MERA, I., GUTIÉRREZ-WING, C., ARGÁNIS-JUÁREZ, C. & VILCHIS-NESTOR, A. R. 2017a. Reduction of maghemite to magnetite over 304SS, in the presence of silver nanoparticles. *Surface and Coatings Technology,* 324**,** 338-344.

MARTÍNEZ-MERA, I., GUTIÉRREZ-WING, C., ARGÁNIS-JUÁREZ, C. & VILCHIS-NESTOR, A. R. 2017b. Reduction of maghemite to magnetite over 304SS, in the presence of silver nanoparticles. *Surface & Coatings Technology,* 324**,** 338-344.

MAURYA, N. S., MITTAL, A. K., CORNEL, P. & ROTHER, E. 2006. Biosorption of dyes using dead macro fungi: Effect of dye structure, ionic strength and pH. *Bioresource technology,* 97**,** 512-521.

MORCALI, M. H., ZEYTUNCU, B., AKTAS, S., YUCEL, O. & GULLUOGLU, A. N. 2013. Platinum adsorption from chloride media using carbonized biomass and commercial sorbent. *Minerals & Metallurgical Processing,* 30**,** 129-136.

MORISADA, S., RIN, T., OGATA, T., KIM, Y.-H. & NAKANO, Y. 2012. Adsorption recovery of rhodium(III) in acidic chloride solutions by amine-modified tannin gel. *Journal of applied polymer science,* 126**,** E34-E38.

MOSLEMI, H., SHAMSI, P. & HABASHI, F. 2011. Pyrite and pyrrhotite open circuit potentials study: Effects on flotation. *Minerals Engineering,* 24**,** 1038-1045.

NAVARRO, P., ALVAREZ, R., VARGAS, C. & ALGUACIL, F. J. 2004. On the use of zinc for gold cementation from ammoniacal–thiosulphate solutions. *Minerals engineering,* 17**,** 825-831.

NAVARRO, P., VARGAS, C., ALONSO, M. & ALGUACIL, F. J. 2007. Towards a more environmentally friendly process for gold: models on gold adsorption onto activated carbon from ammoniacal thiosulfate solutions. *Desalination,* 211**,** 58-63.

NIKIFOROV, V. N., GOLDT, A. E., GUDILIN, E. A., SREDIN, V. G. & IRHIN, V. Y. 2014a. Magnetic properties of maghemite nanoparticles. *Bulletin of the Russian Academy of Sciences: Physics,* 78**,** 1075-1080.

NIKIFOROV, V. N., GOLDT, A. E., GUDILIN, E. A., SREDIN, V. G. & IRHIN, V. Y. 2014b. Magnetic properties of maghemite nanoparticles. *Bulletin of the Russian Academy of Sciences. Physics,* 78**,** 1075-1080.

NIKOLOSKI, A. N. & ANG, K.-L. 2013. Review of the Application of Ion Exchange Resins for the Recovery of Platinum-Group Metals From Hydrochloric Acid Solutions. *Mineral Processing and Extractive Metallurgy Review,* 35**,** 369-389.

NIKOLOSKI, A. N. & ANG, K.-L. 2014. Review of the Application of Ion Exchange Resins for the Recovery of Platinum-Group Metals From Hydrochloric Acid Solutions. Taylor & Francis Group.

NIMIBOFA, A., TOBIN, E. A., DAVID, S. N., DONBEBE, W. & DIXON, D. E. 2017. Equilibrium, kinetic and thermodynamic studies of the uptake of copper by layered double hydroxide. *Hemijska industrija,* 71**,** 429-437.

NYIRŐ-KÓSA, I., REČNIK, A. & PÓSFAI, M. 2012. Novel methods for the synthesis of magnetite nanoparticles with special morphologies and textured assemblages. *An Interdisciplinary Forum for Nanoscale Science and Technology,* 14**,** 1-10.

ODIO, O. F., LARTUNDO-ROJAS, L., SANTIAGO-JACINTO, P., MARTÍNEZ, R. & REGUERA, E. 2014. Sorption of Gold by Naked and Thiol-Capped Magnetite Nanoparticles: An XPS Approach. *Journal of physical chemistry. C,* 118**,** 2776-2791.

OLUWASOLA, E. A., HAININ, M. R. & AZIZ, M. M. A. 2015. Evaluation of asphalt mixtures incorporating electric arc furnace steel slag and copper mine tailings for road construction. *Transportation Geotechnics,* 2**,** 47-55.

ORABY, E. A., EKSTEEN, J. J. & TANDA, B. C. 2017. Gold and copper leaching from gold-copper ores and concentrates using a synergistic lixiviant mixture of glycine and cyanide. *Hydrometallurgy,* 169**,** 339-345.

PAIVA, A. P., ORTET, O., CARVALHO, G. I. & NOGUEIRA, C. A. 2017. Recovery of palladium from a spent industrial catalyst through leaching and solvent extraction. *Hydrometallurgy,* 171**,** 394-401.

PARK, I., TABELIN, C. B., SENO, K., JEON, S., INANO, H., ITO, M. & HIROYOSHI, N. 2020. Carrier-microencapsulation of arsenopyrite using Al-catecholate complex: nature of oxidation products, effects on anodic and cathodic reactions, and coating stability under simulated weathering conditions. *Heliyon,* 6**,** e03189-e03189.

PARK, I., TABELIN, C. B., SENO, K., JEON, S., ITO, M. & HIROYOSHI, N. 2018. Corrigendum to “Simultaneous suppression of acid mine drainage formation and arsenic release by Carrier-microencapsulation using aluminum-catecholate complexes” [Chemosphere 205C (2018) 414–425]. *Chemosphere (Oxford),* 209**,** 1021-1021.

PARK, Y. J. & FRAY, D. J. 2009. Recovery of high purity precious metals from printed circuit boards. *Journal of hazardous materials,* 164**,** 1152-1158.

PARKINSON, G. S. 2016. Iron oxide surfaces. *Surface Science Reports,* 71**,** 272-365.

PEEK, E., BARNES, A. & TUZUN, A. 2011a. Nickeliferous pyrrhotite – "Waste or resource?". *Minerals Engineering,* 24**,** 625-637.

PEEK, E., BARNES, A. & TUZUN, A. 2011b. Nickeliferous pyrrhotite – "Waste or resource?". *Minerals engineering,* 24**,** 625-637.

PELLENZ, L., DE OLIVEIRA, C. R. S., DA SILVA JÚNIOR, A. H., DA SILVA, L. J. S., DA SILVA, L., ULSON DE SOUZA, A. A., DE SOUZA, S. M. D. A. G. U., BORBA, F. H. & DA SILVA, A. 2023. A comprehensive guide for characterization of adsorbent materials. *Separation and purification technology,* 305**,** 122435.

PEREZ, J. P. H., FOLENS, K., LEUS, K., VANHAECKE, F., VAN DER VOORT, P. & DU LAING, G. 2019. Progress in hydrometallurgical technologies to recover critical raw materials and precious metals from low-concentrated streams. *Resources, conservation and recycling,* 142**,** 177-188.

RAHMAYANTI, M., SANTOSA, S. J. & SUTARNO, S. 2016. Comparative study on the adsorption of [AuCl4]– onto salicylic acid and gallic acid modified magnetite particles. *Indonesian journal of chemistry,* 16**,** 329-337.

RAMESH, A., HASEGAWA, H., SUGIMOTO, W., MAKI, T. & UEDA, K. 2008. Adsorption of gold(III), platinum(IV) and palladium(II) onto glycine modified crosslinked chitosan resin. *Bioresour Technol,* 99**,** 3801-9.

RANJBAR, R., NADERI, M., OMIDVAR, H. & AMOABEDINY, G. 2014. Gold recovery from copper anode slime by means of magnetite nanoparticles (MNPs). *Hydrometallurgy,* 143**,** 54-59.

RAO, C. R. M. & REDDI, G. S. 2000. Platinum group metals (PGM); occurrence, use and recent trends in their determination. *TrAC, Trends in analytical chemistry (Regular ed.),* 19**,** 565-586.

RITCEY, G. M. 2005. Tailings management in gold plants. *Hydrometallurgy,* 78**,** 3-20.

SAFARZADEH, M. S., HORTON, M. & VAN RYTHOVEN, A. D. 2018. Review of Recovery of Platinum Group Metals from Copper Leach Residues and Other Resources. *Mineral processing and extractive metallurgy review,* 39**,** 1-17.

SAGNOTTI, L. 2007. *Iron sulfides,* Dordrecht, Dordrecht, Netherlands: Springer.

SAGNOTTI, L., MACRI, P. & EGLI, R. 2007. Magnetic properties of atmospheric particulate matter (PM10) in the Latium region (Italy): an empirical approach to evaluate natural and anthropogenic inputs. *Geophysical research abstracts*.

SAMAN, N., AHMAD KAMAL, N. A., LYE, J. W. P. & MAT, H. 2020. Synthesis and characterization of CTAB-silica nanocapsules and its adsorption behavior towards

Pd(II) ions in aqueous solution. *Advanced powder technology : the international journal of the Society of Powder Technology, Japan,* 31**,** 3205-3214.

SANTOYO SALAZAR, J., TRUONG PHUOC, L., IHIAWAKRIM, D., BEGIN-COLIN, S., POURROY, G., PEREZ, L., DE ABRIL, O., VAZQUEZ, M. & GRENECHE, J.-M. 2011. Magnetic iron oxide nanoparticles in 10-40 nm range: Composition in terms of magnetite/maghemite ratio and effect on the magnetic properties. *Chemistry of Materials,* 23**,** 1379-1386.

SARKAR, S., SARKAR, S. & BISWAS, P. 2017. Effective utilization of iron ore slime, a mining waste as adsorbent for removal of Pb(II) and Hg(II). *Journal of environmental chemical engineering,* 5**,** 38-44.

SENG, S., TABELIN, C. B., MAKINO, Y., CHEA, M., PHENGSAART, T., PARK, I., HIROYOSHI, N. & ITO, M. 2019. Improvement of flotation and suppression of pyrite oxidation using phosphate-enhanced galvanic microencapsulation (GME) in a ball mill with steel ball media. *Minerals Engineering,* 143.

SHEARER, G. C., CHAVAN, S., BORDIGA, S., SVELLE, S., OLSBYE, U. & LILLERUD, K. P. 2016. Defect Engineering: Tuning the Porosity and Composition of the Metal–Organic Framework UiO-66 via Modulated Synthesis. *Chemistry of materials,* 28**,** 3749-3761.

SHEN, L., QIAO, Y., GUO, Y., MENG, S., YANG, G., WU, M. & ZHAO, J. 2014. Facile co-precipitation synthesis of shape-controlled magnetite nanoparticles. *Ceramics International,* 40**,** 1519-1524.

SHEN, S., GUISHEN, L., PAN, T., HE, J. & GUO, Z. 2011a. Selective adsorption of Pt ions from chloride solutions obtained by leaching chlorinated spent automotive catalysts on ion exchange resin Diaion WA21J. *J Colloid Interface Sci,* 364**,** 482-9.

SHEN, S., GUISHEN, L., PAN, T., HE, J. & GUO, Z. 2011b. Selective adsorption of Pt ions from chloride solutions obtained by leaching chlorinated spent automotive catalysts on ion exchange resin Diaion WA21J. *Journal of Colloid And Interface Science,* 364**,** 482-489.

SHI, Z., BONNEVILLE, S., KROM, M. D., CARSLAW, K. S., JICKELLS, T. D., BAKER, A. R. & BENNING, L. G. 2011. Iron dissolution kinetics of mineral dust at low pH during simulated atmospheric processing. *Atmospheric chemistry and physics,* 11**,** 995-1007.

SIDHU, P. S., GILKES, R. J. & POSNER, A. M. 1977. Mechanism of the low temperature oxidation of synthetic magnetites. *Journal of Inorganic and Nuclear Chemistry,* 39**,** 1953-1958.

STEINLECHNER, S. & ANTREKOWITSCH, J. 2015. Potential of a Hydrometallurgical Recycling Process for Catalysts to Cover the Demand for Critical Metals, Like PGMs and Cerium. *The Journal of The Minerals, Metals & Materials Society (TMS),* 67**,** 406-411.

SUN, S. & MURRAY, C. B. 1999. Synthesis of monodisperse cobalt nanocrystals and their assembly into magnetic superlattices (invited). *Journal of Applied Physics,* 85**,** 4325-4330.

SUN, Z., XIAO, Y., AGTERHUIS, H., SIETSMA, J. & YANG, Y. 2016. Recycling of metals from urban mines – a strategic evaluation. *Journal of Cleaner Production,* 112**,** 2977-2987.

SWAMI, R. K., PUNDHIR, N. K. S. & MATHUR, S. 2007. Kimberlite Tailings. *Transportation Research Record: Journal of the Transportation Research Board,* 1989-2**,** 131-134.

SYED, S. 2012. Recovery of gold from secondary sources—A review. *Hydrometallurgy,* 115-116**,** 30-51.

TABELIN, C. B., IGARASHI, T., VILLACORTE-TABELIN, M., PARK, I., OPISO, E. M., ITO, M. & HIROYOSHI, N. 2018. Arsenic, selenium, boron, lead, cadmium, copper, and zinc in naturally contaminated rocks: A review of their sources, modes of enrichment, mechanisms of release, and mitigation strategies. *The Science of the total environment,* 645**,** 1522-1553.

TABELIN, C. B., SASAKI, R., IGARASHI, T., PARK, I., TAMOTO, S., ARIMA, T., ITO, M. & HIROYOSHI, N. 2017a. Simultaneous leaching of arsenite, arsenate, selenite and selenate, and their migration in tunnel-excavated sedimentary rocks: I. Column experiments under intermittent and unsaturated flow. *Chemosphere,* 186**,** 558-569.

TABELIN, C. B., SASAKI, R., IGARASHI, T., PARK, I., TAMOTO, S., ARIMA, T., ITO, M. & HIROYOSHI, N. 2017b. Simultaneous leaching of arsenite, arsenate, selenite and selenate, and their migration in tunnel-excavated sedimentary rocks: II. Kinetic and reactive transport modeling. *Chemosphere,* 188**,** 444-454.

TABELIN, C. B., VEERAWATTANANUN, S., ITO, M., HIROYOSHI, N. & IGARASHI, T. 2017c. Pyrite oxidation in the presence of hematite and alumina: I. Batch leaching experiments and kinetic modeling calculations. *Science of the Total Environment,* 580**,** 687-698.

TABELIN, C. B., VEERAWATTANANUN, S., ITO, M., HIROYOSHI, N. & IGARASHI, T. 2017d. Pyrite oxidation in the presence of hematite and alumina: I. Batch leaching experiments and kinetic modeling calculations. *Sci Total Environ,* 580**,** 687-698.

TANINOUCHI, Y.-K., WATANABE, T. & OKABE, T. H. 2017. Recovery of Platinum Group Metals from Spent Catalysts Using Electroless Nickel Plating and Magnetic Separation. *Materials Transactions,* 58**,** 410-419.

THOMAS, W. J. & CRITTENDEN, B. D. 1998. *Adsorption technology and design,* Oxford ;, Butterworth-Heinemann.

TONG, S., DENG, H., WANG, L., HUANG, T., LIU, S. & WANG, J. 2018. Multi-functional nanohybrid of ultrathin molybdenum disulfide nanosheets decorated with cerium oxide nanoparticles for preferential uptake of lead (II) ions. *Chemical engineering journal (Lausanne, Switzerland : 1996),* 335**,** 22-31.

TUNCUK, A., STAZI, V., AKCIL, A., YAZICI, E. Y. & DEVECI, H. 2012. Aqueous metal recovery techniques from e-scrap: Hydrometallurgy in recycling. *Minerals Engineering,* 25**,** 28-37.

UHEIDA, A., IGLESIAS, M., FONTAS, C., HIDALGO, M., SALVADO, V., ZHANG, Y. & MUHAMMED, M. 2006a. Sorption of palladium(II), rhodium(III), and platinum(IV) on Fe(3)O(4) nanoparticles. *J Colloid Interface Sci,* 301**,** 402-8.

UHEIDA, A., IGLESIAS, M., FONTÀS, C., HIDALGO, M., SALVADÓ, V., ZHANG, Y. & MUHAMMED, M. 2006b. Sorption of palladium(II), rhodium(III), and platinum(IV) on Fe 3O 4 nanoparticles. *Journal of Colloid And Interface Science,* 301**,** 402-408.

UMEDA, H., SASAKI, A., TAKAHASHI, K., HAGA, K., TAKASAKI, Y. & SHIBAYAMA, A. 2011. Recovery and Concentration of Precious Metals from Strong Acidic Wastewater. *MATERIALS TRANSACTIONS,* 52**,** 1462-1470.

VEČEŘ, M. & POSPÍŠIL, J. 2012. Stability and Rheology of Aqueous Suspensions. *Procedia Engineering,* 42**,** 1720-1725.

VLASSOPOULOS, D. & WOOD, S. A. 1990a. Geochim. cosmochim. acta: Erratum to vlassopoulos and wood (1990) "Gold speciation in natural waters: I. Solubility and hydrolysis of gold in aqueous solution." 54, 3–12. *Geochimica et cosmochimica acta,* 54**,** 1849-1849.

VLASSOPOULOS, D. & WOOD, S. A. 1990b. Gold speciation in natural waters: I. Solubility and hydrolysis reactions of gold in aqueous solution. *Geochimica et Cosmochimica Acta,* 54**,** 3-12.

WANG, C.-B. & ZHANG, W.-X. 1997. Synthesizing Nanoscale Iron Particles for Rapid and Complete Dechlorination of TCE and PCBs. *Environmental science & technology,* 31**,** 2154-2156.

WANG, L., TIAN, C., MU, G., SUN, L., ZHANG, H. & FU, H. 2012. Magnetic nanoparticles/graphitic carbon nanostructures composites: Excellent magnetic separable adsorbents for precious metals from aqueous solutions. *Materials research bulletin,* 47**,** 646-654.

WANG, M., TAN, Q., CHIANG, J. F. & LI, J. 2017a. Recovery of rare and precious metals from urban mines—A review. *Frontiers of Environmental Science & Engineering,* 11.

WANG, M., TAN, Q., CHIANG, J. F. & LI, J. 2017b. Recovery of rare and precious metals from urban mines —— A review. *Frontiers of environmental science & engineering,* 11**,** 3-19.

WANG, Z., XU, C., WANG, S., GAO, J. & AI, T. 2016. Utilization of magnetite tailings as aggregates in asphalt mixtures. *Construction and Building Materials,* 114**,** 392-399.

WANG, Z., ZHANG, B., YE, C. & CHEN, L. 2018. Recovery of Au(III) from leach solutions using thiourea functionalized zeolitic imidazolate frameworks (TUZIF-8). *Hydrometallurgy,* 180**,** 262-270.

WIDLER, A. M. & SEWARD, T. M. 2002. The adsorption of gold(I) hydrosulphide complexes by iron sulphide surfaces. *Geochimica et cosmochimica acta,* 66**,** 383-402.

WU, C., ZHU, X., WANG, Z., YANG, J., LI, Y. & GU, J. 2017. Specific Recovery and In Situ Reduction of Precious Metals from Waste To Create MOF Composites with Immobilized Nanoclusters. *Industrial & engineering chemistry research,* 56**,** 13975-13982.

WU, F., ZHAO, T., YAO, Y., JIANG, T., WANG, B. & WANG, M. 2020. Recycling supercapacitor activated carbons for adsorption of silver (I) and chromium (VI) ions from aqueous solutions. *Chemosphere (Oxford),* 238**,** 124638-124638.

XIANG, Y., CHEN, X., CAO, C., DING, S., XU, L. & LIU, G. 2020. High performance and selectivity recovery of Au(III) from waste solution using the RFU resin. *Reactive & functional polymers,* 154**,** 104637.

XIAO, D., LU, T., ZENG, R. & BI, Y. 2016. Preparation and highlighted applications of magnetic microparticles and nanoparticles: a review on recent advances. *Mikrochimica Acta,* 183**,** 2655-2675.

XU, G.-R., AN, Z.-H., XU, K., LIU, Q., DAS, R. & ZHAO, H.-L. 2021. Metal organic framework (MOF)-based micro/nanoscaled materials for heavy metal ions removal: The cutting-edge study on designs, synthesis, and applications. *Coordination chemistry reviews,* 427**,** 213554.

XU, Y. & ZHANG, W.-X. 2000. Subcolloidal Fe/Ag Particles for Reductive Dehalogenation of Chlorinated Benzenes. *Industrial & engineering chemistry research,* 39**,** 2238-2244.

YANG, S.-T., YANLI, C., HAIFANG, W., GANGBO, L. I. U., SHENG, C., YANWEN, W., YUANFANG, L. I. U. & AONENG, C. A. O. 2010. Folding/aggregation of graphene oxide and its application in Cu2+ removal. *Journal of colloid and interface science,* 351**,** 122-127.

YAO, C., CHEN, S., WANG, L., DENG, H. & TONG, S. 2019. Low cost and rapid fabrication of copper sulfides nanoparticles for selective and efficient capture of noble metal ions. *Chemical engineering journal (Lausanne, Switzerland : 1996),* 373**,** 1168-1178.

YOO, J., KIM, H.-S., PARK, S.-Y., KWON, S., LEE, J., KOO, J. & SEO, Y.-S. 2020. Instantaneous integration of magnetite nanoparticles on graphene oxide assisted by ultrasound for efficient heavy metal ion retrieval. *Ultrasonics sonochemistry,* 64**,** 104962-104962.

ZAZYCKI, M. A., TANABE, E. H., BERTUOL, D. A. & DOTTO, G. L. 2017a. Adsorption of valuable metals from leachates of mobile phone wastes using biopolymers and activated carbon. *Journal of Environmental Management,* 188**,** 18-25.

ZAZYCKI, M. A., TANABE, E. H., BERTUOL, D. A. & DOTTO, G. L. 2017b. Adsorption of valuable metals from leachates of mobile phone wastes using biopolymers and activated carbon. *J Environ Manage,* 188**,** 18-25.

ZHANG, H., RITCHIE, I. M. & LA BROOY, S. R. 2001. Electrochemical Oxidation of Gold and Thiourea in Acidic Thiourea Solutions. *Journal of the Electrochemical Society,* 148**,** D146-D153.

ZHANG, L., ZENG, Y. & CHENG, Z. 2016. Removal of heavy metal ions using chitosan and modified chitosan: A review. *Journal of molecular liquids,* 214**,** 175-191.

ZHANG, W.-X. 2003. Nanoscale Iron Particles for Environmental Remediation: An Overview. *Journal of nanoparticle research : an interdisciplinary forum for nanoscale science and technology,* 5**,** 323.

ZHANG, Y., LIU, S., XIE, H., ZENG, X. & LI, J. 2012. Current Status on Leaching Precious Metals from Waste Printed Circuit Boards. *Procedia Environmental Sciences,* 16**,** 560-568.

ZHANG, Y., XU, Q., ZHANG, S., LIU, J., ZHOU, J., XU, H., XIAO, H. & LI, J. 2013. Preparation of thiol-modified Fe3O4@SiO2nanoparticles and their application for gold recovery from dilute solution. *Separation and Purification Technology,* 116**,** 391-397.

ZHANG, Z. & ZHANG, F.-S. 2014a. Selective recovery of palladium from waste printed circuit boards by a novel non-acid process. *Journal of Hazardous Materials,* 279**,** 46-51.

ZHANG, Z. & ZHANG, F. S. 2014b. Selective recovery of palladium from waste printed circuit boards by a novel non-acid process. *J Hazard Mater,* 279**,** 46-51.

ZHAO, J., WANG, C., WANG, S., ZHANG, L. & ZHANG, B. 2019a. Augmenting the adsorption parameters of palladium onto pyromellitic acid-functionalized nanosilicas from aqueous solution. *Colloids and surfaces. A, Physicochemical and engineering aspects,* 578**,** 123581.

ZHAO, J. S. & DAI, J. H. 2014. Kinetics and Mechanism of Platinum Pressure-Cyanide Dissolution. *Applied Mechanics and Materials,* 522-524**,** 424-428.

ZHAO, M., HUANG, Z., WANG, S. & ZHANG, L. 2020. Ultrahigh efficient and selective adsorption of Au(III) from water by novel Chitosan-coated MoS2 biosorbents: Performance and mechanisms. *Chemical engineering journal (Lausanne, Switzerland : 1996),* 401**,** 126006.

ZHAO, M., LI, X., HUANG, Z., WANG, S. & ZHANG, L. 2021. Facile cross-link method to synthesize chitosan-based adsorbent with superior selectivity toward gold ions: Batch and column studies. *International journal of biological macromolecules,* 172**,** 210-222.

ZHAO, M., ZHAO, J., HUANG, Z., WANG, S. & ZHANG, L. 2019b. One pot preparation of magnetic chitosan-cystamine composites for selective recovery of Au(III) from the aqueous solution. *International journal of biological macromolecules,* 137**,** 721-731.

ZHAO, S., FAN, J. & SUN, W. 2014. Utilization of iron ore tailings as fine aggregate in ultra-high performance concrete. *Construction and Building Materials,* 50**,** 540-548.

ZHOU, S., HU, C., XU, W., MO, X., ZHANG, P., LIU, Y. & TANG, K. 2020. Fast recovery of Au (III) and Ag(I) via amine-modified zeolitic imidazolate framework-8. *Applied organometallic chemistry,* 34**,** n/a.